

Serous business: delineating the broad spectrum of diseases with subretinal fluid in the macula

Dijk, E.H.C. van; Boon, C.J.F.

Citation
Dijk, E. H. C. van, & Boon, C. J. F. (2021). Serous business: delineating the broad spectrum of diseases with subretinal fluid in the macula. *Progress In Retinal And Eye Research*, *84*. doi:10.1016/j.preteyeres.2021.100955

Version:	Publisher's Version
License:	Creative Commons CC BY 4.0 license
Downloaded from:	https://hdl.handle.net/1887/3213227

Note: To cite this publication please use the final published version (if applicable).

Progress in Retinal and Eye Research 84 (2021) 100955

Contents lists available at ScienceDirect

Progress in Retinal and Eye Research

journal homepage: www.elsevier.com/locate/preteyeres

Serous business: Delineating the broad spectrum of diseases with subretinal fluid in the macula

Elon H.C. van Dijk [a], Camiel J.F. Boon [a,b,*]

[a] Department of Ophthalmology, Leiden University Medical Center, Albinusdreef 2, 2333 ZA, Leiden, the Netherlands
[b] Department of Ophthalmology, Amsterdam University Medical Centers, University of Amsterdam, Meibergdreef 9, 1105 AZ, Amsterdam, the Netherlands

ARTICLE INFO

Keywords:
Central serous chorioretinopathy (CSC)
Differential diagnosis
Retinal disease
Serous fluid accumulation
Serous maculopathy

ABSTRACT

A wide range of ocular diseases can present with serous subretinal fluid in the macula and therefore clinically mimic central serous chorioretinopathy (CSC). In this manuscript, we categorise the diseases and conditions that are part of the differential diagnosis into 12 main pathogenic subgroups: neovascular diseases, vitelliform lesions, inflammatory diseases, ocular tumours, haematological malignancies, paraneoplastic syndromes, genetic diseases, ocular developmental anomalies, medication-related conditions and toxicity-related diseases, rhegmatogenous retinal detachment and tractional retinal detachment, retinal vascular diseases, and miscellaneous diseases. In addition, we describe 2 new clinical pictures associated with macular subretinal fluid accumulation, namely serous maculopathy with absence of retinal pigment epithelium (SMARPE) and serous maculopathy due to aspecific choroidopathy (SMACH). Differentiating between these various diseases and CSC can be challenging, and obtaining the correct diagnosis can have immediate therapeutic and prognostic consequences. Here, we describe the key differential diagnostic features of each disease within this clinical spectrum, including representative case examples. Moreover, we discuss the pathogenesis of each disease in order to facilitate the differentiation from typical CSC.

1. Introduction

Central serous chorioretinopathy (CSC) is a relatively common chorioretinal disease that typically presents with a sudden disruption of central vision. This vision loss is caused by a detachment of the neurosensory retina due to an accumulation of serous subretinal fluid (SRF) in the macula. However, abnormalities may extend well beyond the posterior pole, possibly leading to only mild visual complaints. Middle-aged men are most commonly affected, despite the fact that an older age does not rule out a first-time presentation of CSC, especially in women. Both corticosteroid use and endogenous hypercortisolism, as well as several genetic factors, have been found to increase the risk of developing CSC (Brinks et al., 2021; Daruich et al., 2015; de Jong et al., 2015; Kaye et al., 2020; van Dijk et al., 2016a, 2017b; van Rijssen et al., 2019b).

A wide variety of other diseases and conditions can also present with serous SRF in the macula and can therefore clinically mimic CSC (Table 1). Since the differentiation between these diseases and CSC can be challenging, we discuss the extensive differential diagnosis of CSC. Moreover, we describe the pathogenic mechanisms specific to the various diseases that contribute to this differential diagnosis. These diseases can be broadly categorised into the following 12 main pathogenic subgroups:

1. Neovascular diseases
2. Vitelliform lesions
3. Inflammatory diseases
4. Ocular tumours
5. Haematological malignancies
6. Paraneoplastic syndromes
7. Genetic diseases
8. Ocular developmental anomalies
9. Medication-related conditions and toxicity-related diseases
10. Rhegmatogenous retinal detachment and tractional retinal detachment
11. Retinal vascular diseases
12. Miscellaneous diseases

A thorough medical history, including medical conditions, medication use, and familial eye diseases, as well as the nature and pattern of

* Corresponding author. Department of Ophthalmology, Amsterdam University Medical Centers, University of Amsterdam, Meibergdreef 9, 1105 AZ, Amsterdam, the Netherlands.
E-mail address: camiel.boon@amsterdamumc.nl (C.J.F. Boon).

https://doi.org/10.1016/j.preteyeres.2021.100955
Received 30 November 2020; Received in revised form 14 February 2021; Accepted 19 February 2021
Available online 11 March 2021
1350-9462/© 2021 The Authors. Published by Elsevier Ltd. This is an open access article under the CC BY license (http://creativecommons.org/licenses/by/4.0/).

Abbreviations

AMD	age-related macular degeneration
BDUMP	bilateral diffuse uveal melanocytic proliferation
BM	Bruch's membrane
CACD	central areolar choroidal dystrophy
CNV	choroidal neovascularisation
CSC	central serous chorioretinopathy
FA	fluorescein angiography
FAF	fundus autofluorescence
HELLP	haemolysis, elevated liver enzymes, and low platelet
ICGA	indocyanine green angiography
IgM	immunoglobulin type M
IRF	intraretinal fluid
MEK	mitogen-activated protein kinase kinase inhibitor
MEKAR	mitogen-activated protein kinase kinase inhibitor-associated retinopathy
OCT	optical coherence tomography
OCTA	optical coherence tomography angiography
PCV	polypoidal choroidal vasculopathy
PDT	photodynamic therapy
RPE	retinal pigment epithelium
SMARPE	serous maculopathy with absence of retinal pigment epithelium
SMACH	serous maculopathy due to aspecific choroidopathy
SRF	subretinal fluid
VEGF	vascular endothelial growth factor

the symptoms, can help when evaluating the differential diagnoses of CSC. In addition, fundoscopy and non-invasive imaging methods such as optical coherence tomography (OCT) and OCT angiography (OCTA) of the retina and choroid, as well as fundus autofluorescence (FAF), can show key features which can help differentiate between the causes of serous maculopathy. In many cases, fluorescein angiography (FA) and indocyanine green angiography (ICGA) can be valuable for evaluating the retinal and choroidal circulation in order to identify the presence of fluid leakage and/or other abnormalities. In this manuscript, we discuss the main differential diagnostic features of each disease subgroup. We also provide the general pathophysiological background and information regarding the pathogenesis of these diseases, together with case examples, to further facilitate the differentiation between these diseases and typical CSC.

2. The functional unit consisting of the neurosensory retina, retinal pigment epithelium, Bruch's membrane, and choroid

2.1. The neurosensory retina

The neurosensory retina has a complex structure, consisting of neuronal layers and cells that are highly organised and cross-connected. The blood vessels arising from the central retinal artery deliver blood to all cells in the retina except the photoreceptors. The inner blood-retinal barrier is formed by tight junctions between the endothelial cells in the retinal vessels; this barrier is important for maintaining retinal homeostasis and preventing the accumulation of intraretinal fluid (IRF)(Daruich et al., 2018; Klaassen et al., 2013). The macula is the central part of the retina encircled by temporal vascular arcades and contains both rods and cones. The centre of the macula contains the 1.5-mm diameter fovea (also known as the fovea centralis). The fovea contains a dense concentration of primarily M cones (sensitive to medium-wavelength light in the visible spectrum) and L cones (sensitive to long-wavelength light in the visible spectrum), as well as S cones (sensitive to short-wavelength light in the visible spectrum) and rods(Roorda and Williams, 1999; Solomon and Lennie, 2007). The foveal centre (also known as the foveola) is 0.35 mm in diameter and contains the highest concentration of cones in the retina. In the foveola, the inner nuclear layer and the ganglion cell layer are laterally displaced, leading to a structural depression known as the foveal pit(Ahnelt, 1998; Curcio et al., 1990).

The photoreceptors, which serve as the first-order neurons in the visual system, absorb photons, which initiates the visual cycle and causes a change in the neuron's membrane potential. This electrochemical signal is then propagated through the cell membrane and transmitted via synapses to the higher-order neuronal networks in the visual system. The phototransduction cascade occurs in the photoreceptor's outer segments, which contain up to 1000 flat membranous structures that greatly increase the surface area and phototransduction efficiency. These photoreceptor outer segments are closely surrounded by the retinal pigment epithelium (RPE) microvilli, which phagocytose the outer segments shed by the RPE(Hollenberg and Lea, 1988). Every 24 h, the RPE phagocytoses approximately 10% of the photoreceptor outer segments. This process is important, as these oldest distal outer segments contain the highest concentrations of potentially toxic by-products of the visual cycle that therefore need to be digested and degraded by the RPE(Schmitz-Valckenberg et al., 2020; Sparrow et al., 2012). In addition, the apposition between the outer photoreceptor structures and the apical RPE surface is essential, as part of the visual cycle and the regeneration of visual pigment occurs in the RPE (Lamb and Pugh, 2004), although the cone cells also have an alternative process for recycling intraretinal visual pigments(Wang and Kefalov, 2011).

The photoreceptors receive oxygen and metabolites from the choroid. Thus, an abundant oxygen supply from the choroid is extremely important, as the photoreceptor inner segments have one of the highest rates of oxygen consumption per unit weight in the human body (Wangsa-Wirawan and Linsenmeier, 2003). Phagocytosis of photoreceptor outer segments, proper functioning of the visual cycle, and molecular exchange are all critically dependent upon a normal anatomical and functional relationship between the photoreceptors and the RPE (Wangsa-Wirawan and Linsenmeier, 2003).

2.2. Retinal pigment epithelium

The intimate relationship between the photoreceptors and RPE monolayer is optimised by the numerous apical RPE microvilli surrounding the photoreceptors' distal outer segments. The neuroretina is attached to the RPE to a certain extent via the so-called interphotoreceptor matrix that envelops the cone cells(Ishikawa et al., 2015). The transport of metabolites and ions between the photoreceptors and the choriocapillaris is mediated by the RPE, which forms an outer blood-retinal barrier(Fields et al., 2020; Rizzolo et al., 2011). Cell-cell junctions in the RPE are formed by tight junctions, adherens junctions, and gap junctions; thus, the directed transport of nutrients from the choroid to the outer retina, and the removal of waste products, water, and ions from the outer retina to the choroid, is tightly regulated. In the RPE, cell volume, pH, and transepithelial transport are regulated by the polarised insertion of ion channels, transporters, and other proteins in the apical and basolateral RPE membrane compartments. Under normal conditions, the RPE efficiently transports water and solutes away from the subretinal space (i.e. between the neuroretina and the RPE) to the choroid(Dvoriashyna et al., 2020; Reichhart and Strauss, 2014). This outward movement of molecules across the RPE depends primarily on active ionic transport and – to a lesser extent – the higher oncotic pressure (i.e. colloid osmotic pressure) in the choroid compared to the retina(Dvoriashyna et al., 2020; Reichhart and Strauss, 2014).

The RPE also plays an essential role in many other processes(Strauss,

Table 1
Differential diagnosis of central serous chorioretinopathy.

	Disease	Clinical characteristics and differential diagnostic aspects	Treatment options	References	Figure
Ocular neovascular disease	Subretinal neovascularisation in context of pachychoroid neovasculopathy	Older age, presence of neovascular network on ICGA (sometimes FA), and OCTA, neovascularisation over areas of choroidal thickening and thickened Haller's layer vessels ('pachyvessels')	Intravitreal anti-VEGF injections	(Cheung et al., 2019; Pang and Freund, 2015)	2A-F
	Polypoidal choroidal vasculopathy	Older age, presence of polypoidal dilatations on OCT and ICGA, sometimes with concurrent non-polypoidal neovascularisation on ICGA and OCT	Intravitreal anti-VEGF injections and/or (reduced-settings or full-settings) photodynamic therapy	(Cheung et al., 2018; Cheung et al., 2019; Coscas et al., 2015; Spaide et al., 1995; Yannuzzi et al., 1990)	2G-K
	Neovascular age-related macular degeneration	Presence of drusen in combination with or without vitelliform lesion, neovascular lesion on OCT, OCTA, FA (and ICGA)	Intravitreal anti-VEGF injections	(Bergen et al., 2019; Mehta et al., 2018)	2L-N
	Other conditions with subretinal neovascularisation	- High myopia: chorioretinal atrophy adjacent to optic disc, oblique insertion of optic disc, macular pigment abnormalities, thin choroid - Angioid streaks (often in pseudoxanthoma elasticum): early onset, bilateral deep retinal red-brown bands, optic disc drusen, peripheral round atrophic scars - Multifocal choroiditis: yellow-white punched-out round spots deep to the retina, women < 50 years - Choroidal rupture: yellow-white subretinal streak, history of blunt eye trauma	Intravitreal anti-VEGF injections	(Aguilar and Green, 1984; Chatziralli et al., 2019; Ikuno, 2017; Kohno et al., 2000; Slakter et al., 1997; Wyszynski et al., 1988)	2O-Q
Vitelliform lesions	Autosomal dominant Best vitelliform macular dystrophy and autosomal recessive bestrophinopathy due to *BEST1* gene mutations	Positive family history, bilateral disease, vitelliform lesion on fundoscopy, serous detachment on OCT, filled with hyperreflective material, hyperautofluorescence on FAF, no focal leakage on FA, no choroidal hyperpermeability on ICGA, absent or markedly decreased light rise on electro-oculography, mutations in the *BEST1* gene	No treatment available, intravitreal anti-VEGF injections in case of neovascularisation	(Boon et al., 2009b; Boon et al., 2013b)	3A-D
	Acute exudative polymorphous vitelliform maculopathy	Multiple, bilateral well-defined serous macular detachments, subretinal accumulation of yellow-white material, hyperautofluorescence on FAF, no focal leakage on FA/ICGA	No treatment available	(Barbazetto et al., 2018; Gass et al., 1988)	3E-H
	Adult-onset foveomacular vitelliform dystrophy	Either unilateral or bilateral small (<1 disc diameter) round foveal yellowish subretinal lesions, hyperautofluorescence on FAF, central hypofluorescence with a hyperfluorescent ring on FA (with late staining of vitelliform lesion), either non- or hypofluorescent changes on ICGA	No treatment available	(Chowers et al., 2015; Pierro et al., 2002; Querques et al., 2011; Spaide, 2004)	3I–K
	Vitelliform lesions secondary to age-related macular degeneration	Presence of drusen in combination with surrounding vitelliform detachment, underlying confluent drusen	AREDS formula supplements (intravitreal anti-VEGF injections in case of neovascularisation)	(Bergen et al., 2019; Mehta et al., 2018)	3L-N & 3O-Q
	Vitelliform lesions in the context of other diseases	- Epiretinal membrane - Vitreomacular traction - Persistent SRF after retinal reattachment surgery	Either observation or surgical intervention (vitrectomy)	(Querques and delle Noci, 2007; Spaide, 2008)	3R-T
Inflammatory diseases	Vogt-Koyanagi-Harada disease	Harada disease: only ocular signs, including vitritis and optic disc oedema Rapid onset, young age, bilateral in 95% of cases, cystoid outer retinal fluid on OCT, numerous central leakage points on FA, in some cases with serous inferior retinal detachment, early hyperfluorescence on ICGA At least 3 of the following findings to establish the diagnosis Vogt-Koyanagi-	Corticosteroids, other systemic immunosuppressive medication	(O'Keefe and Rao, 2017; Shin et al., 2015)	4A-G

(*continued on next page*)

Table 1 (*continued*)

	Disease	Clinical characteristics and differential diagnostic aspects	Treatment options	References	Figure
		Harada disease: bilateral chronic iridocyclitis, posterior uveitis, neurologic signs, cutaneous signs			
	White dot syndromes (e.g. acute posterior multifocal placoid pigment epitheliopathy)	Rapid onset with progressive marked vision loss and often slow recovery, female predominance, relatively young age, (placoid) subretinal (yellow-white) lesions on fundoscopy, OCT, and FA, hypofluorescent changes on late-phase ICGA	Local and/or oral corticosteroids, other systemic immunosuppressive medication (intravitreal anti-VEGF injections in case of neovascularisation)	Birnbaum et al. (2010)	4H–N
	Posterior scleritis	Middle-aged women, presentation with deep pain, hyperaemia of the conjunctiva and large scleral vessels, painful eye movements, choroidal folds, serous retinal detachment, and optic disc oedema on examination, fluid in the sub-Tenon space around the optic disc (T-sign) on B-scan ultrasonography, no leakage on FA/ICGA	Corticosteroids, other systemic immunosuppressive medication	(Agrawal et al., 2016; McCluskey et al., 1999)	4O-R
	Sarcoidosis	Nodules on conjunctiva and anterior, intermediate or posterior uveitis on examination, retinal vasculitis, small round atrophic granulomas in inferior peripheral fundus Systemic disease: granulomas in different organs, mainly lungs, skin, and lymphatic system	Corticosteroids, other systemic immunosuppressive medication	(Nunes et al., 2007; Watts et al., 2000)	4S–V
	Unilateral acute idiopathic maculopathy	Presentation soon after a flu-like illness, young age, swelling of outer retina with elevated and disrupted ellipsoid zone on OCT, spontaneous and quite rapid resolution of SRF, vitritis on examination, no leakage on FA and no hyperfluorescence on ICGA	Observation	(Beck et al., 2004; Freund et al., 1996; Hughes et al., 2012; Yannuzzi et al., 1991)	5A-F
Ocular tumours	Choroidal naevus and melanoma	Hyperpigmented (sometimes amelanotic) and elevated choroidal mass on fundoscopy, low internal reflectivity on B-scan ultrasonography, solid choroidal mass on OCT, multiple areas of pinpoint leakage on FA (choroidal melanoma), blockage of fluorescence on ICGA Focal leakage on FA may be seen in case of neovascularisation	Naevi: regular checks, melanomas may be treated with brachytherapy, proton therapy, or enucleation based on staging (intravitreal anti-VEGF injections in case of neovascularisation, sometimes photodynamic therapy in case of serous SRF leaking from naevus without neovascularisation)	(Higgins et al., 2016; Shields et al., 2019)	6A-F
	Choroidal metastases	Yellow-white elevated choroidal lesions, sometimes multifocal and bilateral, minority of patients is not known with a primary tumour at the moment of ocular presentation, high internal reflectivity on B-scan ultrasonography, irregular hyperreflective spots in the photoreceptor layer and RPE layer, in combination with choroidal mass on OCT, early hypofluorescence and late leakage on FA, blockage of choroidal fluorescence on ICGA at the location of the tumour	Observation, chemotherapy, immunotherapy, hormone therapy, whole eye irradiation	(Arepalli et al., 2015; Shields et al., 1997a, 1997b)	6Q-S
	Circumscribed cavernous choroidal haemangioma	Elevated orange-red mass on fundoscopy, elevated choroidal lesion with mixed reflectivity characteristics on OCT that fit within the vascular nature of the tumour, mild diffuse hyperfluorescence on early-phase FA with increasing diffuse leakage throughout the later phases, rapid filling of tumour vessels and late 'wash-out' phenomenon on ICGA, high internal reflectivity on B-scan ultrasonography	Photodynamic therapy	(Rahman et al., 2013; Shields et al., 2001)	6G-P
	Choroidal osteoma	Young women, well-defined bone structure in papillary or macular region, absence of echoes posterior to the tumour on B-scan	Observation (intravitreal anti-VEGF injections in case of neovascularisation)	(Rao and Gentile, 2010; Shields et al., 2007, 2015; Song et al., 2010; Yahia et al., 2008)	7A-D

(*continued on next page*)

Table 1 (*continued*)

	Disease	Clinical characteristics and differential diagnostic aspects	Treatment options	References	Figure
		ultrasonography, hyperreflective horizontal lamellar lines on OCT between choroid and tumour tissue, hyperfluorescent changes on late-phase FA and ICGA			
Haematological malignancies	Waldenström macroglobulinaemia	Bilateral macular serous retinal detachments, no focal leakage on FA, no choroidal hyperpermeability on ICGA, hyperviscosity-related retinopathy on fundoscopy (in some cases) Overproduction of the monoclonal immunoglobulin type M, blood hyperviscosity	Chemotherapy, radiotherapy, bone marrow transplantation. No evidence-based effective treatment of retinal lesions.	(Baker et al., 2013; Thomas et al., 1983)	8A-D
	Choroidal lymphoma	Presentation between fifth and seventh decade Multifocal, yellow-whitish choroidal infiltrates on fundoscopy, homogenous hyperreflective sub-RPE infiltration (primary vitreoretinal lymphoma) or deep choroidal infiltration (choroidal lymphoma) on OCT	Thorough systemic screening to assess the presence of a systemic lymphoma External beam radiotherapy, intravitreal methotrexate, intravitreal rituximab	(Arias et al., 2013; Barry et al., 2018; Matsuo et al., 1998)	8I–P and 8Q-Z
	Leukaemia	In majority of patients: cotton wool spots, haemorrhages, vascular tortuosity In minority of patients: bilateral foveal SRF, multifocal granular hyperfluorescence on FA, dot-like choroidal hyperfluorescence without leakage on ICGA Thrombocytopaenia, anaemia, and leukocytopenia, leukaemic blasts in the bone marrow	Chemotherapy, steroids, radiation therapy, stem cell transplantation	(Malik et al., 2005; Moulin et al., 2010)	8AA-AF
Paraneoplastic syndromes	Bilateral diffuse uveal melanocytic proliferation (BDUMP)	Several elevated pigmented bilateral uveal lesions and progressive cataract, association with (usually) non-ocular tumours; RPE atrophy and irregularity on examination, early hyperfluorescence on FA, corresponding to the RPE changes and RPE detachments, granular hyperfluorescent changes on ICGA	Plasmapheresis and plasma exchange	(Duong et al., 2006; Gass et al., 1990; Klemp et al., 2017)	8E-H
	Paraneoplastic vitelliform maculopathy	Relationship with cutaneous and uveal melanoma; vitelliform lesions, anti-RPE and anti-retinal auto-antibodies in serum	No treatment available	(Nagiel et al., 2017; Rahimy and Sarraf, 2013)	9I-II
Genetic diseases	Best vitelliform macular dystrophy and autosomal recessive bestrophinopathy due to *BEST1* gene mutations	see 'Vitelliform diseases'	No treatment available	(Boon et al., 2009b; Boon et al., 2013b)	3A-D
	RP1L1-associated occult macular dystrophy	*RP1L1* gene mutation, autosomal dominant inheritance Poor visual acuity despite very few abnormalities on fundoscopy, thickened and blurry ellipsoid line on OCT in the early stage of disease, which is disrupted and absent in the late phase, few abnormalities on FAF, no focal leakage on FA/ICGA	No treatment available	Takahashi et al. (2014)	10A-B
	Central areolar choroidal dystrophy due to *PRPH2* gene mutations	*PRPH2* gene mutation, autosomal dominant inheritance Moderate atrophic RPE changes in the stage 1 and 2, geographic atrophy in the stage 3 and 4, highly symmetrical FAF abnormalities, no leakage on FA, no hyperfluorescent changes on ICGA	No treatment available	(Boon et al., 2008; Boon et al., 2009a)	10C-E
	Pseudoxanthoma elasticum and serous fluid	*ABCC6* gene mutation, autosomal recessive inheritance Angioid streaks (bilateral deep retinal red-brown bands radiating from optic disc), thin choroid on OCT, no focal leakage on FA (unless in case of subretinal neovascularisation), no CSC-like hyperfluorescent zones on	Intravitreal anti-VEGF injections in case of neovascularisation	(Hansen et al., 2014; Karampelas et al., 2013)	10F-J

(*continued on next page*)

Table 1 (*continued*)

	Disease	Clinical characteristics and differential diagnostic aspects	Treatment options	References	Figure
		ICGA Localised skin changes ('plucked chicken' appearance), premature atherosclerosis, gastrointestinal and cardiovascular complications			
Ocular developmental anomalies	Dome-shaped macula	Inward macular deviation with a thickened underlying sclera, together with relatively thin choroid, especially on vertical OCT scan	No good evidence on effective treatment	Caillaux et al. (2013)	11A-F
	Tilted disc with inferior staphyloma	Anterior position of the upper and temporal portion of the tilted optic disc, oblique axis of the optic disc with an inferonasal crescent-shaped region, mild situs inversus of the retinal vessels, attenuation of the choroid and depigmented RPE in the staphylomatous inferior part of the eye SRF is visible on horizontal and vertical OCT scan, but vertical OCT scan shows the inferior staphyloma, in which SRF occurs in the watershed zone of thicker to thinner choroid, no focal leakage on FA/ICGA	No good evidence on effective treatment	(Cohen et al., 1998; Nakanishi et al., 2008)	11G-L
	Optic disc pit	Congenital unilateral abnormality of the optic disc (grey 'pit') on fundoscopy, no focal leakage on FA, no choroidal hyperpermeability on ICGA, connection of SRF to optic disc and retinoschisis-like intraretinal fluid on OCT	Conservative approach may be preferable initially. Consider treatment (e.g. vitrectomy, juxtapapillary laser photocoagulation in cases with progressive vision loss)	(Bloch et al., 2019; Jain and Johnson, 2014)	11M-P
	Uveal effusion syndrome	Most often in middle-aged hyperopic men, localised areas of RPE hypertrophy and hyperplasia ('leopard spots') on examination, together with peripheral choroidal detachment and sometimes concomitant non-rhegmatogenous retinal detachment with shifting SRF; in the acute phase, 'leopard spots' correspond to hyperfluorescent areas on FA, which later become a mixture of hyper- and hypofluorescence, early granular hyperfluorescence on ICGA, choroidal detachment on B-scan ultrasonography	No good evidence on effective treatment	(Elagouz et al., 2010; Gass and Jallow, 1982; Uyama et al., 2000)	11Q-T
	Focal choroidal excavation with secondary serous subretinal fluid	Concavity in the choroid, with normal overlying retinal architecture	No good evidence on effective treatment	Chung et al. (2017)	11U-X
	Macular choroidal macrovessel	Large tortuous choroidal vessel temporally in the macula, no leakage on FA, early filling on ICGA	No good evidence on effective treatment	(Dalvin et al., 2021; Lima et al., 2011)	11Y-AB
	Torpedo maculopathy	Hypo- or hyperpigmented lesion of the RPE, temporally to the fovea with a tip pointing toward the fovea, some hyperpigmentation of edges, lack of autofluorescence on FAF and no leakage on FA	No treatment available or necessary	(Roseman and Gass, 1992; Shirley et al., 2018)	11AC-AE
Medication-related conditions and toxicity-related disease	MEK inhibitor-associated retinopathy (MEKAR)	Onset of SRF associated with MEK inhibitor treatment (targeted treatment for metastatic tumours), bilateral and symmetrical, sometimes multifocal serous retinal detachments, no pachychoroid or RPE detachments on OCT, no leakage on FA, no light rise on electro-oculography	Observation, without discontinuation of treatment	(Urner-Bloch et al., 2014; van Dijk et al., 2015)	12A-C
	Checkpoint inhibitors causing birdshot-like chorioretinopathy (e.g. pembrolizumab)	Onset of SRF associated with checkpoint inhibitor treatment (for metastatic tumours), macular oedema, retinal vasculitis on examination	Local corticosteroid injections	(Minos et al., 2016; Miyakubo et al., 2019; Obata et al., 2019; Priem and Oosterhuis, 1988; Wong et al., 2012)	12D-F
	Hair dyes containing aromatic amines (para-phenylenediamine and 5-	Similar to MEKAR. Onset of SRF soon after the use of specific commercial hair dye containing aromatic amines, no pachychoroid or RPE detachments	Observation	Faure et al. (2020)	12G-I

(*continued on next page*)

Table 1 (*continued*)

	Disease	Clinical characteristics and differential diagnostic aspects	Treatment options	References	Figure
	diamine sulphate) causing serous retinopathy	on OCT, no leakage on FA and no hyperfluorescent abnormalities on ICGA			
	Poppers maculopathy	Either unilateral or bilateral yellow subretinal (foveal) deposit on fundoscopy, disruption of the ellipsoid zone and slight retinal elevation on OCT, no pachychoroid or RPE detachments on OCT, no leakage on FA	Observation, with discontinuation of poppers use	(Davies et al., 2012; Rewbury et al., 2017)	12J-L
Rhegmatogenous retinal detachment and tractional retinal detachment		Acute (or in rare cases gradual) onset of symptoms, such as visual field loss, central vision loss when macula is affected; history of flashes, floaters, and vision loss; pigment in the vitreous, peripheral retinal breaks, and peripheral extension of retinal detachment on examination	Laser photocoagulation, scleral buckling, vitrectomy	Steel (2014)	13A-F & 13G-I
Retinal vascular disease	Diabetic macular oedema	Diabetes mellitus in medical history; other features characteristic of diabetic retinopathy on examination (haemorrhages, microaneurysms, cotton wool spots, hard exudates)	Intravitreal anti-VEGF injections and/or corticosteroid treatment, with or without laser treatment	(Catier et al., 2005; Otani et al., 1999; Ozdemir et al., 2005)	–
	Retinal vein occlusion	Retinal haemorrhages, cotton wool spots, and vein occlusion on examination, non-perfusion on FA	Intravitreal anti-VEGF injections and/or corticosteroid treatment, with or without laser treatment	(Celik et al., 2016; Gallego-Pinazo et al., 2013)	–
	Acute hypertensive retinopathy	Retinal haemorrhages, cotton wool spots, and blood vessel occlusion on examination, increased choroidal thickness on OCT in the acute phase A similar clinical picture may be observed in pregnant women with pre-eclampsia	Treatment of hypertension	(Fraser-Bell et al., 2017; Grosso et al., 2005)	–
	Pregnancy-related serous maculopathy	Multifocal areas of SRF accumulation on OCT, together with intraretinal cystoid changes and outer retinal changes, hyperfluorescent changes corresponding to dye staining in the subretinal space on FA, choroidal filling defects on ICGA Hypertensive complications of pregnancy, e.g. (pre-)eclampsia	Observation	(Erbagci et al., 2008; Van Rysselberge et al., 2020)	13J-L
Miscellaneous	Serous maculopathy with absence of retinal pigment epithelium (SMARPE)	SRF accumulates due to absence of RPE, no drusen, early hyperfluorescence on FA, no pronounced abnormalities on ICGA	No good evidence on effective treatment	None	14A-J
	Serous maculopathy secondary to RPE dysfunction due to confluent drusen	Drusen, signs of age-related macular degeneration/drusen in other eye	AREDS formula supplements (intravitreal anti-VEGF injections in case of neovascularisation)	Cukras et al. (2010)	13M-O
	Serous maculopathy due to aspecific choroidopathy (SMACH)	Atrophic RPE changes and hyperpigmentations on fundoscopy, irregular and thickened RPE on OCT, elevated by a thickened and irregular and structurally altered choroid, early blockage of fluorescein on FA with staining and leakage on mid- to late-phase, variable fluorescence changes on ICGA	No good evidence on effective treatment	None	15A-J

Abbreviations: AREDS, Age-related Eye Disease Study; CSC, central serous chorioretinopathy; FA, fluorescein angiography; FAF, fundus autofluorescence; ICGA, indocyanine green angiography; MEK, mitogen-activated protein kinase kinase; MEKAR, MEK inhibitor-associated retinopathy; OCT, optical coherence tomography; OCTA, optical coherence tomography angiography; RPE, retinal pigment epithelium; SRF, subretinal fluid; VEGF, vascular endothelial growth factor.

2005). For example, the RPE both forms and maintains 2 extracellular matrixes known as the interphotoreceptor matrix and Bruch's membrane (BM). The pigmentation of RPE cells is based on melanin, which is packed primarily in melanosomes in the apical compartment of the RPE cell; importantly, the central macula contains the highest concentration of RPE melanosomes(Weiter et al., 1986). Melanin in the RPE has both a photoprotective function by absorbing scattered light and an antioxidant function. With ageing, melanin itself can become oxidised, and the number of melanosomes decreases; in addition, the number of complex melanin-containing granules increases, including melanolysosomes and toxic melanolipofuscin granules. The RPE also appears to play a key role in the retina's immunological microenvironment(Anderson et al., 2010). The RPE tight junctions form the outer blood-retinal barrier, which protects the neuroretina from direct contact with the choroidal blood flow. Together with the absence of lymphatics in the subretinal area, this accounts for an essential part of immune privilege in these tissues(Jiang et al., 1993; Wenkel and Streilein, 2000). Moreover, activity of macrophages and antigen presenting cells is locally modulated by the RPE (Wenkel and Streilein, 1998; Zamiri et al., 2005). Finally, the RPE secretes a variety of growth factors and structure-regulating factors such as

vascular endothelial growth factor (VEGF). In the healthy eye, these factors are beneficial for maintaining both structure and function, and RPE-derived VEGF is believed to play an important role in ocular development, particularly with respect to the development and maintenance of the choriocapillaris(Blaauwgeers et al., 1999). Under pathological conditions, however, RPE-derived factors such as VEGF can be detrimental. For example, an overexpression of VEGF has been shown to promote the formation of choroidal neovascularisation (CNV) in age-related macular degeneration (AMD) and other ocular diseases (Witmer et al., 2003). The RPE's permeability can also be affected by various factors such as pro-inflammatory cytokines, oxidative stress, angiogenic molecules such as VEGF, matrix metalloproteinases, the inflammatory effects of mast cell–derived factors, and complement activation(Daruich et al., 2018; Lakkaraju et al., 2020; Mullins et al., 2014; Xia and Rizzolo, 2017).

Similar to the differences in photoreceptors, the characteristics of the RPE also differ between the central and peripheral retina(Boulton and Dayhaw-Barker, 2001). For example, the density of RPE cells decreases moving from the fovea to the peripheral retina, and the ratio of photoreceptors to RPE cells is highest in the macula. In addition, RPE cells in the macula are taller, have a smaller diameter, and contain more melanin granules compared to peripheral RPE cells. Also similar to photoreceptors, RPE cells are among the highest consumers of energy in the body. Although both light and oxygen are essential for vision, they can also promote the formation of reactive oxygen species, which can cause photochemical damage to the retina(Organisciak and Vaughan, 2010). Finally, the number of RPE cells generally decreases with age, placing an increased burden on the remaining cells(Panda-Jonas et al., 1996).

2.3. Bruch's membrane

Bruch's membrane separates the RPE from the choriocapillaris and consists of 3 layers, with a central elastic layer bordered on either side by a collagenous layer. The elastic layer of BM is thicker moving from the fovea to the periphery, and the overall thickness of BM increasing with age (Chong et al., 2005; Ramrattan et al., 1994), with increased deposits of collagen, lipids, and other substances such as complement components(Guymer et al., 1999). These ageing-related changes can disrupt BM integrity and can cause a sharp decrease in the transport of transepithelial fluid and nutrients, particularly in the macula, where BM is thinnest(Booij et al., 2010). In addition, the BM becomes more fragile with age, thereby increasing the risk of neovascular ingrowth. Subretinal deposits, including basal laminar deposits, basal linear deposits, and drusen (the precursors of AMD) can develop preferentially between the basement membrane of the RPE and the inner collagenous layer of BM(Anderson et al., 2010; van der Schaft et al., 1992).

2.4. Choroid

The choroid, a thin vascular network below BM, consists of the choriocapillaris layer, 2 layers with larger blood vessels, and the suprachoroid layer. These 4 layers contain blood vessels, fibroblasts, immune-competent cells, melanocytes, and supporting tissue (Nickla and Wallman, 2010). The choroid receives blood from the ophthalmic artery, which sends short posterior ciliary arteries into the eye, where they divide further to form smaller arteries. In the posterior pole of the eye, the choriocapillaris has a lobular structure, with a main arteriole surrounded by draining venules(Hayreh, 1990; Mrejen and Spaide, 2013; Spaide, 2020).

The choriocapillaris contains a dense network of capillaries, whereas the underlying 2 layers contain medium-sized arteries and arterioles (Sattler's layer) and larger vessels (Haller's layer). Finally, the suprachoroid layer sets the boundary of the choroid(Nickla and Wallman, 2010). Among middle-aged individuals (i.e. 40-50 years of age), choroidal thickness is approximately 300 μm (Entezari et al., 2018; Imamura et al., 2009), and this generally decreases with age. Choroidal thickness also varies with axial length; individuals with an axial elongation generally have a thinner choroid than individuals with decreased axial length(Fujiwara et al., 2009; Morgan et al., 2018; Wang et al., 2015).

The choroid receives the highest rate of blood flow per unit weight of any tissue in the human body in order to provide sufficient levels of oxygen and nutrition to the retina and remove waste products(Parver et al., 1980; Wangsa-Wirawan and Linsenmeier, 2003). This high blood flow also allows for the dissipation of thermal energy due to light absorption, thereby helping to stabilise tissue temperature(Bill et al., 1983; Parver et al., 1982). Conversely, both the structure and function of the choriocapillaris requires the constitutive secretion of VEGF by the RPE. The choriocapillaris has a polarised structure, with fenestrations in the capillary wall at the internal surface facing BM/RPE. Soluble VEGF is needed for the development and maintenance of these fenestrations (Saint-Geniez et al., 2009), which play an important role in the flow of nutrients toward the RPE and ensuring sufficient molecular exchange at the choroid-BM-RPE-neurosensory retina interface. These choriocapillary vascular fenestrations also allow the dye fluorescein, which is used during FA, to diffuse into the extravascular space, whereas larger molecules such as indocyanine green are unable to enter the extravascular space(Pino, 1985; Tornquist et al., 1990). Unlike the vessels in the choriocapillaris, the medium-sized blood vessels in Sattler's layer and the large blood vessels in Haller's layer do not contain fenestrations.

The choroid appears to lack a mechanism for autoregulating blood flow; however, neural innervation and myogenic mechanisms may play a role in regulating choroidal blood flow(Spaide, 2020). For example, sympathetic stimulation increases choroidal vascular resistance and decreases blood flow, whereas parasympathetic stimulation causes choroidal vascular dilation, increasing blood flow(Granstam and Nilsson, 1990; Reiner et al., 2018).

The characteristics of the outflow through the vortex veins can affect choroidal blood flow in both health and disease(Spaide, 2020). Moreover, the choroid secretes several growth factors and enzymes, including matrix metalloproteinases, tissue plasminogen activator, basic fibroblast growth factor, and transforming growth factor beta (Nickla and Wallman, 2010), all of which have found to regulate eye growth and/or scleral remodelling(Boote et al., 2020; Hu et al., 2009). As mentioned above, the choroid contains a wide range of immune cells, including macrophages, dendritic cells, and mast cells, as well as complement factors, all of which also play an important role in ocular health and disease(Anderson et al., 2002, 2010; Boon et al., 2009d; McMenamin et al., 2019). With age, a number of choroidal properties decrease, including thickness, choriocapillary blood flow, and the density and diameter of choroidal vessels(Chong et al., 2005).

Melanocytes in the choroid absorb scattered light and may also protect against oxidative stress, although high oxygen partial pressure and high light exposure of choroidal melanocytes increase the risk of malignant melanoma(Daruich et al., 2018). The choroid has a higher protein concentration than the retina and vitreous, and the retina is less permeable to water than the RPE(Kirchhof and Ryan, 1993; Marmor, 1990). This set of properties facilitates the osmotic movement of water from the vitreous to the choroid, provided that cellular barriers such as the outer blood-retinal barrier of the RPE are intact. Thus, in addition to the polarised location and function of ion channels and transporters in the RPE, the osmotic gradient from the vitreous and the retina to the choroid also helps keep the neurosensory retina attached to the RPE (Kirchhof and Ryan, 1993; Marmor, 1990).

2.5. Unique characteristics that predispose the macula to subretinal fluid accumulation

The macula is particularly sensitive to the accumulation of SRF in many of the diseases discussed in this manuscript. Several factors underlie this high susceptibility to macular SRF accumulation and depend

largely on the underlying aetiology, as well as structural and functional differences that exist between the macula and peripheral areas of the involved tissues. For example, gene expression varies between the neurosensory retina, RPE, BM, and choroid, and the spatial expression of retinal genes also changes with age(Cowan et al., 2020; Ishibashi et al., 2004; Kociok and Joussen, 2007; Sharon et al., 2002; van Soest et al., 2007). In addition, shape, density, and function of photoreceptors and RPE cells vary topographically and change with age(Boulton and Dayhaw-Barker, 2001; Boulton et al., 1994; Curcio, 2001; Curcio et al., 1990). For example, the central fovea contains exclusively L and M cones, whereas the macula surrounding the fovea also contains large numbers of rods and S cones (Curcio et al., 1990, 1991), and these parafoveal rods are particularly vulnerable to ageing-related changes (Curcio, 2001; Curcio et al., 1993). Moreover, the RPE cells in the macula have the highest levels of enzyme activity(Boulton et al., 1994). Because macular RPE cells serve the highest density of photoreceptors, this could explain why the macular RPE contains the highest amounts of lipofuscin and its toxic compounds, which originate from degradation of the metabolic and structural elements in the visual cycle(Feeney-Burns et al., 1984; Sparrow and Boulton, 2005; Weiter et al., 1986). The density of RPE cells decreases from the fovea to the peripheral retina (Dorey et al., 1989). The macula also contains macular pigment in the neuroretina, and the central RPE contains higher amounts of melanin, melanolipofuscin, and melanolysosomes compared to the extramacular RPE(Kijlstra et al., 2012; Sparrow and Boulton, 2005). Finally, BM is thinnest in the macula and most vulnerable to ageing-related changes such as a decrease in the transport of fluids and nutrients within this region(Chong et al., 2005).

The highest rate of choroidal blood flow occurs in the macula, and the choroid is significantly thicker in the macula compared to the periphery(Entezari et al., 2018; Margolis and Spaide, 2009; Yoneya and Tso, 1987). The centre of the macula appears to be particularly vulnerable to choroidal vascular disorders, as this region contains several watershed zones, receiving blood supply from the most distal part of 2 arteries(Hayreh, 1975, 2004). However, the foveal cones appear to be more resilient to degenerative processes compared to the rods, giving rise to the phenomenon known as 'foveal sparing', in which foveal structure and function are relatively spared in many macular diseases characterised by chorioretinal atrophy(Bax et al., 2019; Saksens et al., 2014).

3. Why is visual acuity relatively preserved in some diseases involving macular subretinal fluid?

Because of their extremely high metabolic activity and oxygen consumption levels, photoreceptors are highly dependent on the RPE and choroid for molecular exchange and oxygen. Based on animal studies, photoreceptors are estimated to receive approximately 90% of their required oxygen from the choroidal circulation, and 10% from the inner retinal circulation(Ahmed et al., 1993; Linsenmeier and Braun, 1992). Thus, it is somewhat striking that visual acuity can be relatively preserved for several years in some disease categories that involve serous detachment of the neuroretina in the fovea. Several factors may play a role in this phenomenon. For example, cones appear to have less oxygen demand compared to rods. In addition, the central fovea may benefit from a supply of oxygen and molecular exchange from the perifoveal vascular plexus, particularly in cases involving macular SRF accumulation in which molecular exchange between the RPE and choroid is compromised. Moreover, the cones appear to be more resistant to both damage and ageing than the rods; remarkably, the total number of foveal cones is relatively stable with ageing(Curcio et al., 1993). Nevertheless, the visual cycle is interrupted in cases of serous photoreceptor detachment from the RPE, which normally provides several essential steps in the regeneration of visual pigments. One possible explanation why visual acuity can remain reasonably well preserved under these circumstances may be that the Müller cells may provide cones with an alternative intraretinal visual cycle(Wang and Kefalov, 2011).

It is a remarkable finding that patients with neovascular AMD may have a relatively preserved vision when SRF is present. A certain amount of persistent SRF may therefore be acceptable or even favourable when treating with anti-VEGF agents(Daruich et al., 2018; Mehta et al., 2018). Another surprising finding is that although some diseases involving macular SRF (e.g. CSC and Best vitelliform macular dystrophy) have relatively preserved long-term visual acuity, other causes of serous SRF accumulation such as rhegmatogenous retinal detachment are generally associated with a rapid, severe loss of central vision. Some diseases are characterised by relatively stable, gradual-onset macular SRF within a 'closed compartment' delineated by an attached neuroretina and underlying RPE, thereby allowing for a reasonable level of molecular exchange, ion exchange, and oxygen diffusion, even though the outer photoreceptors are no longer embedded in the apical surface of their normal housekeeper cells in the RPE. The physiological composition of the SRF in many diseases involving a 'closed compartment' of macular SRF may be more favourable than in other conditions such as the SRF associated with a rhegmatogenous retinal detachment. In the case of a rhegmatogenous detachment, the macular detachment generally has a relatively rapid onset, with potentially more acute and more severe damage occurring in the detached photoreceptors. In addition, the composition of the SRF (which is primarily liquefied vitreous) in a rhegmatogenous retinal detachment likely differs significantly from the SRF composition in 'closed compartment' SRF accumulation, thereby possibly having a stronger effect on photoreceptor function(Quintyn and Brasseur, 2004). A recent study found marked differences between the molecular profile of the SRF in CSC and rhegmatogenous retinal detachment(Kowalczuk et al., 2018). Nevertheless, visual acuity can also be extremely poor in some cases of 'closed compartment' SRF accumulation, for example in macular photoreceptor dystrophies with primary photoreceptor degeneration and in certain cases involving severe ischaemia such as ischaemic retinal venous occlusion(Celik et al., 2016; Yamaguchi et al., 2006).

4. Central serous chorioretinopathy

4.1. Clinical characteristics of CSC

4.1.1. Presentation and classification of CSC

Most symptomatic patients with CSC experience a sudden decrease in vision, loss of stereopsis, and/or metamorphopsia (distorted vision), together with changes in colour and contrast vision; thus, CSC is generally associated with a decrease in quality of life(Breukink et al., 2017; Sahin et al., 2014). However, abnormalities can extend well beyond the posterior pole, and will induce only mild visual complaints in a subset of CSC patients. CSC encompasses a clinical spectrum, making it challenging for clinicians in terms of reporting the disease and determining its prognosis(Kaye et al., 2020; Singh et al., 2019). Indeed, high levels of disagreement have been reported among experienced retinal specialists(Singh et al., 2019). Although 2 main subtypes are generally distinguished – acute CSC and chronic CSC – other disease subtypes have also been described, including recurrent CSC, persistent CSC, and inactive CSC(Singh et al., 2019). However, the classification of CSC is controversial, and several types for classification have been proposed(Chhablani and Cohen, 2020; Daruich et al., 2015; Yannuzzi, 2010). It is unclear whether these various subtypes represent either a continuum or distinct disease entities, despite being part of the same pachychoroid spectrum and despite overlap in genetic risk factors (Cheung et al., 2019; Daruich et al., 2015; Mohabati et al., 2020c; van Rijssen et al., 2019b).

The distinction between acute CSC and chronic CSC has been studied extensively and has often been based on the duration of ocular complaints and SRF accumulation, combined with the presence (in chronic CSC) or absence (in acute CSC) of atrophic RPE changes(van Dijk et al.,

2018a; van Rijssen et al., 2019b). Patients with chronic CSC generally present with poorer visual acuity compared to patients with acute CSC, and up to 40% of chronic CSC patients present with bilateral SRF(Gackle et al., 1998). However, most patients with chronic CSC also develop subclinical changes such as changes in the RPE and/or abnormalities visible on ICGA in the fellow eye(van Dijk et al., 2019).

4.1.2. *Epidemiology and risk factors of CSC*

The mean annual incidence of CSC is 9.9 per 100,000 males and 1.7 per 100,000 females (Kitzmann et al., 2008), with a reported male-to-female ratio of up to 8:1(Gemenetzi et al., 2010; Wang et al., 2008). However, the incidence of CSC is likely underestimated, as asymptomatic CSC can be diagnosed by the presence of extramacular SRF, as observed in the contralateral eye and in family members of patients with CSC(Lehmann et al., 2015; van Dijk et al., 2019; Weenink et al., 2001). CSC is most often diagnosed in middle-aged patients who are therefore still of working age. The peak age at onset for CSC is 40–50 years but varies widely(Castro-Correia et al., 1992; Gilbert et al., 1984; Spaide et al., 1996). Women and patients who are relatively older at diagnosis have an increased risk of either presenting with CNV or developing CNV later in the disease course(Fung et al., 2012; Pang and Freund, 2015; Schatz et al., 1992).

A specific form of acute CSC can occur during pregnancy, with acute-onset macular SRF, and some of these patients present with the striking finding of subretinal whitish fibrin-like material in the serous detachment(Maggio et al., 2015; Said-Ahmed et al., 2012). Although CSC can occur in uncomplicated pregnancies, some CSC cases present in association with pregnancy-induced hypertension complications such as pre-eclampsia (see section 15.4). In general, CSC resolves with no sequelae within 3 months after pregnancy, although severe vision loss can occur in rare cases(Maggio et al., 2015).

CSC is considered a multifactorial disease. The most clinically relevant risk factor of CSC is corticosteroid use, which has been found to increase the risk of developing CSC by up to 37-fold, even with minimal use(Carvalho-Recchia et al., 2002; Haimovici et al., 2004). Another risk factor is hypercortisolism (Cushing's syndrome), and CSC can even be the presenting symptom in patients with oligosymptomatic Cushing's syndrome(Bouzas et al., 2002; van Dijk et al., 2016a). Several genetic risk factors have also been associated with CSC and are discussed in section 4.2. CSC has also been associated with a relatively short axial length, but CSC can still occur in patients with an increased axial length and myopia(Chatziralli et al., 2017; Ersoz et al., 2019; Yzer et al., 2012).

SRF can resolve spontaneously in both acute CSC and chronic CSC. For example, in the VICI randomised controlled trial comparing oral eplerenone treatment to placebo in chronic CSC, 30% of patients in the placebo group had a complete resolution of SRF at their 1-year follow-up visit(Lotery et al., 2020). However, up to 51% of patients with untreated acute CSC experience at least 1 recurrence(Ficker et al., 1988; Matet

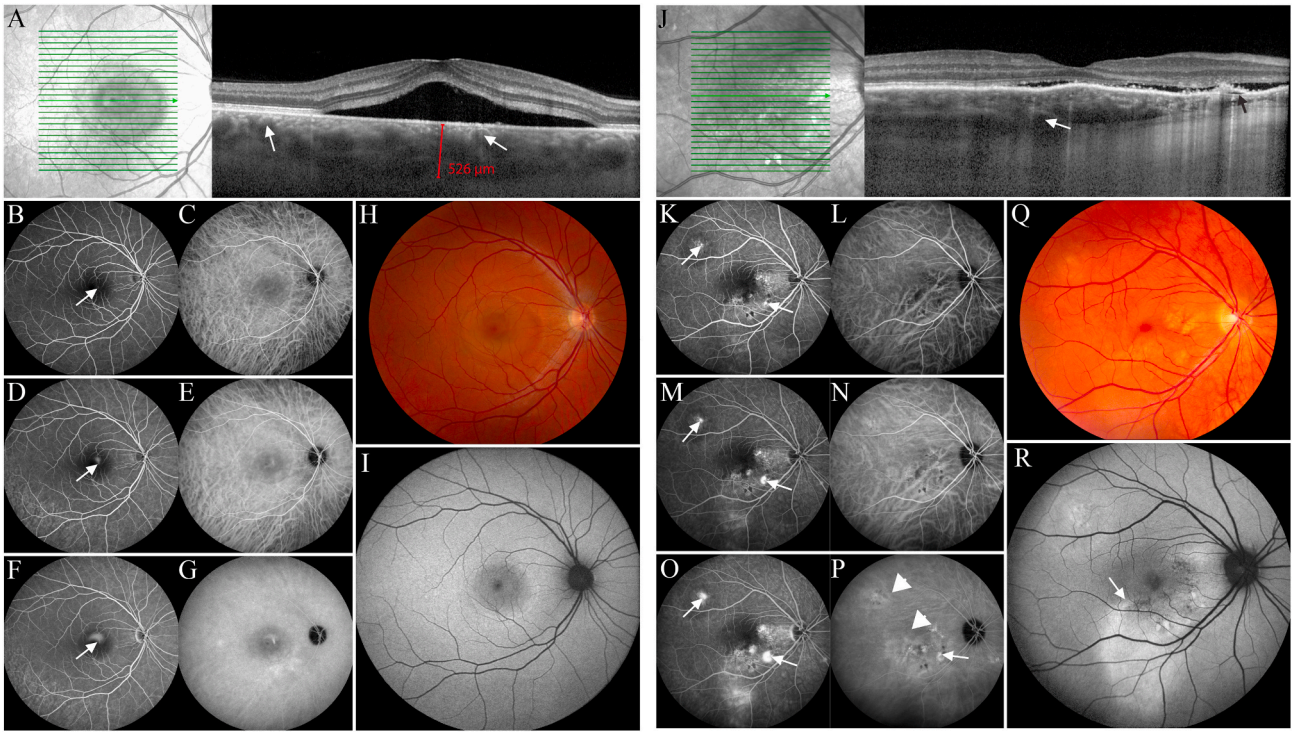


Fig. 1. An overview of characteristics on multimodal imaging in acute (**A-I**) and chronic (**J-R**) central serous chorioretinopathy (CSC).
(**A-I**) Multimodal imaging of a 34-year-old man diagnosed with **acute CSC.**
Optical coherence tomography (OCT; A) shows foveal subretinal fluid overlying a thick choroid (526 µm with 'pachyvessels' (white arrows). On fluorescein angiography there is a focal area of hyperfluorescent dye leakage, which increases and ascends in the subretinal space to produce a 'smoke stack' leakage pattern (white arrows, B, D, F). On indocyanine green angiography there is a similar leakage pattern with additional hyperfluorescent areas of choroidal vascular hyperpermeability in the late phase (G). The serous detachment seen on OCT (A) and colour fundus photography (H) has a slightly hyperautofluorescent border on fundus autofluorescence (I).
(**J-R**) Multimodal imaging of a 44-year-old man with **chronic CSC.**
Subretinal fluid, photoreceptor outer segment atrophy, a small retinal pigment epithelial detachment (black arrow), choroidal thickening, and dilated veins in Haller's layer (white arrow) are present on OCT (J). Focal areas of hyperfluorescent leakage (white arrows) are seen at 1 min (K), 3 min (M), and 6 min (O) fluorescein angiography. Indocyanine green angiography typically shows large choroidal vessels and choroidal vascular hyperpermeability, visible as characteristic hyperfluorescent multifocal 'ink blot' leakage (arrowheads) in the mid-to-late phase (L, N, P). Colour fundus photography shows irregular pigmentary abnormalities, some of which correspond to the areas of leakage and atrophic RPE changes on fluorescein angiography (Q). Fundus autofluorescence shows irregular and multifocal, mostly hyperautofluorescent abnormalities, including a hyperautofluorescent 'descending tract' (white arrow) induced by chronic subretinal fluid.

et al., 2018). A similar recurrence rate has been reported in patients with untreated chronic CSC(Fok et al., 2011; Gilbert et al., 1984). Notably, few patients with chronic CSC have a previous history of acute CSC (Mohabati et al., 2018b).

4.1.3. Fundus findings in CSC

A serous detachment of the neuroretina is visible on fundoscopy in patients with CSC either with or without detachment of the RPE. This neurosensory detachment is typically round or oval, with no sign of haemorrhage (Fig. 1H and Q), and yellow subretinal deposits may be visible in the vicinity of the detachment. A bullous retinal detachment can also occur, but is a relatively rare manifestation of chronic CSC (Balaratnasingam et al., 2016a). Moreover, subretinal fibrin has been reported in a small subset of CSC patients, particularly in pregnant patients(Ie et al., 1993; Rezai and Eliott, 2004).

RPE changes – either focal or multifocal – are common, although these changes are more prevalent in chronic CSC than in acute CSC. These RPE changes can include changes in pigment, RPE thickening, and atrophy of the RPE. If present, RPE degeneration can present in either a 'descending tract' or 'teardrop' pattern (Fig. 1O and R) due to gravitational tracking of the SRF(Daruich et al., 2015; Kaye et al., 2020; Yannuzzi, 2010). In rare cases of severe chronic CSC, atrophic RPE changes in the inferior retinal area can be extensive, with scattered bone spicule–like hyperpigmentation, resulting in an incorrect diagnosis of sectorial retinitis pigmentosa.

4.1.4. OCT and OCT angiography findings in CSC

On OCT, SRF often presents together with increased choroidal thickness, and choroidal abnormalities are believed to be the primary underlying abnormality in CSC. OCT may reveal focal SRF accumulation at the fovea (Fig. 1A and J), whereas in some patients multifocal SRF accumulations due to multiple sites of leakage can be present. In acute CSC, the SRF generally resolves spontaneously, resulting in a good prognosis in terms of retinal anatomy and visual function(van Rijssen et al., 2019b; Wang et al., 2008; Wong et al., 2004). Enhanced-depth imaging of the choroid often reveals dilated large vessels in Haller's layer, with thinning of the overlying smaller vessels in Sattler's layer and the choriocapillaris. Most patients with CSC present with 1 or more RPE detachments, as well as irregular and/or atrophic RPE alterations that can be relatively subtle(Ahlers et al., 2009; Yang et al., 2013). In a subset of patients with CSC, mid-to hyperreflective material below a shallow RPE detachment and above BM can be seen, suggesting the possible presence of neovascular material(Fung et al., 2012; Pang and Freund, 2015; Schatz et al., 1992). Using en face OCT and the choroidal vascularity index can especially be useful in these patients(Kim et al., 2020; Wong et al., 2021).

IRF, which usually occurs together with SRF and active leakage on FA, has been referred to as 'posterior cystoid retinal degeneration' and most often presents in the papillomacular region(Mohabati et al., 2020b; Piccolino et al., 2008). Diffuse atrophic RPE alterations, also known as diffuse retinal pigment epitheliopathy, are a typical finding in severe chronic CSC and have been linked to corticosteroid use(Polak et al., 1995). These atrophic abnormalities can expand over time (Mohabati et al., 2018b), and some patients may even present with a severe chronic CSC phenotype with extensive atrophic RPE changes and posterior cystoid retinal degeneration(Mohabati et al., 2018a, 2018b, 2020b).

The use of OCT angiography (OCTA), a non-invasive method to measure the movement of blood cells within blood vessels, is increasing rapidly in retinal and chorioretinal diseases, including CSC(Spaide et al., 2018a). This tool may provide additional insights into retinal and/or choroidal abnormalities that occur in CSC, adding to the existing knowledge obtained using contrast imaging modalities. Importantly, OCTA may play an essential role in detecting subretinal neovascular tissue (Spaide et al., 2018a), in addition to the clinical signs of CNV visible on conventional OCT (e.g. mid-to hyperreflective material below a flat irregular RPE detachment) and ICGA (e.g. presence of a well-demarcated neovascular membrane). OCTA may also be useful in detecting CNV in normal-looking fellow eyes(Spaide et al., 2018a). Hypoperfusion and low flow in the choriocapillaris have been observed on OCTA and are hypothesised to be caused by hyperperfusion in the surrounding areas(Teussink et al., 2015). An increase in hydrostatic pressure has also been seen in these surrounding areas and could result in RPE damage and SRF leakage(De Bats et al., 2018). Finally, reduced choriocapillary perfusion is believed to causes ischaemia in adjacent retinal structures due to insufficient oxygen delivery, which may increase the retina's susceptibility to develop SRF(Teussink et al., 2015).

4.1.5. Fluorescein angiography findings in CSC

In general, acute CSC is characterised by a focal leak that is visible on FA and leads to the transient accumulation of SRF(Ahlers et al., 2009; Yang et al., 2013). The phenomena known as 'smokestack leakage' – an ascending area of hyperfluorescence with subtle lateral diffusion due to the convection currents of fluid containing a low concentration of fluorescein (Fig. 1B, D, and F) – and/or an 'ink blot' leakage pattern – a gradual expansion of a round hyperfluorescent area from a central pinpoint of fluorescein leakage – are typical of acute CSC(Bujarborua et al., 2010; Wang et al., 2008). In chronic CSC, areas of leakage visible on FA can be either focal or multifocal (Fig. 1K, M, and O).(van Rijssen et al., 2019a) In acute CSC and chronic CSC, pooling of fluorescein under the detached RPE can be seen on FA, whereas window defects can be seen in areas of RPE atrophy.

4.1.6. Indocyanine green angiography in CSC

Choroidal abnormalities can be visualised using ICGA. Some choroidal areas have a delay in vascular filling during the early phase of ICGA, visible as focal hypofluorescent areas(Kitaya et al., 2003; Prunte and Flammer, 1996). However, early-phase ICGA in CSC often shows areas of large, dilated, and – in some cases – densely packed choroidal vessels (Fig. 1C and L). Mid-to late-phase ICGA reveals the typical choroidal vascular hyperpermeability, presenting as focal hyperfluorescent staining of the inner choroid with indistinct borders in the posterior pole and in some cases in the mid-periphery (Fig. 1E and N). (Piccolino and Borgia, 1994; Spaide et al., 1996) With progressive ICGA phases, these focal hyperfluorescent areas develop into 'ink blot'-like indistinct regions of hyperfluorescent centrifugal leakage of indocyanine green (Fig. 1G and P). Most acute CSC cases have a single area of focal leakage visible on both FA and ICGA, although abnormalities visible on ICGA can be considerably more extensive and/or multifocal in these cases. In contrast, extensive hyperfluorescent choroidal abnormalities and multifocal areas of leakage are more common in chronic CSC (Fig. 1K–P) (Eandi et al., 2005).

4.1.7. Fundus autofluorescence findings in CSC

FAF imaging can be used to measure RPE metabolism, as this imaging modality shows the presence of the autofluorescent molecule lipofuscin (Schmitz-Valckenberg et al., 2020), a degradation product formed during the phagocytosis and processing of photoreceptor outer segments by the RPE. An accumulation of lipofuscin causes hyperautofluorescent changes, whereas RPE atrophy and/or signal blockage causes hypo-autofluorescence(Senba, 1985; von Ruckmann et al., 1995). The active fluorophore N-Retinyl-N-retinylidene ethanolamine (A2E) is the first and best characterised component of lipofuscin(Yung et al., 2016).

In CSC, hypo-autofluorescence has been described to occur at the site of leakage on FA (Eandi et al., 2005), whereas hyperautofluorescent abnormalities can be found at the site of prolonged neuroretinal detachment (Fig. 1I and R).(Ho and Yannuzzi, 2008; Wang et al., 2008) In chronic CSC, FAF gravitational tracts can appear as regions of hyperautofluorescent and/or hypo-autofluorescent areas that typically originate at the macula and optic disc and extend inferiorly after prolonged SRF accumulation (Fig. 1R). Interestingly, the direction of these gravitational tracts has been associated with the side on which the

patient usually sleeps(Pang et al., 2014). Over time, granular regions of hypo-autofluorescent changes can become more confluent in patients with chronic CSC(Lee et al., 2016; Zola et al., 2018).

4.1.8. Treatment of CSC

Although a broad range of treatment modalities have been reported for CSC, the preferred treatment varies widely in practice, and the treatment of CSC is controversial(Mehta et al., 2017; van Rijssen et al., 2019b). Based on a large body of evidence obtained from retrospective studies and from the PLACE trial, the first randomised controlled trial for chronic CSC, half-dose (or half-fluence) photodynamic therapy (PDT) is considered both safe and effective for treating chronic CSC and should be the treatment of choice in these patients whenever available(van Dijk et al., 2018a; van Rijssen et al., 2019b). To perform this half-dose PDT, patients have to receive 3 mg/m^2 verteporfin, which is half of the verteporfin dose that was originally used to treat neovascular AMD patients (Newman, 2016). In contrast, observation for a few months may be the preferred approach in acute CSC, although reduced-setting PDT may be considered in specific circumstances, for example in patients who require optimal vision for their profession(Chan et al., 2008; Mohabati et al., 2020a; van Dijk et al., 2020b; van Rijssen et al., 2019b). Most clinicians recommend treatment based on the corresponding area(s) of hyperfluorescence on ICGA, as these choroidal abnormalities form the basis of the disease, and hyperfluorescent changes on FA are often more localised, carrying the risk of under-treatment with FA-guided PDT. However, localisation of the ICGA-based PDT spot can be chosen by taking into consideration areas of SRF on OCT and focal leakage on FA, in addition to the corresponding underlying changes in hyperfluorescence on ICGA. The size of the PDT spot can often be as large as up to 7 mm without compromising safety. In cases of multifocal leakage in which the leakage area cannot be included within a single PDT spot, the macular area (if affected) can be treated first, exactly 15 min after the start of the verteporfin infusion, over a period of 10 min, and the second area (e.g. above the optic disc) can be treated immediately after the start of macular treatment (with a standard treatment time of 83 s), with no overlap between these subsequent treatment spots(van Dijk et al., 2020b).

A large body of evidence suggests that PDT has an excellent short-term and long-term safety profile in CSC – regardless of whether or not the fovea is included in the treatment spot – even with a second treatment applied to the same eye(Silva et al., 2013; van Rijssen et al., 2019b). Reduced-setting PDT has also been found to be both safe and effective for treating SRF in patients with severe chronic CSC (Mohabati et al., 2018b), as well as in patients with chronic CSC who present with visual complaints due to extrafoveal SRF(van Dijk et al., 2017a). In addition, in patients with chronic CSC with posterior cystoid retinal degeneration, PDT is considered the most successful treatment in terms of complete resolution of this degeneration(Mohabati et al., 2020b). In chronic CSC, a second application of half-dose PDT was found to be less effective at achieving complete resolution of SRF compared to the first application of PDT(van Dijk et al., 2018a). Importantly, however, there are currently no indications that a second application of PDT within a few months of the first application increases the risk of either retinal or chorioretinal atrophy(van Dijk et al., 2018a; van Rijssen et al., 2019b). A lack of response to PDT and/or the recurrence of SRF following PDT for chronic CSC is more common in male patients, patients with diffuse leakage on FA, patients without intense changes in hyperfluorescence on ICGA, older patients, and patients with low visual acuity prior to treatment, for reasons that are currently unknown(Matet et al., 2018; van Rijssen et al., 2018).

The most commonly reported alternative treatments for chronic CSC are oral mineralocorticoid receptor antagonists (e.g. eplerenone), micropulse laser treatment, and focal thermal laser photocoagulation. The initial enthusiasm regarding the use of eplerenone for CSC, which was based on relatively small – and mostly retrospective – studies (Bousquet et al., 2013; Daruich et al., 2015; van Rijssen et al., 2019b), has been tempered by the results of the VICI randomised controlled trial, which found that eplerenone was not more effective at treating chronic CSC compared to placebo(Lotery et al., 2020). A possible explanation for this finding may be the limited number of mineralocorticoid receptors expressed in the choroid(Brinks et al., 2018). The use of another, potentially more potent mineralocorticoid antagonist, spironolactone, is less attractive, as this compound is less selective for the mineralocorticoid receptor and also affects the androgen receptor and the progesterone receptor. Because of this reduced selectivity, spironolactone has more adverse side effects than eplerenone, including sex hormone-related adverse events such as gynaecomastia in men and breast tenderness in both men and women(Danjuma et al., 2014; Lainscak et al., 2015).

Micropulse laser treatment has also been advocated as a potentially effective treatment for CSC. Short duty cycle micropulse laser supposedly has an effect on RPE and photoreceptors, being relatively selective in terms of cell damage, as observed in studies in humans and in other species.(Sivaprasad et al., 2010; Yu et al., 2005). However, the exact mechanism of action and evidence for efficacy are subject of controversy (van Rijssen et al., 2020a). The anatomical and functional efficacy of micropulse laser treatment appears to be inferior to half-dose PDT based on the results of the only available randomised controlled trial (PLACE trial) and subsequent PLACE trial reports(van Dijk et al., 2018a; van Rijssen et al., 2019a, 2019b, 2020a). Using a cross-over approach in which micropulse laser treatment is applied after a previous failure of primary half-dose PDT was also found to not significantly improve either anatomical or functional outcome, whereas cross-over treatment with half-dose PDT after a previous micropulse laser treatment was more effective(van Rijssen et al., 2020b). Focal thermal laser photocoagulation in CSC should only be used in patients with extrafoveal leakage, as complications such as scotomas and CNV may occur after treatment (Ficker et al., 1988). However, compared to no treatment, focal laser photocoagulation in CSC has been found not to significantly affect best-corrected visual acuity and recurrence rate(Ficker et al., 1988; Robertson, 1986; Robertson and Ilstrup, 1983).

Performing prospective studies in CSC has been found to be essential, as acute CSC and even chronic CSC tend to show spontaneous SRF resolution, which could have resulted in numerous scientifically flawed claims of treatment efficacy in CSC in the past(Lotery et al., 2020; Luttrull, 2016; van Rijssen et al., 2020a).

A variety of other therapeutic approaches have been proposed for CSC, but most have a low level of evidence regarding their efficacy(van Rijssen et al., 2019b). With CSC, it is particularly important to assess treatment efficacy using the appropriate outcome measures and prospective randomised controlled trials, given that up to 30% of patients with chronic CSC with a history of chronic SRF leakage can have a complete resolution of SRF without treatment(Lotery et al., 2020; van Rijssen et al., 2020a).

4.2. Pathogenesis of CSC

Despite the identification of several risk factors and ability to detect primary abnormalities in the choroid and RPE, the precise pathogenesis of CSC is poorly understood(Kaye et al., 2020; van Rijssen et al., 2019b).

CSC is likely choroidal in origin, and thinning, ischaemia, and/or inflammation at the level of the choriocapillaris have been suggested to cause increased choroidal permeability. Although the affected areas tend to have an attenuated choriocapillaris and Sattler's layer, the large vessels forming the outer choroid (i.e. Haller's layer) are often dilated, resulting in an overall thicker choroid (i.e. pachychoroid), which can be observed on OCT imaging of the choroid and on mid-phase ICGA (Cheung et al., 2019; Daruich et al., 2015; Gemenetzi et al., 2010; Liew et al., 2013; Nicholson et al., 2013; Prunte and Flammer, 1996). Importantly, the definition of pachychoroid-related disease has shifted away from only an abnormally thick choroid (for example >350 μm in an eye with a normal axial length) to a more detailed morphological

definition. For this definition, several aspects such as focal or diffuse choroidal thickening, 'pachyvessels' (dilated choroidal vessels in Haller's layer with a diameter of up to 300 μm that can terminate abruptly), attenuation of choriocapillaris and intermediate vessels within Sattler's layer, and choroidal vascular hyperpermeability should be taken into account(Cheung et al., 2019; Gal-Or et al., 2018; Warrow et al., 2013). Still, it is important to address that numerous different definitions are used for terms such as pachychoroid and pachyvessels(Spaide, 2021).

This combination of abnormalities can lead to focal – and in some cases, more extensive – damage to the RPE outer blood-retinal barrier, RPE atrophy due to hypoperfusion of the choriocapillaris, decreased RPE adhesion with subsequent RPE detachment, and changes in ion and water transport(Dansingani et al., 2016; Daruich et al., 2015; Kaye et al., 2020; van Rijssen et al., 2019b). When a focal disruption occurs in the RPE outer blood-retinal barrier, water, electrolytes, and proteins can leak into the subretinal space(Wang et al., 2008). Similar choroidal abnormalities and increased choroidal thickness have also been described in the fellow eye of more than half of all patients with CSC, despite the absence of visual complaints in that eye(Chen et al., 2017; Iida et al., 1999; Tsujikawa et al., 2010). Thus, abnormalities in both the choroid and RPE often exist before the occurrence of SRF in many patients with CSC. These abnormalities, which may represent a *forme fruste* of CSC, are sometimes referred to as pachychoroid pigment epitheliopathy(Cheung et al., 2019; Warrow et al., 2013).

Although the choroid appears to have limited mechanisms for autoregulating blood flow, changes in these mechanisms may be a contributing underlying factor in CSC, as an increase in ocular perfusion pressure (measured as the difference between arterial blood pressure and intraocular pressure) was observed in patients during exercise (Spaide, 2020; Tittl et al., 2005). The putative association between CSC and several systemic diseases also indicates the existence of either a molecular effect on choroidal vessels or a global dysregulation of these vessels(Nathaniel Roybal et al., 2018). Because the choroidal circulation is regulated by the sympathetic nervous system, this system has been suggested to play a role in the pathogenesis of CSC(Nathaniel Roybal et al., 2018). In addition, the relative obstruction of venous outflow through the vortex veins may also play a role in the pathogenesis of CSC (Pang et al., 2014; Spaide, 2020; Spaide and Cheung, 2020; Spaide et al., 2021).

Hormonal factors may also be involved in the pathogenesis of CSC, as corticosteroid use is a major risk factor of CSC and CSC is far more prevalent among men than among women, although the precise mechanisms are poorly understood(Daruich et al., 2015; van Haalen et al., 2018; van Rijssen et al., 2019b). Interestingly, the risk of CSC increases in women with ageing, possibly due to changes in hormonal balance, but the underlying mechanism is currently unknown(Bousquet et al., 2016; Bujarborua et al., 2013; Lahousen et al., 2016; Setrouk et al., 2016).

Mineralocorticoid receptor sensitivity may play a role in the pathogenesis of CSC (Bousquet et al., 2013; Zhao et al., 2012), although recent clinical and experimental studies have cast doubt on the relevance of this receptor in CSC(Brinks et al., 2018; Lotery et al., 2020). Moreover, stress and shift work have been associated with CSC, although conflicting results have been reported(Matet et al., 2018; van Haalen et al., 2018, 2019). Pregnancy and having a type A personality have also been suggested as risk factors of CSC, and both have been linked to changes glucocorticoid metabolism (Goichot et al., 1998; Haimovici et al., 2003; Scheer et al., 2009), although conflicting results indicate that additional study is needed(Conrad et al., 2014; van Haalen et al., 2018, 2019).

Finally, a variety of genetic risk factors have been identified in CSC, including single nucleotide polymorphisms in the *CFH* gene (encoding complement factor H) (de Jong et al., 2015; Hosoda et al., 2018; Miki et al., 2014; Moschos et al., 2016; Schellevis et al., 2018), the *C4B* gene (encoding complement factor 4B) (Breukink et al., 2015), and the *NR3C2* gene, which encodes the mineralocorticoid receptor(van Dijk et al., 2017b). Moreover, CSC has been associated with the *ARMS2* gene (encoding age-related macular degeneration susceptibility 2) (de Jong et al., 2015), the *CDH5* gene (encoding cadherin 5) (Schubert et al., 2014), and the *SLC7A5* gene (encoding solute carrier family 7 member 5)(Miki et al., 2018). Recently, the *VIPR2* gene, which encodes vasoactive intestinal peptide receptor 2, has been linked to increased choroidal thickness, thereby increasing the susceptibility to develop CSC. However, the fact that not all patients with pachychoroid develop CSC, a second, currently unknown step likely plays a role in the pathogenesis of CSC(Hosoda et al., 2018).

Despite variability in the clinical presentation and severity of CSC, different CSC phenotypes have genetic overlap, indicating that non-genetic factors may play a more prominent role in determining the clinical course of CSC(Mohabati et al., 2020c). Unlike AMD, to date no systemic abnormalities in the complement system have been identified in CSC(van Dijk et al., 2017c). The complement system is a key mechanism of innate immunity with several physiologic activities, including the elimination of micro-organisms and damaged cells(Boon et al., 2009d). Interestingly, there have been reports of an association between CSC and infections such as *Helicobacter pylori*(Liu et al., 2016). Although these possible associations with infections are far from firmly established, they are not far-fetched, as the complement pathway plays a pivotal part in innate immunity against infectious invaders(Boon et al., 2009d).

In the following sections, we will discuss additional disease categories that may present with serous SRF accumulation in the macula.

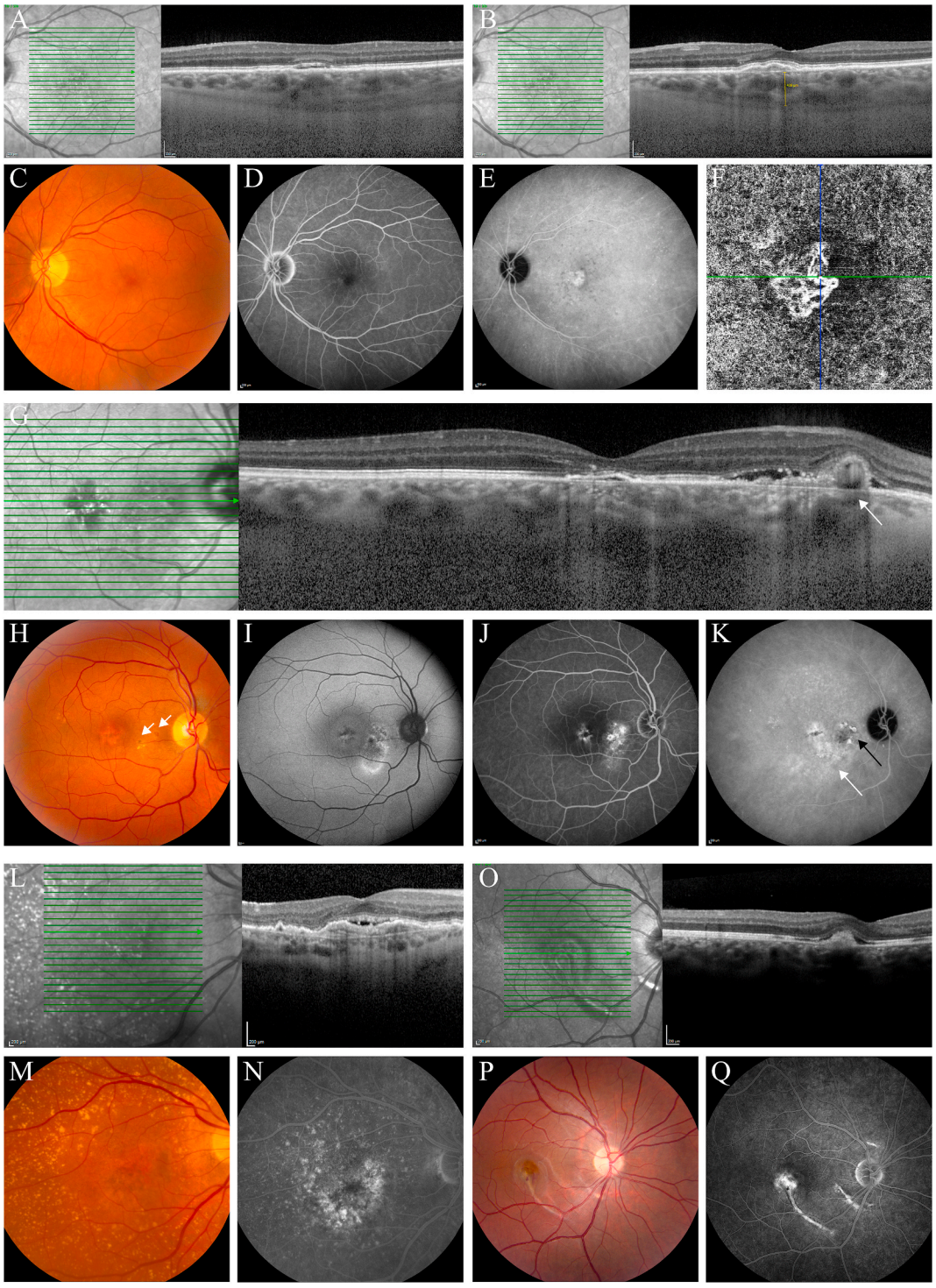
5. Neovascular diseases

A broad range of retinal and chorioretinal diseases can present with CNV (also known as macular neovascularisation). CNV can present as a subtle, relatively 'flat' type of sub-RPE (type 1) CNV (i.e. CNV-1), requiring a high index of suspicion and multimodal imaging to establish a diagnosis. There are several findings on imaging that can indicate a neovascular component when confronted with serous SRF in the macula; these findings include: 1) a relatively broad, flat RPE detachment on OCT with mid-reflective sub-RPE material corresponding to neovascular tissue (instead of the hyporeflective fluid signal in cases of uncomplicated CSC), 2) evidence of CNV-1 on OCTA together with the absence of a clear 'hot spot' of focal leakage on FA, and 3) a well-demarcated, moderately hyperfluorescent neovascular membrane on ICGA. In addition, CNV generally presents in older patients compared to uncomplicated CSC, and the prevalence of CNV is similar between men and women(Fung et al., 2012; Pang and Freund, 2015; Schatz et al., 1992).

5.1. Pachychoroid neovasculopathy

5.1.1. Clinical characteristics

Pachychoroid neovasculopathy is a form of CNV-1 that develops above zones of choroidal thickening, with pathologically dilated blood vessels in Haller's layer and attenuation of the overlying choriocapillaris and the blood vessels in Sattler's layer (Fig. 2A and B). Pachychoroid neovasculopathy is considered part of the pachychoroid disease spectrum(Cheung et al., 2019; Dansingani et al., 2016; Pang and Freund, 2015). Patients with pachychoroid neovasculopathy are presumed to have primary CNV-1, with no prior history of CSC. Multimodal imaging in these patients shows CNV-1, with no changes that could indicate other causes of subretinal neovascularisation such as AMD (e.g. no drusen in either the affected eye or the fellow eye), myopic degeneration (i.e. no choroidal thinning), and other types of degeneration (Fig. 2C). A shallow RPE detachment is often seen on OCT (Fig. 2A and B), and mid-to hyperreflective material below this shallow RPE detachment and above BM indicate the possible presence of neovascular material. Enhanced-depth OCT imaging often shows the underlying thickened choroid and the dilated vasculature in Haller's layer. On OCTA, the CNV may be clearly visible (Fig. 2F), and the angiographic signs in pachychoroid neovasculopathy may resemble findings in chronic CSC.



(caption on next page)

Fig. 2. An overview of several ocular neovascular diseases that are part of the differential diagnosis of central serous chorioretinopathy.
(**A-F**) Multimodal imaging of the left eye of a 75-year-old female patient with **pachychoroid neovasculopathy.**
The foveal optical coherence tomography (OCT) scan (A) in this patient showed a shallow accumulation of subretinal fluid (SRF), and a relatively thick choroid. An OCT scan inferiorly to the fovea (B) showed a flat irregular detachment of the retinal pigment epithelium (RPE), with a mid-reflective accumulation beneath it. Some enlarged choroidal vessels could be seen in this area. The fundus photograph (C) showed relatively mild RPE alterations. The fluorescein angiography (FA; D) in this patient showed very few macular abnormalities, and no focal leakage. On indocyanine green angiography (ICGA; E) relatively localised hyperfluorescent changes were present, which were more demarcated and surrounded by some small areas of hypofluorescence, in contrast to typical central serous chorioretinopathy (CSC). This area was compatible with a possible subretinal neovascularisation. ICGA did not show additional areas of indistinct hyperfluorescent choroidal ('ink blot') leakage (Fig. 1I), that is commonly seen in some disease presentations with a pachychoroid background such as CSC. The type 1 (sub-RPE) macular neovascularisation (MNV-1) was clearly visible on OCT angiography (F).
(**G-K**) Multimodal imaging of the right eye of a 57-year-old male patient with a history of **central serous chorioretinopathy**, which was eventually **complicated by type 1 (sub-RPE) macular neovascularisation with polypoidal choroidal vasculopathy**.
The foveal OCT scan (G) in this patient showed a shallow RPE detachment in the fovea, together with SRF and a larger RPE detachment nasally to the fovea. Irregular, mostly mid-reflective abnormalities could be seen below this larger RPE detachment, suggestive of neovascular tissue (MNV-1), and possibly a polypoidal vascular structure at the larger dome-shaped part of the RPE detachment (white arrow). On the fundus photograph (H), atrophic RPE alterations were seen foveally, with slightly whitish abnormalities in the nasal part of the macula, indicative of exudation in association with neovascular/polypoidal tissue. A round pink-red subretinal structure (white arrow) corresponded to the round lesion on OCT (white arrow in G) and hyperfluorescent round area on ICGA (black arrow in K), representing the polypoidal lesion. Fundus autofluorescence (FAF; I) showed irregular hyperautofluorescent and hypo-autofluorescent abnormalities. On mid-phase FA (J), relatively indistinct leakage was most clearly observed in the area nasally to the fovea. ICGA (K) revealed more indistinct areas of hyperfluorescent changes typical of chronic CSC below the fovea and superotemporally and inferotemporally in the macula (white arrow). In addition, this ICGA image showed a more well-demarcated hyperfluorescent area in the nasal macula, compatible with neovascular tissue, with some round-to-oval hyperfluorescent lesions with a hypofluorescent halo at the nasal edge of the neovascular tissue, characteristic of polypoidal choroidal vasculopathy (black arrow).
(**L-N**) Multimodal imaging of the right eye of a 71-year-old woman with **neovascular age-related macular degeneration.**
The foveal OCT scan (L) in this patient revealed SRF, above a broad RPE detachment with underlying mid-reflective neovascular material. On fundus photography (M), foveal RPE alterations were seen without clear fibrosis or haemorrhage. Extensive drusenoid subretinal deposits were present in the peripheral macula and in the retinal areas around the vascular arcades. In contrast to typical CSC, there was no focal leakage on FA (N), but rather diffuse, indistinct sub-RPE leakage discretely visible through atrophic RPE window defects, compatible with MNV-1.
(**O-Q**) Multimodal imaging of the right eye of a 19-year-old male patient with a **subretinal neovascularisation**, 7 months **after** previous **choroidal rupture due to blunt trauma.**
An OCT scan (O) showed a hyperreflective accumulation or scar, and a trace of SRF beneath the retina. On fundoscopy (P), 2 yellow-white streaks of choroidal rupture were observed in the macula, concentric to the optic disc, together with haemorrhages and some subretinal fibrosis at the neovascularisation at the upper edge of the larger temporal choroidal rupture. FA (Q) revealed staining and some leakage in this area in the late phase, compatible with secondary subretinal neovascularisation.

Early-to-mid-phase ICGA may show a relatively well-demarcated area of focal choroidal hyperpermeability, thus highlighting the neovascular membrane (Fig. 2E). In addition, some patients present with additional areas of indistinct hyperfluorescent choroidal (i.e. 'ink blot') leakage, which is typical of a pachychoroid background. However, leakage on FA is generally less distinct in pachychoroid neovasculopathy compared to active CSC (Fig. 2D), due to the presence of a neovascular membrane. In these cases, OCTA could provide additional information(Carnevali et al., 2017). The clinical progression of pachychoroid neovasculopathy to polypoidal choroidal vasculopathy (PCV) has also been described (Cheung et al., 2019; Manayath et al., 2018).

It can be difficult to determine whether or not there is a subretinal neovascular component present below an RPE detachment, even using all currently available multimodal imaging tools, including FA, ICGA, OCT, and OCTA. Thus, making a differential diagnosis with uncomplicated CSC – and the resulting decision regarding the primary treatment – can be challenging. Because a patient can have a previous – but undocumented – episode of CSC, it may not always be possible to determine whether the patient presents with primary CNV in the context of pachychoroid neovasculopathy or presents with CNV that is secondary to CSC. Nevertheless, all types of active CNV may require treatment with intravitreal injections of anti-VEGF medication. Some clinicians also apply PDT in order to also treat the underlying pachychoroid component of the disease, in some cases reducing the number of anti-VEGF injections required; however, only a limited amount of evidence has been published to date in support of this 2-component treatment approach (Kitajima et al., 2020; Matsumoto et al., 2020; Roy et al., 2019).

5.1.2. Pathogenesis

Choroidal abnormalities in the pachychoroid spectrum can damage the RPE, resulting in pachychoroid pigment epitheliopathy. This subtle clinical presentation may be considered a *forme fruste* of CSC, presenting as mild atrophic RPE changes and/or RPE detachments together with reduced fundus tessellation – without SRF – in an area of thickened choroid, dilated vessels in Haller's layer, and attenuated vessels in both Sattler's layer and the choriocapillaris. Eventually, the resulting disruption in the integrity of the interface between BM and the RPE can lead to an accumulation of SRF via a leak in the RPE in the context of CSC without CNV-1 (Cheung et al., 2019; Dansingani et al., 2016; Warrow et al., 2013).

5.2. Polypoidal choroidal vasculopathy

5.2.1. Clinical characteristics

PCV (also known as aneurysmal type 1, or sub-RPE, neovascularisation) generally presents at an older age compared to CSC and has a more equal incidence in men and women, which together with some key findings on fundoscopy and multimodal imaging may help differentiate PCV from CSC(Lorentzen et al., 2018). In PCV, orange-pink subretinal nodular structures are often visible on fundoscopy; however, these lesions can be subtle. On OCT, a peaked and/or dome-shaped RPE elevation with an underlying hyperreflective subretinal accumulation can be observed, in some cases with a hyporeflective vascular lumen of the polyp; however, it can be difficult to distinguish PCV and CSC based on these OCT images(Yannuzzi et al., 1997). Contrast imaging can often be used to establish the proper diagnosis; for example, PCV can be diagnosed when 1 or more focal nodular areas of hyperfluorescence are visible on early ICGA – either with or without an interconnecting vascular network together with hyperfluorescent – and in some cases nodular – structures on FA(Balaratnasingam et al., 2016c; Cheung et al., 2014; Coscas et al., 2015; Koh et al., 2012, 2013; Lorentzen et al., 2018). The well-defined hyperfluorescent nodules visible on early-phase ICGA are usually surrounded by a halo of hypofluorescence(Koh et al., 2013). Serous and haemorrhagic RPE detachments corresponding with the abnormal findings on ICGA are often present, together with IRF(Ooto et al., 2011). Importantly, although PCV can present as an isolated disease, it can also present as a complication associated with either neovascular AMD or CSC (Fig. 2G–K)..(Yannuzzi et al., 1990, 1997)

In Caucasians, PCV is phenotypically and presumably pathophysiologically more commonly associated with AMD than in Asians with PCV, as a pachychoroid background is more common in Asians(Chang and Cheng, 2020; Coscas et al., 2015; Kokame et al., 2019). Caucasian patients with PCV appear to present with 3 main subtypes of the disease. The first (and largest) subgroup of patients have PCV in the context of typical drusen-associated neovascular AMD, with ≥5 drusen with a diameter of ≥63 μm in both the affected eye and the fellow eye; this subtype is referred to as type A PCV. Patients with type B PCV have PCV together with either a non-polypoidal CNV-1 component or a branching vascular network component, but do not have drusen. Finally, type C PCV is considered an idiopathic form of PCV, presenting without drusen or signs of non-polypoidal CNV-1 or branching vascular network in either the affected eye or the fellow eye. Thus, among these 3 subtypes, only type A PCV presents with typical drusen-associated AMD(van Dijk et al., 2020a).

The first-line treatment for PCV generally consists of intravitreal injections of anti-VEGF medication. This treatment can be supplemented with either full-dose or half-dose PDT in order to improve visual outcome, increase the likelihood of achieving complete regression of the polypoidal lesions, and reduce the number of anti-VEGF injections compared to treatment with anti-VEGF injections alone(Cheung et al., 2018; Koh et al., 2013; Lee et al., 2018; Lim et al., 2020; van Dijk et al., 2018a, 2020b). Focal laser photocoagulation is another treatment option, but can only be used in treating extrafoveal and extramacular polypoidal lesions(Cheung et al., 2018; Gomi et al., 2007).

5.2.2. Pathogenesis

PCV and neovascular AMD have similar environmental and genetic risk factors, and up to 62% of patients who presumably have neovascular AMD may also have a component of PCV(Cheung et al., 2018; Maruko et al., 2007; Sho et al., 2003; Wong et al., 2016). Moreover, the polypoidal lesions in PCV are often associated with a branching vascular network of CNV between BM and the RPE, highlighting the notion that PCV may be a variant of CNV-1(Coscas et al., 2015; Dansingani et al., 2018). Patients with CNV-1 can have a component of aneurysmal dilation (the 'polyp') that is usually located at the edge of the neovascularisation. This aneurysmal dilation is generally referred to as PCV, which strictly speaking appears to be a misnomer, as the neovascular lesions that characterise PCV may not necessarily arise directly from the choroid. However, there is currently no consensus regarding the precise origin of these lesions(Balaratnasingam et al., 2016c).

The exact definition of PCV, and its association with neovascular AMD, are currently the subject of controversy. In fact, PCV appears to encompass a spectrum of presentations with variable pathogenic backgrounds, as only a portion of patients with PCV were shown to have the disease in the context of typical drusen-associated neovascular AMD(van Dijk et al., 2020a). This notion has been supported by clinical experimental evidence, as AMD-related findings of altered immunity can only be reproduced partly when investigated on PCV, likely reflecting that PCV is pathologically different from AMD(Borgersen et al., 2020; Lechner et al., 2016; Subhi et al., 2019a, 2019b). Moreover, PCV has been hypothesised to have a pachychoroid-driven background in some patients, whereas the pathogenesis of the third group – who present with neither drusen nor pachychoroid – is currently unknown(Balaratnasingam et al., 2016c; Dansingani et al., 2018; Spaide et al., 2020a; van Dijk et al., 2020a; Yannuzzi et al., 1997).

5.3. CSC complicated by choroidal neovascularisation with or without polypoidal choroidal vasculopathy

5.3.1. Clinical characteristics

The natural course of CSC can be complicated by CNV (usually type 1) with or without the occurrence of PCV(Balaratnasingam et al., 2016c; Dansingani et al., 2018). This complication, which develops in up to 25% of patients, is more prevalent in patients with long-standing chronic CSC and is generally associated with relatively poor visual outcome(Fung et al., 2012; Mrejen et al., 2019; Shiragami et al., 2018). The risk of developing CNV-1 in CSC has been associated with several factors, including choroidal vascular permeability on late-phase ICGA, sex (with women having a higher risk compared to men), and poor baseline visual acuity(Shiragami et al., 2018). CNV can be detected using a combination of FA to reveal a relatively indistinct leakage and ICGA, which can reveal a well-demarcated area of focal choroidal hyperpermeability highlighting the neovascular membrane on early-to-mid-phase ICGA. The presence of CNV may also be clearly visible on OCTA(Cheung et al., 2019; Manayath et al., 2018).

As in all cases of CNV, these patients should be treated with intravitreal injections of anti-VEGF medication, and this treatment can be supplemented with PDT, for example if PCV is also present(Cheung et al., 2018; Kitajima et al., 2020; Koh et al., 2013; Lee et al., 2018; Lim et al., 2020; Matsumoto et al., 2020; Roy et al., 2019; van Dijk et al., 2018a, 2020b).

5.3.2. Pathogenesis

The precise pathogenesis of CNV in CSC is currently unclear. Long-standing choroidal dysfunction and SRF leakage in CSC can lead to a pro-inflammatory and pro-neovascular environment, resulting in damage to the RPE and BM. This can weaken the barrier preventing the ingrowth of neovascular tissue in the subretinal space. Moreover, ischaemia of the choriocapillaris may also play an important role in driving the formation of neovascular tissue(Chan et al., 2003; Prunte and Flammer, 1996). Finally, PCV can develop in patients with CSC and long-standing CNV-1, presumably occurring as aneurysmal dilations at the edge of the neovascularisation(Fung et al., 2012; Mrejen et al., 2019; Shiragami et al., 2018).

5.4. Neovascular age-related macular degeneration

5.4.1. Clinical characteristics

AMD has clinical overlap with CSC, as both conditions can present with RPE changes and SRF in the macula, which – in the case of neovascular AMD – results from CNV leakage. This SRF leakage can be remarkably stable or can wax and wane despite the presence of neovascular tissue below the RPE, thereby complicating the differentiation between AMD and CSC. Nevertheless, the CNV tends to be more aggressive and progressive in AMD, with a more rapid loss of vision compared to several other diseases involving CNV, such as pachychoroid neovasculopathy. In neovascular AMD, OCT generally shows a larger, broader, and/or more irregular RPE neovascular detachment, with underlying mid-reflective to highly reflective neovascular tissue components (Fig. 2L). Uncomplicated CSC generally presents with hyporeflective fluid below the RPE detachment(s). In contrast to CSC, patients with AMD tend to have a normal or thin choroid without 'pachyvessels'. OCTA can be extremely helpful for detecting subtle cases of CNV in both AMD and CSC cases involving CNV(Rocholz et al., 2019). In contrast to typical CSC, central macular drusen are typically present in neovascular AMD, although CSC patients may present with 'pachydrusen' dispersed in small clusters outside the central macula(Sheth et al., 2020). Moreover, the age at onset for neovascular AMD is over 55 years, in contrast with the age at onset for CSC(Daruich et al., 2015; de Jong, 2006). In most AMD cases, patients also present with drusen in the fellow eye, with no focal 'hot spots' of leakage on FA. In cases involving CNV, a well-demarcated neovascular membrane can be observed on ICGA (Fig. 2L–N), without the typical indistinct hyperfluorescent areas often present in CSC(de Jong, 2006). Patients with neovascular AMD and active CNV should be treated with intravitreal injections of anti-VEGF medication.

5.4.2. Pathogenesis

The exact pathogenesis of AMD is currently unknown. It involves a complex interplay of vascular, metabolic, and inflammatory

mechanisms. For instance, numerous genetic susceptibility factors play a role in AMD (Boon et al., 2008b; Geerlings et al., 2017), interacting with several environmental factors, such as smoking, diet, and infectious triggers. Moreover, structural factors in the macular microenvironment have been found to be involved(Guymer et al., 1999).

Activation and dysregulation of the complement pathway, an important part of the innate immune system, has been thought to be of importance(Boon et al., 2008b, 2013a; Hussain et al., 2020; Kaarniranta et al., 2020; Rozing et al., 2020). Dendritic cells can amplify inflammatory responses, due to complement formation, degradation of the extracellular matrix, and immune complex formation(Hageman et al., 2001).

Sub-RPE drusen, as hallmark lesions of early AMD, are focal deposits between the basement membrane of the RPE and the inner collagenous BM. These deposits contain a combination of extracellular debris that are damaging to the structure and function of the RPE(Bergen et al., 2019; Curcio et al., 2009; Green, 1999). This cocktail of sub-RPE drusenoid debris includes for instance cellular components derived from photoreceptor outer segments and the RPE, cholesterol-rich lipoproteins, complement proteins, and blood-derived compounds(Anderson et al., 2010; Bergen et al., 2019; Curcio, 2018). Reticular pseudodrusen (subretinal drusenoid deposits) are located internal to the RPE and can extend internally through the ellipsoid zone, in contrast to sub-RPE drusen, and are also typically seen in AMD patients. These reticular pseudodrusen are an independent risk factor for progression towards advanced AMD(Spaide et al., 2018b). Although drusen are characteristic lesions of AMD, they are not specific to AMD, as drusen and drusen-like lesions can occur in several other retinal phenotypes(Saksens et al., 2014). Sub-RPE drusen and damage to BM in AMD create a pro-inflammatory and pro-angiogenic environment that increases the risk of CNV formation(Grisanti and Tatar, 2008; Guymer et al., 1999; Nozaki et al., 2006). The formation of type 1 (i.e. 'occult') sub-RPE neovascular tissue (CNV-1) can further damage the RPE and may lead to SRF leakage through the resulting dysfunctional RPE outer blood-retina barrier(Anderson et al., 2010; Bergen et al., 2019; Curcio, 2018; Grisanti and Tatar, 2008; Guymer et al., 1999; Nozaki et al., 2006).

5.5. Other conditions complicated by subretinal neovascularisation

Several other diseases such as high myopia, angioid streaks, multifocal choroiditis, and choroidal rupture can also be complicated by serous SRF in the macula as a result of CNV. However, the clinical picture of these entities differs markedly from CSC, as discussed below.

5.5.1. High myopia

Myopic chorioretinal atrophy adjacent to the optic disc, an oblique insertion of the optic disc, macular pigment abnormalities, and a refractive error of more than −6.00 dioptres (axial length >26 mm) are all common findings in myopic macular degeneration. CNV can develop in up to 10% of patients, often presenting together with 'lacquer cracks' (spontaneous ruptures in BM) and widespread chorioretinal atrophy (Ikuno, 2017). This myopic CNV type can have subtle SRF leakage and some degree of hyperreflective subretinal accumulation above a focal area of RPE that is interrupted by the CNV. In contrast to CSC, RPE detachments are rarely seen on OCT in myopic CNV, and the choroid is often thin. Although relatively localised leakage of the CNV may be visible on FA, ICGA does not show the hyperfluorescent, indistinct 'ink blot' choroidal leakage characteristic of CSC, even if CNV has developed (Ikuno, 2017; Liew et al., 2013; Prunte and Flammer, 1996; Ruiz-Medrano et al., 2019). CNV in high myopia should be treated using intravitreal injections of anti-VEGF medication; this treatment should be continued on a *pro re nata* basis, as the CNV in high myopia usually responds rapidly to anti-VEGF treatment(Ruiz-Medrano et al., 2019).

5.5.2. Angioid streaks

Angioid streaks represent breaks in a thickened, calcified, and abnormally fragile BM, being vulnerable to the development of CNV (Chatziralli et al., 2019). Angioid streaks occur most commonly in pseudoxanthoma elasticum (see section 11.4), but can also occur in other systemic diseases such as Paget's disease, Ehlers–Danlos syndrome, haemoglobinopathies, and other collagen diseases. On fundoscopy, angioid streaks are visible as bilateral red-brown bands deep in the retina, radiating in an irregular pattern away from the optic disc. Additional findings on fundoscopy can include optic disc drusen, peripheral round atrophic scars, and a mottled RPE appearance (peau d'orange)(Chatziralli et al., 2019). On FAF, hypo-autofluorescent fissures can be seen, which are indicative of RPE attenuation and are relatively extensive compared to fundoscopy and FA(Sawa et al., 2006). FA reveals a window defect, as the underlying choriocapillaris is visible due to the RPE absence(Federman et al., 1975).

Angioid streaks are considered to be a primary abnormality in BM, thereby increasing the risk of developing CNV. The presence of angioid steaks in a patient with CNV helps determine the aetiology of the CNV, providing a contrast with CSC. Intravitreal injections of anti-VEGF medication are currently the most effective treatment for CNV in patients with angioid streaks(Chatziralli et al., 2019; Gliem et al., 2013).

5.5.3. Multifocal choroiditis

Multifocal choroiditis is a non-infectious form of posterior uveitis, most commonly seen in relatively young myopic women of Caucasian descent. Multifocal choroiditis has also been described as punctate inner choroidopathy, although controversy exists on the degree of overlap between these entities. Patients can develop 1 or more central choroidal lesions – with possible damage to BM – and CNV formation; these lesions may resolve as atrophic scars. Auto-immunity appears to play a role in the pathogenesis of multifocal choroiditis (de Groot et al., 2020); however, CNV can occur soon after choriocapillaritis, which is visible as hypofluorescent changes on ICGA(Slakter et al., 1997). These hypofluorescent abnormalities on ICGA can be helpful for discriminating between multifocal choroiditis and CSC. In contrast to CSC, leakage from the neovascularisation, as well as 1 or more active choroidal lesions, can be observed on FA in multifocal choroiditis(Parnell et al., 2001; Slakter et al., 1997).

Currently, there is no consensus regarding the treatment of CNV in multifocal choroiditis due to a lack of randomised controlled trials. Nevertheless, CNV in multifocal choroiditis is typically treated with intraocular injections of anti-VEGF medication. Moreover, due to the inflammatory component of this disease, local or systemic steroids, as well as other immunosuppressive treatments, can be added(de Groot et al., 2020; Parodi et al., 2013).

5.5.4. Choroidal rupture

A choroidal rupture is characterised by a yellow-white subretinal streak that runs concentric to the optic disc. This streak can present directly following blunt trauma, but in some cases can be initially obscured by adjacent subretinal blood. A history of blunt eye trauma, after which the choroid, RPE, and BM can stretch and break, is a key factor in the diagnosis. Because it is relatively inelastic, BM is particularly prone to rupturing together with the apposed RPE and choriocapillaris. The occurrence of CNV – which in this context is usually type 2 – can present up to years after choroidal rupture and can present with localised SRF, thus mimicking CSC (Fig. 2O–Q). However, findings on multimodal imaging often differ between CSC and post-choroidal rupture CNV; shortly after blunt eye trauma with choroidal rupture, a blockage of fluorescein on FA can be seen when haemorrhage is present, without evidence of leakage. When CNV develops, localised fluorescein leakage may occur. Moreover, unlike with CSC, ICGA shows the presence of more hypofluorescent streaks compared to the number of hyperfluorescent streaks visible on FA, even shortly after the development of a choroidal rupture(Aguilar and Green, 1984; Kohno et al.,

2000; Wyszynski et al., 1988).

The current treatment for CNV in patients with choroidal rupture is intravitreal injections with anti-VEGF medication(Aguilar and Green, 1984; Wyszynski et al., 1988).

6. Vitelliform lesions

6.1. Best vitelliform macular dystrophy

Best disease (also known as Best vitelliform macular dystrophy) is an autosomal dominant form of macular dystrophy that typically presents with a bilateral vitelliform lesion that can resemble the central neuroretinal detachment in CSC (Fig. 3A–D) and is discussed in detail in Chapter 11.

6.2. Acute exudative polymorphous vitelliform maculopathy

6.2.1. Clinical characteristics

Acute exudative polymorphous vitelliform maculopathy is characterised by multiple, bilateral, well-defined serous macular detachments that vary in size. Inner retinal cystoid changes can also be seen on OCT, and over time, yellow-to-white material can accumulate within the serous detachments (Fig. 3E–H). To date, no genetic variants have been linked to this disease.

Multimodal imaging is the key to distinguish between CSC and acute exudative polymorphous vitelliform maculopathy. For example, no hyperfluorescent changes can be seen on FA in patients with acute exudative polymorphous vitelliform maculopathy. Moreover, on ICGA the observed hyperfluorescence in acute exudative polymorphous vitelliform maculopathy is correlated with the lesions visible on fundoscopy, while the 'ink blot' hyperfluorescent changes typical of CSC are not present. On FAF, typical hyperautofluorescence of the polymorphous deposits is another important feature specific to acute exudative polymorphous vitelliform maculopathy and can be important in distinguishing this disease from CSC, as both hyperautofluorescent and hypo-autofluorescent changes on FAF can be seen in CSC (Fig. 3F) (Eandi et al., 2005; Ho and Yannuzzi, 2008; Wang et al., 2008).

Visual acuity usually recovers spontaneously within several months to years in patients with acute exudative polymorphous vitelliform maculopathy(Barbazetto et al., 2018; Gass et al., 1988). Finally, certain forms of paraneoplastic retinopathy and autosomal recessive bestrophinopathy can closely resemble acute exudative polymorphous vitelliform maculopathy and should be excluded in cases of doubt(Boon et al., 2009b, 2009c).

6.2.2. Pathogenesis

Impaired RPE function has been suggested to cause SRF in acute exudative polymorphous vitelliform maculopathy(Barbazetto et al., 2018). In contrast, other groups have suggested that inflammation causes a change in choroidal permeability, with secondary RPE dysfunction and an accumulation of lipofuscin(Vaclavik et al., 2007).

6.3. Adult-onset foveomacular vitelliform dystrophy

6.3.1. Clinical characteristics

Adult-onset foveomacular vitelliform dystrophy is a heterogeneous group of macular disorders, part of the pattern dystrophies, characterised by a round yellowish subretinal vitelliform deposit in the fovea that can occur unilaterally or bilaterally and can present multifocally (Fig. 3I–K).(Boon et al., 2007; Chowers et al., 2015) In typical cases, the vitelliform lesions are smaller in size than the diameter of the optic disc and no drusen are visible on fundoscopy, OCT, and/or FA. In patients without a dominant family history with late onset, these features, in particular the presence of drusen, are more consistent with AMD (see section 6.4), which has a more guarded prognosis (Balaratnasingam et al., 2016b). Based on the clinical onset and findings on multimodal imaging, the distinction between this condition and CSC is relatively straightforward. For example, with adult-onset foveomacular vitelliform dystrophy visual complaints generally begin between the fourth and sixth decade, often with a gradual onset of visual symptoms. In addition, unlike CSC, OCT typically does not reveal RPE detachments. With adult-onset foveomacular vitelliform dystrophy, FA typically shows a central area of hypofluorescence surrounded by a hyperfluorescent ring, without focal leakage and with staining of the lesion in late-phase FA. Moreover, ICGA generally shows either normal fluorescence or hypofluorescent changes due to blockage by the vitelliform material, which is in contrast to CSC. Hyperautofluorescence of the lesions is often visible on FAF due to the accumulation of lipofuscin and/or lipofuscin precursors within the vitelliform lesion and the RPE(Chowers et al., 2015; Renner et al., 2004).

Currently, no viable treatment options are available for adult-onset foveomacular vitelliform dystrophy. Although the disease can remain relatively stable over many years, progression to foveal atrophy and/or CNV can occur after the age of 50–60, leading to a marked loss of central vision(Chowers et al., 2015; Querques et al., 2011).

6.3.2. Pathogenesis

In addition to the clinical variability, adult-onset foveomacular vitelliform dystrophy also has genetic heterogeneity. Autosomal dominant mutations in the *PRPH2*, *BEST1*, *IMPG1*, *IMPG2* genes have been reported as the most common causes in patients when a genetic defect is identified, which is the case in the minority of patients(Chowers et al., 2015; Gass, 1974).

A separation between the outer retina and the RPE has been suggested to lead to an accumulation of subretinal material, including pigment molecules, lipofuscin-laden macrophages, and shed photoreceptor outer segments; excess production of photoreceptor outer segments and/or impaired uptake of photoreceptor outer segments may play a role in this process(Chowers et al., 2015; Querques et al., 2011). In contrast to CSC, no focal RPE leak or dysfunctional choroid is associated with adult-onset foveomacular vitelliform dystrophy(Chowers et al., 2015; Querques et al., 2011).

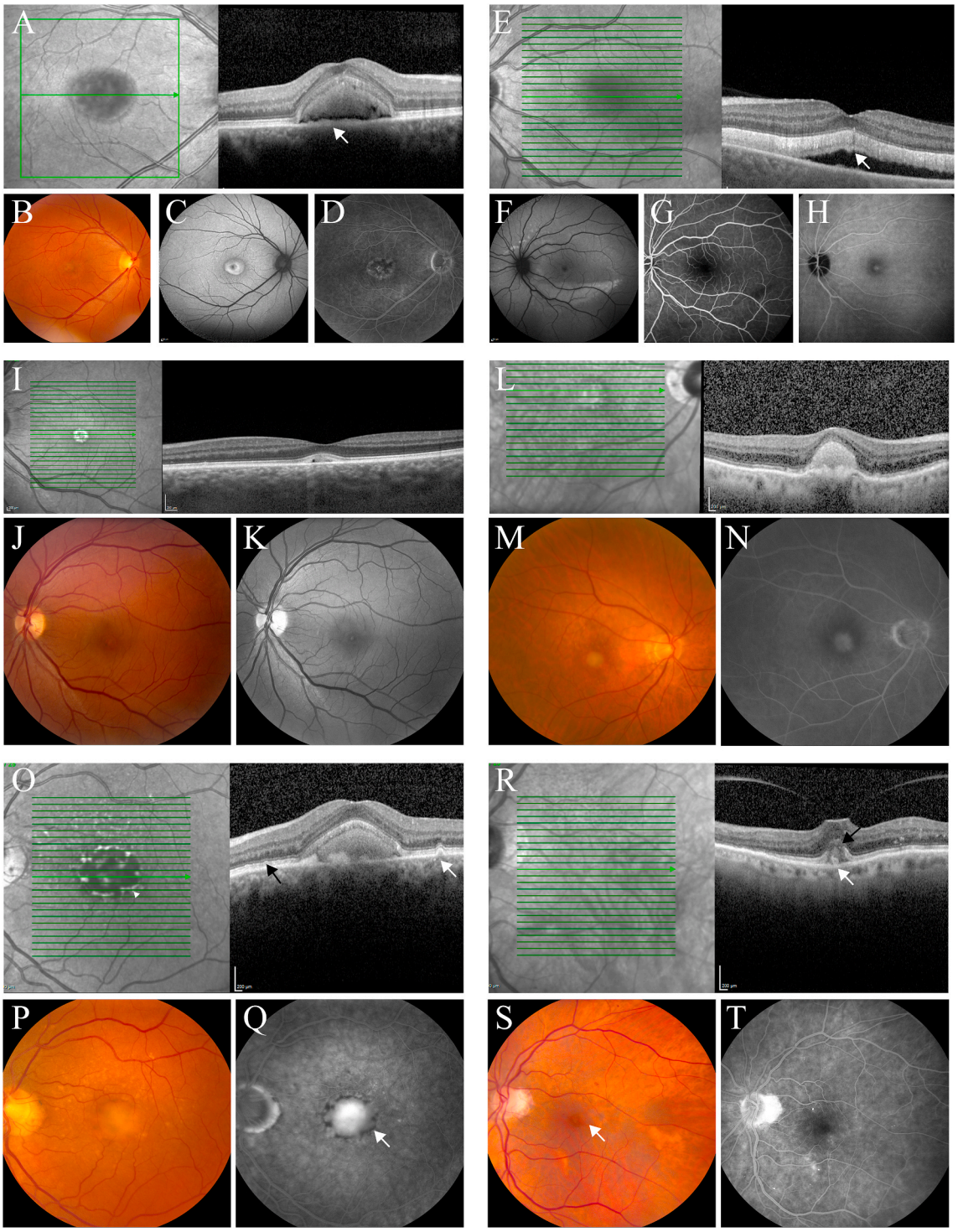
6.4. Vitelliform lesions secondary to age-related macular degeneration

6.4.1. Clinical characteristics

Patients with AMD can develop acquired vitelliform lesions due to drusen-associated RPE dysfunction (Fig. 3L–Q)(Lima et al., 2012). Vitelliform lesions in the context of AMD are often located above a large RPE detachment that results from a confluence of soft drusen. However, these lesions may also be associated with subretinal drusenoid deposits (i.e. reticular pseudodrusen) without sub-RPE drusen (Spaide et al., 2019); in this case, the vitelliform lesions will appear more whitish – rather than yellowish – in colour because the lesion is located above the RPE(Spaide and Curcio, 2010).

SRF can also occur in non-neovascular AMD, and 3 morphological patterns of SRF have recently been described for this disease entity: 1) a crest of SRF above the apex of a large drusenoid RPE detachment, 2) SRF at the junction between several confluent drusen, and 3) an accumulation of low-lying SRF over confluent drusen(Hilely et al., 2020). This SRF, which occurs in the absence of CNV, has been suggested to arise from RPE decompensation and RPE pump failure. The majority of these drusen and drusenoid RPE detachments resolve spontaneously without requiring treatment(Hilely et al., 2020; Lek et al., 2018; Sikorski et al., 2011).

CSC and AMD have some clinical overlap; for example, both conditions can present with RPE changes and vitelliform lesions (Spaide, 2004), and both can be complicated by CNV. However, typical CSC does not present with central macular drusen, although some CSC patients can present with dispersed clusters of drusen-like lesions called 'pachydrusen'(Spaide, 2018). AMD usually presents in patients over the age of 60, in contrast to CSC, which usually presents in patients under



(caption on next page)

Fig. 3. An overview of several vitelliform lesions that are part of the differential diagnosis of central serous chorioretinopathy.
(**A-D**) Multimodal imaging of the right eye of a 53-year-old male patient with **Best vitelliform macular dystrophy**, who had an absent light rise on the electro-oculogram, and carried a p.Arg218His mutation in the *BEST1* gene.
Optical coherence tomography (OCT; A) showed a serous detachment of the macula, filled with hyperreflective material, and a somewhat thickened retinal pigment epithelium (RPE) line beneath it (white arrow). This hyperreflective material in the subretinal space is presumed to consist mainly of an accumulation of photoreceptor outer segments, which cannot be phagocytosed due to a lack of apposition of the outer photoreceptor tips and the apical surface of the RPE. The yellowish vitelliform lesion was also seen on fundoscopy (B). Fundus autofluorescence (FAF; C) imaging shows the hyperautofluorescent lesion, as lipofuscin and/or its precursors molecules accumulate under the macula. Fluorescein angiography (FA; D) revealed mainly hypofluorescence due to blockage by the vitelliform material, with some late staining of the vitelliform subretinal space. In contrast to central serous chorioretinopathy, there is no focal leakage, because there is no focal defect in the outer blood-retinal barrier of the RPE.
(**E-H**) Multimodal imaging of the left eye of a 43-year-old male patient with **acute exudative polymorphous vitelliform maculopathy.**
On the foveal OCT scan (E), a hyperreflective accumulation (white arrow; presumably accumulated photoreceptor outer segments) under the retina was seen, together with subretinal fluid. FAF (F) showed multifocal hyperautofluorescent abnormalities: a large area inferior in the macula - possibly subretinal material that gravitated inferiorly in the subretinal space – as well as some lesions superonasally to the optic disc. FA (G) revealed no marked abnormalities except some inferior blockage of the background fluorescence by the subretinal material, whereas indocyanine green angiography (ICGA) showed only very mild hyperfluorescent changes in the fovea.
(**I–K**) Multimodal imaging of the left eye of a 47-year-old male patient with **adult-onset foveomacular vitelliform dystrophy** without a family history of macular disease.
OCT (I) revealed a small hyperreflective lesion bilaterally under the fovea. Fundoscopy (J) and red-free fundus photography (K) showed a small vitelliform lesion in the fovea. No mutations were found in the known macular dystrophy genes.
(**L-N**) Multimodal imaging of the right eye of a 84-year-old female patient with a **vitelliform lesion secondary to age-related macular degeneration with reticular pseudodrusen** (subretinal drusenoid deposits).
A hyperreflective vitelliform lesion was seen on OCT (L), together with a shallow RPE detachment and some retinal pseudodrusen. Fundus photography (M) showed the yellow-white vitelliform lesion, surrounded by some whitish reticular pseudodrusen, that are better visible as hyporeflective spots on the infrared reflectance image in L. FA (N) showed some staining of the vitelliform lesion, without focal leakage or evidence of neovascularisation.
(**O-Q**) Multimodal imaging of the left eye of a 70-year-old male patient with a **vitelliform lesion secondary to age-related macular degeneration with a mixture of cuticular drusen** (below the RPE; white arrow) **and reticular pseudodrusen** (subretinal drusenoid deposits, above the RPE; black arrow).
The OCT scan (O) showed a subretinal hyperreflective accumulation under the fovea, between the neuroretina and the RPE, with an irregular RPE layer beneath it. Fundus photography (P) showed a vitelliform lesion with surrounding smaller and larger drusen. On late-phase FA (Q) the vitelliform lesion showed hyperfluorescent staining without focal leakage, some hypofluorescent blockage of its edges (white arrow) by either dense subretinal material or RPE hypertrophy that corresponded to hyperreflective areas on infrared reflectance (arrowhead in O), surrounded by hyperfluorescent small cuticular drusen.
(**R-T**) Multimodal imaging of the left eye of a 90-year-old male patient with a **vitelliform lesion in the context of vitreofoveal traction.**
The OCT scan (R) showed vitreofoveal traction, with a secondary foveal vitelliform lesion that shows irregular (mostly hyper)reflectivity between the RPE (white arrow) and what was left of the ellipsoid zone of the photoreceptors (black arrow). The fundus photograph (S) showed a subtle, small vitelliform lesion in the fovea (white arrow), together with some microaneurysms in this diabetic patient. This small vitelliform lesion did not correspond to any abnormalities on FA (T), which only highlighted some microaneurysms.

the age of 60(Daruich et al., 2015; de Jong, 2006). In addition, unlike CSC most cases of AMD present with drusen in the fellow eye, with no focal 'hot spots' of leakage visible on FA and no multifocal 'ink blot' hyperfluorescent choroidal areas on ICGA(Daruich et al., 2015; de Jong, 2006; Lima et al., 2012). Finally, patients who present with a relatively large RPE detachment due to confluent soft drusen have a markedly increased risk of developing geographic atrophy and/or CNV within a few years(Balaratnasingam et al., 2016b, 2017).

6.4.2. *Pathogenesis*

Impaired phagocytosis of photoreceptor outer segments by diseased RPE leads to vitelliform lesions secondary to AMD (Arnold et al., 2003), and several mechanisms have been suggested to play a role in this process. First, an accumulation of a combination of sub-RPE drusenoid debris has been found to impair several RPE functions, including its phagocytotic activity and pump function, thus resulting in SRF leakage (Anderson et al., 2010; Bergen et al., 2019; Curcio, 2018; Grisanti and Tatar, 2008; Guymer et al., 1999; Nozaki et al., 2006). Second, an increase in lipofuscin in the RPE can impair RPE function, for example reducing phagocytosis(Sundelin et al., 1998). Finally – and independent of the presence of lipofuscin – RPE cells can lose their polarity with ageing, with a subsequent decrease in cellular function(Lima et al., 2012).

6.5. *Vitelliform lesions in the context of other diseases*

Vitelliform lesions have also been described in the context of other diseases (Chowers et al., 2015), including CSC(Spaide, 2004). Vitelliform material can accumulate in patients in whom the photoreceptors are mechanically separated from the RPE, for example in patients with an epiretinal membrane (Querques and delle Noci, 2007), vitreomacular traction (Fig. 3R–T) (Spaide, 2008), and persistent SRF following retinal reattachment surgery(Rashaed, 2013). These clinical pictures can be distinguished based on the patient's medical history and OCT imaging (Spaide, 2008). Macular vitelliform lesions have also been described in several systemic conditions, including pseudoxanthoma elasticum (Freund et al., 2011), mitochondrial retinal dystrophy (de Laat et al., 2013), as well as with several toxic conditions (see Chapter 13). (Urner-Bloch et al., 2014).

Altered RPE function also plays an essential role in vitelliform lesions in the context of the aforementioned systemic conditions(Chowers et al., 2015). For example, the number of RPE cells and pigment granules in the remaining RPE cells are decreased in pseudoxanthoma elasticum (Audo et al., 2007; Freund et al., 2011; Hansen et al., 2014). In toxic conditions such as mitogen-activated protein kinase kinase (MEK) inhibitor-associated retinopathy (MEKAR), impaired RPE pump function has been suggested to underlie both the accumulation of SRF and the occurrence of vitelliform lesions(van Dijk et al., 2015).

7. Inflammatory diseases

A range of inflammatory diseases is included in the differential diagnosis of CSC, as these diseases can cause SRF leakage, for example due to choroiditis and increased RPE permeability. In the paragraphs below we have included the most important diseases. However, sympathetic ophthalmia, Bartonella neuroretinitis, Lyme disease, and syphilis may also present with SRF or a SRF-like appearance(Habot-Wilner et al., 2011; Subudhi et al., 2017; Yoo et al., 2009). Some of the inflammatory diseases can also be complicated by CNV.

7.1. Vogt-Koyanagi-Harada disease

7.1.1. Clinical characteristics

Vogt-Koyanagi-Harada disease is a severe bilateral granulomatous panuveitis that typically affects younger individuals (20–50 years old). In Vogt-Koyanagi-Harada disease, T cells target melanocytes in various ocular tissues, leading to vitritis, optic disc oedema, and serous retinal detachments. Four clinical stages of the disease can be discerned, namely the prodromal, acute uveitic, convalescent, and chronic recurrent stages, and many patients present with extraocular manifestations, including pleiocytosis (an abnormally high number of lymphocytes in the cerebrospinal fluid), poliosis (an absence of melanin in the hair), vitiligo, alopecia, and dysacusis(O'Keefe and Rao, 2017; Read et al., 2000; Shin et al., 2015). When only ocular signs are present, the condition is called Harada disease. According to criteria established by the American Uveitis Society, a diagnosis of Vogt-Koyanagi-Harada disease requires 1 or more findings from at least 3 of the following 4 groups of symptoms: 1) bilateral chronic iridocyclitis, 2) posterior uveitis, 3) neurological symptoms, and 4) cutaneous abnormalities(Read and Rao, 2000). However, recent studies suggest that the 'eye-only' presentation of Vogt-Koyanagi-Harada disease may actually be much more common than the syndromic presentation of Vogt-Koyanagi-Harada(Du et al., 2016).

Acute Vogt-Koyanagi-Harada disease and CSC have a certain degree of clinical overlap, as exudative retinal detachments can occur together with choroidal thickening – clearly visible on OCT – in the acute phase. However, several features are important for distinguishing between these 2 diseases. For example, in 95% of Vogt-Koyanagi-Harada cases the fellow eye is affected within 2 weeks after the onset of disease. In addition, vitritis, optic disc oedema, and serous retinal detachments are common features of Vogt-Koyanagi-Harada but are extremely rare in CSC. On early FA, the irregular fluorescence combined with multiple pinpoint regions of leakage at the RPE level and the blurred margins of the optic disc in a patient with Vogt-Koyanagi-Harada disease differ markedly from the single – or few – focal 'hot spots' of leakage that are typically present in CSC (Figs. 1H and 4C–D). Moreover, ICGA typically shows early hyperfluorescence together with early-to-mid-phase hypofluorescence in patients with Vogt-Koyanagi-Harada disease, which is in contrast to the increased choroidal permeability combined with localised or – in some cases, multifocal – hyperfluorescent 'ink blot' leakage visible on mid-to late-phase ICGA in CSC cases (Fig. 4A–G). In the advanced stage of Vogt-Koyanagi-Harada disease, choroidal thinning occurs, and patches of yellow discolouration may be visible on fundoscopy, a finding that differs from CSC(Sahoo et al., 2019).

Vogt-Koyanagi-Harada disease is treated using an initial high dose of corticosteroids, after which the dosage can be reduced gradually over several months. In contrast, this treatment is contraindicated in CSC, as steroid treatment generally leads to a worsening of the clinical picture (O'Keefe and Rao, 2017; Read et al., 2000; Shin et al., 2015). Over the long term, steroid-sparing immunomodulatory drugs are used to manage patients with Vogt-Koyanagi-Harada disease in order to minimise the occurrence of complications such as cataract, glaucoma, subretinal fibrosis, and CNV(O'Keefe and Rao, 2017).

7.1.2. Pathogenesis

Vogt-Koyanagi-Harada disease has been suggested to arise from an auto-immune process driven by T cells that react against an as-yet unidentified antigen associated with melanocytes(Moorthy et al., 1995; Read and Rao, 2000). Cutaneous injury and viral infection may play a role in triggering the disease in some patients, causing a sensitisation to the antigen. Moreover, genetic factors may also play a role in increasing the susceptibility to develop the disease(O'Keefe and Rao, 2017; Rathinam et al., 1999). The detachment of the neurosensory retina in patients with Vogt-Koyanagi-Harada disease is believed to be caused by an exudative process, as the fluid in the subretinal space is typically proteinaceous(O'Keefe and Rao, 2017; Read and Rao, 2000). Finally, in the acute phase of the disease choroidal thickening can occur in areas of inflammation, causing RPE damage and hyperpermeability, resulting in an accumulation of SRF(O'Keefe and Rao, 2017; Read and Rao, 2000).

7.2. White dot syndromes

7.2.1. Clinical characteristics

The white dot syndromes encompass a group of multifocal inflammatory conditions characterised by numerous yellow or white dots of unknown origin involving the retina and the choroid. This group of syndromes includes acute posterior multifocal placoid pigment epitheliopathy, acute zonal occult outer retinopathy, birdshot chorioretinopathy, multiple evanescent white dot syndrome, multifocal choroiditis (Fig. 4H–N), punctate inner choroidopathy, and serpiginous choroiditis. Most of the white dot syndromes are more common in women than in men and typically present under the age of 50. The occurrence of a serous retinal detachment has been described in patients with punctate inner choroidopathy, acute posterior multifocal placoid pigment epitheliopathy, and multiple evanescent white dot syndrome (Amer et al., 2015; Birnbaum et al., 2010; Chao et al., 2015), thus showing a certain degree of clinical overlap with CSC(Sahoo et al., 2019). Similar to CSC, several white dot syndromes can be complicated by CNV, thus requiring intravitreal anti-VEGF therapy(Birnbaum et al., 2010; Chao et al., 2015; Watzke et al., 1984).

The clinical distinction between white dot syndromes and CSC is usually straightforward. In white dot syndromes, typical yellow-whitish lesions involving the retina and the choroid are present in the posterior pole. In addition, hypo-autofluorescent changes are visible on FAF, and FA shows early hypofluorescence and late hyperfluorescence(Birnbaum et al., 2010; Chao et al., 2015; Watzke et al., 1984). On ICGA, late hypofluorescent lesions can be seen and are typically more widespread compared to the white dots visible on fundoscopy, reflecting the underlying inflammation of the choriocapillaris and choroid; these hypofluorescent areas are in contrast to the hyperfluorescent abnormalities present in CSC(Obana et al., 1996).

Unlike CSC, some of the white dot syndromes can be treated using local and/or systemic corticosteroids, followed by corticosteroid-sparing immunosuppressive therapy(Birnbaum et al., 2010; Chao et al., 2015; Obana et al., 1996; Watzke et al., 1984).

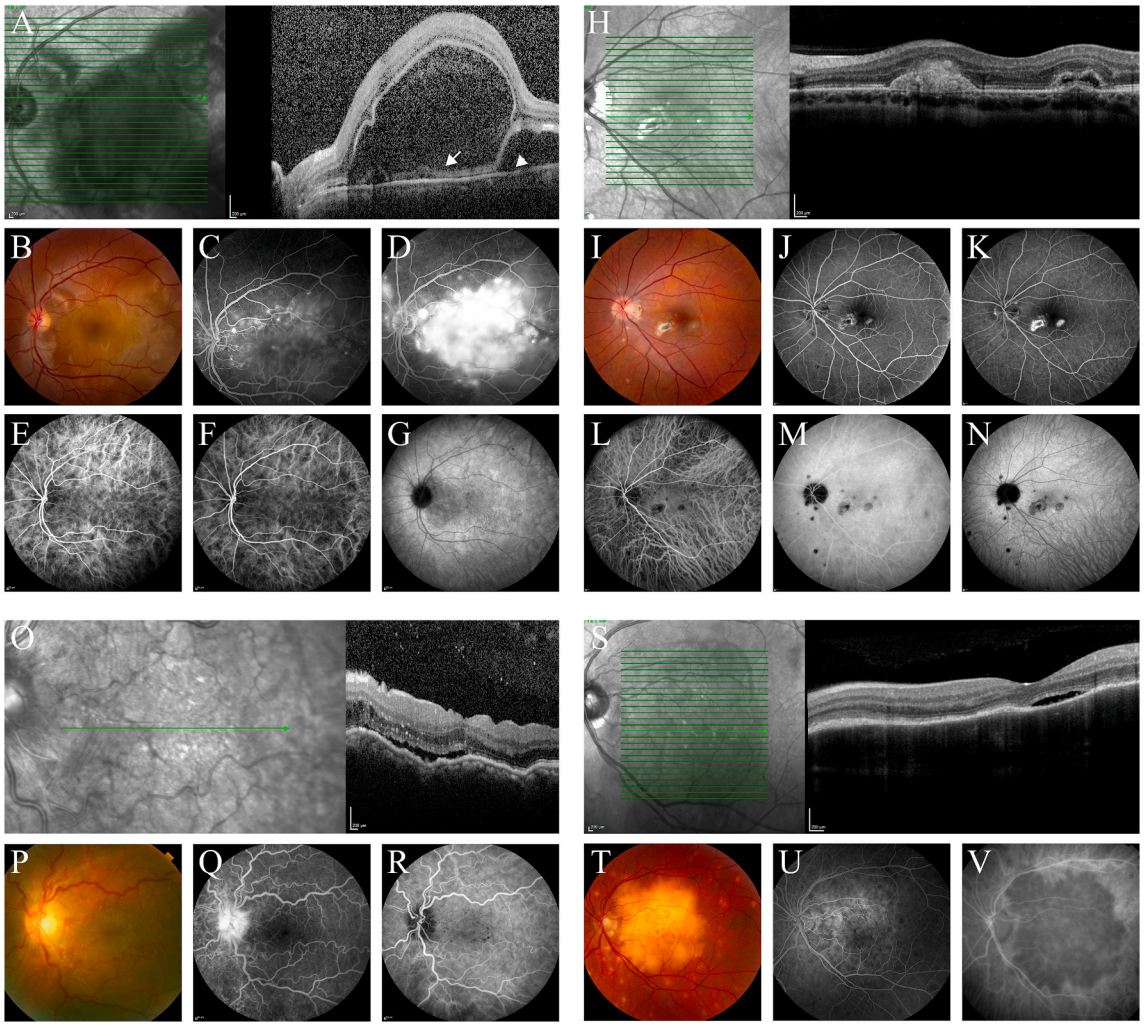
7.2.2. Pathogenesis

The origin of the white dot syndromes is unclear; however, several environmental and genetic factors are believed to play a role(Kuiper et al., 2015; Verhagen et al., 2018). Given the female preponderance of this group of diseases, an auto-immune predisposition is suspected and is supported by genetic studies involving immune-related loci(Márquez et al., 2017). In white dot syndromes without CNV, the main cause of serous SRF leakage is likely hyperpermeability and inflammation of the choroid and RPE(Birnbaum et al., 2010; Chao et al., 2015; Obana et al., 1996; Watzke et al., 1984).

7.3. Posterior scleritis

7.3.1. Clinical characteristics

Posterior scleritis is most prevalent among middle-aged women and can be either idiopathic or associated with an inflammatory or auto-immune disease such as rheumatoid arthritis, systemic lupus erythematosus, or Crohn's disease. Patients with posterior scleritis typically present with moderate to severe pain behind the eye, particularly when moving the eye. Moreover, patients can also present with proptosis and/or other signs of orbital disease. Several abnormalities can appear on fundoscopy, including choroidal folds, serous retinal detachment, and optic disc oedema. In addition to the presence of a neurosensory detachment, several features are often present in both CSC and posterior scleritis, including increased choroidal thickness on OCT and multiple pinpoint leakage foci on FA (Fig. 4O–R). In contrast, hyperaemia of the



(caption on next page)

Fig. 4. An overview of inflammatory diseases that are part of the differential diagnosis of central serous chorioretinopathy.
(**A-G**) Multimodal imaging of the left eye of a 25-year-old female patient of Middle Eastern origin, with rapid bilateral central vision loss within 5 days due to **Vogt-Koyanagi-Harada disease.**
At presentation, the optical coherence tomography (OCT) scan (A) showed both intraretinal and subretinal fluid (SRF) in both eyes. Note that the largest fluid collection is within the outer neuroretina, not below it, because its outer layer consists of an ellipsoid-like hyperreflective line (white arrow), not the underlying retinal pigment epithelium (RPE; white arrowhead). The visual acuity in this eye was 20/200 at presentation. The fundus photograph of the left eye (B) showed an extensive yellowish central serous retinal detachment with several adjacent satellite lesions. No cells in the anterior chamber and the vitreous were seen. Fundoscopy of the right eye showed similar findings. Early- (C) and mid-phase fluorescein angiography (FA; D) showed extensive hyperfluorescence from multiple pinpoints of profuse leakage at the RPE level. Indocyanine green angiography (ICGA) had not been performed at the first visit. However, when the extent of the ophthalmological abnormalities had decreased after treatment with high-dose steroids, early-, mid, and late-phase ICGA (E–G) still showed hypofluorescent abnormalities that are compatible with Vogt-Koyanagi-Harada disease. The visual acuity in this eye was 20/20, at that visit.
(**H–N**) Multimodal imaging of the left eye of a 22-year-old female patient with **multifocal choroiditis.**
OCT (H) showed a relatively shallow, irregular SRF accumulation temporally to the fovea, together with a shallow RPE detachment. Nasally to the fovea, a hyperreflective lesion was present, that involved the RPE and disrupted the normal outer retinal architecture. Both lesions were compatible with macular neovascularisation: the temporal lesion being a new, active neovascular lesion, while the nasal lesion was compatible with a fibrotic neovascularisation, with possibly some persistent neovascular activity in the irregular central part of the lesion. Colour fundus photography (I) showed several small round yellow to white dots in the posterior pole, together with a larger whitish fibrotic subretinal lesion inferonasally to the fovea, and a yellow-greenish subretinal lesion inferotemporally to the fovea corresponding to the active neovascular lesion in H. The latter 2 lesions were hyperfluorescent on FA (J–K), with leakage in the mid-phase (K). On early-, mid-, and late-phase ICGA (L–N), the small yellow-white dots on fundoscopy were visible as hypofluorescent areas, representing the underlying choroidal inflammation, together with the 2 larger, mostly hypofluorescent neovascular lesions. The visual acuity in this eye was 20/20.
(**O-R**) Multimodal imaging of the left eye of a 47-year-old male patient with **posterior scleritis** [Courtesy of Joeri de Hoog, MD].
This patient initially complained of pain in both eyes, which was already present for a year at the moment of ophthalmological imaging. Multimodal imaging revealed a similar clinical picture in both eyes, with only a few cells in both the anterior chamber and the vitreous. The visual acuity at the time of presentation was 16/20 in the left eye. OCT (O) showed the irregular surface of a thickened choroid, together with shallow SRF, some intraretinal fluid and hyperreflective dots in the outer retinal layers. Fundoscopy (P) also showed the choroidal folds and serous retinal detachment, as well as some indistinct peripapillary fluid accumulation. On mid-phase FA (Q), leakage of the optic disc was observed, together with subtle diffuse hyperfluorescent RPE changes nasally to the optic disc, but without focal leakage and atrophic RPE changes that would have been typical of central serous chorioretinopathy. Mid-phase ICGA (R) showed only subtle hyperfluorescent and hypofluorescent changes.
(**S–V**) Multimodal imaging of the left eye of a 52-year-old male patient with **sarcoidosis**.
He only had mild visual complaints of blurred vision that had been present for almost a year, and his visual acuity was 20/22. Although he was known with previous pulmonary sarcoidosis, this disease had been quiescent for years, and immunosuppressive medication had been discontinued for already 8 years.
On the foveal OCT scan (S) of this patient, SRF was seen. A large, prominent white-yellow lesion was seen centrally on fundoscopy (T), with some secondary RPE changes. The lesion was surrounded by several satellite lesions. There were no cells in either the anterior chamber or vitreous. Early-phase FA (U) and mid-phase ICGA (V) showed mainly hypofluorescent changes, without focal leakage, compatible with blockage of fluorescence by a granuloma in the context of sarcoidosis. In the other eye, no abnormalities were present.

conjunctiva and painful eye movements can occur in posterior scleritis, but do not occur in CSC. Moreover, CSC presents with a diffusely thickened choroid, and posterior scleritis with a localised thickening of the sclerochoroidal area. Finally, B-scan ultrasonography often reveals fluid in the sub-Tenon's space around the optic disc (the so-called 'T-sign') in posterior scleritis(Agrawal et al., 2016; McCluskey et al., 1999; Sahoo et al., 2019).

Systemic corticosteroids are generally prescribed to patients with posterior scleritis. In some patients, this treatment can be either supplemented with or replaced by steroid-sparing immunomodulatory drugs(Agrawal et al., 2016; McCluskey et al., 1999).

7.3.2. Pathogenesis

Posterior scleritis is an immune-mediated process in which inflammation posterior to the extraocular muscles leads to circumscribed thickening of the sclerochoroidal area; an overlying serous retinal detachment is often present as well. In addition, inflammatory cells such as T cells and macrophages increase and attempt to infiltrate the deep episcleral tissue. However, the precise mechanism that leads to SRF accumulation is unknown(McCluskey et al., 1999).

7.4. Sarcoidosis

7.4.1. Clinical characteristics

Sarcoidosis is a multisystem disorder of unknown origin in which granulomas develop in various organs and tissues, particularly the lungs and the lymphatic system. The most common presenting symptoms in sarcoidosis are dry cough, weight loss, fatigue, eye and/or skin manifestations, fever, and night sweats(Nunes et al., 2007). Ocular involvement has been reported in up to 50% of patients with some stage of sarcoidosis, affecting virtually any part of the eye. Nodular granulomas in the conjunctiva and anterior, intermediate, and posterior uveitis with choroidal granulomas (Fig. 4S–V) are commonly – albeit variably – present(Nunes et al., 2007). A serous retinal detachment is rarely a presenting symptom in ocular sarcoidosis, but can be associated with an underlying granulomatous lesion in the choroid (Fig. 4T) (Watts et al., 2000). Unlike CSC, sarcoidosis is more common in women and generally presents with signs of ocular inflammation. In sarcoidosis, vasculitis can be seen on FA together with an absence of hyperfluorescent leakage on ICGA (Fig. 4S–V) (Nunes et al., 2007; Watts et al., 2000).

7.4.2. Pathogenesis

Although the aetiology of sarcoidosis is currently unknown, several factors have been proposed to play a role, particularly auto-immunity and genetics(Iannuzzi et al., 2007; Valeyre et al., 2014). Retinal detachments in sarcoidosis may arise from exudate and occur most often in patients with large nodular chorioretinal granulomas(Nunes et al., 2007; Watts et al., 2000). In patients with this type of granuloma, detachment of the neurosensory retina can be the result of increased fluid leakage via a dysfunctional RPE due to increased metabolic activity in response to the underlying choroidal granuloma(Nunes et al., 2007; Watts et al., 2000).

7.5. Unilateral acute idiopathic maculopathy

7.5.1. Clinical characteristics

Unilateral acute idiopathic maculopathy was first described by Yannuzzi and colleagues in 1991(Yannuzzi et al., 1991). This macular disease often occurs in young adults, inducing a sudden and severe loss of vision due to outer photoreceptor abnormalities, with swelling of the outer retina, including an elevated and disrupted ellipsoid zone that can resemble macular SRF accumulation. Patients commonly report having a flu-like illness that precedes their ocular complaints. The retinal changes in unilateral acute idiopathic maculopathy can mimic the SRF

accumulation observed in CSC; moreover, these changes often resolve rapidly and spontaneously, which is also similar to CSC. However, in contrast to CSC unilateral acute idiopathic maculopathy does not have leakage on FA, and ICGA does not show the hyperfluorescent abnormalities that are typical of CSC (Fig. 5A–E).(Freund et al., 1996) The recommended approach for unilateral acute idiopathic maculopathy is conservative treatment(Beck et al., 2004; Freund et al., 1996; Hughes et al., 2012; Yannuzzi et al., 1991).

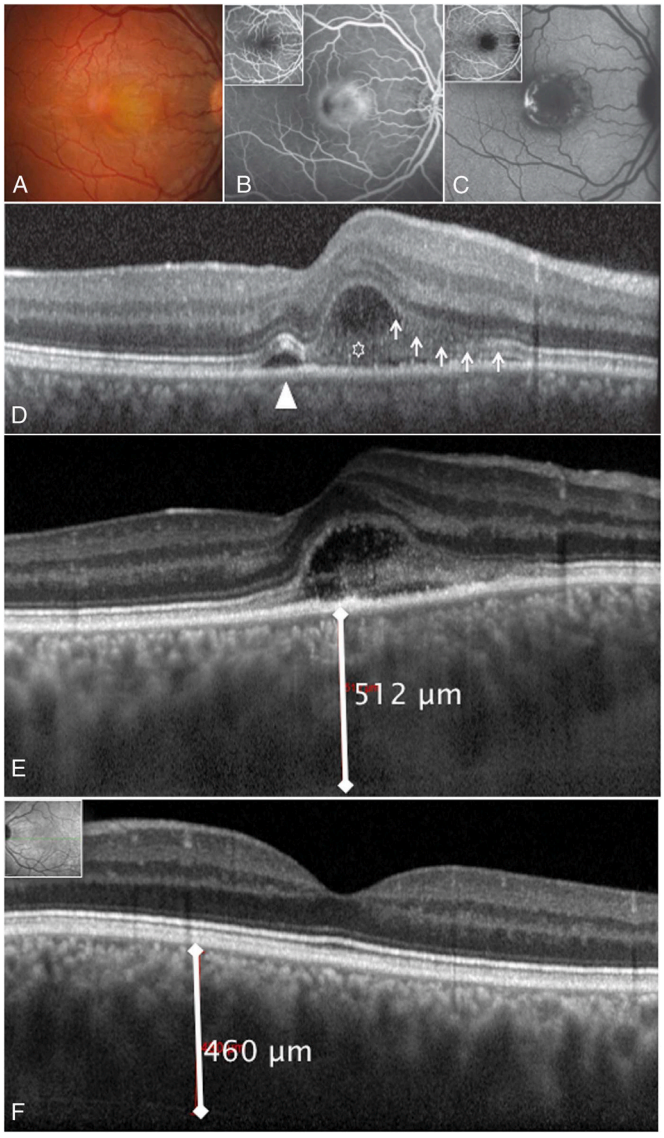


Fig. 5. Multimodal imaging of a 30-year-old male patient with **unilateral acute idiopathic maculopathy** (UAIM) [Courtesy of Mayer Srour, MD].
The patient had previous flu-like symptoms and elevated coxsackievirus A16 antibody titers. Fundus colour photograph (A) showed, during the acute phase of UAIM, a yellow-white lesion at the macula of the right eye. Early-to-late-phase fluorescein angiography (B) revealed late hyperfluorescence (staining and pooling) from the macular lesion. Early-to-late-phase indocyanine green angiography (C) showed a persistent hypofluorescent lesion in the macular area surrounded by a hyperfluorescent halo. Spectral-domain optical coherence tomography (D–E) showed the swelling of the outer retina with the inner segment/outer segment junction that appears elevated and disrupted (small arrows, and arrowhead). Spectral-domain optical coherence tomography also revealed hyperreflective exudation and a pocket of hyporeflective fluid in the subretinal space (D-E; asterisk in D). Enhanced-depth imaging optical coherence tomography revealed a subfoveal thickened choroid (E) compared with fellow eye (F) (512 µm versus 460 µm).

7.5.2. Pathogenesis

Unilateral acute idiopathic maculopathy may be caused by an inflammatory process that predominantly affects the outer retina and the RPE. The coxsackievirus, which causes hand, foot, and mouth disease in children and has been linked to unilateral acute idiopathic maculopathy by several groups, possibly causes inflammatory swelling of the outer retina and an elevated and disrupted ellipsoid zone (Beck et al., 2004; Demirel et al., 2014; Hughes et al., 2012; Srour et al., 2013) either by direct viral infection or by a reactive phenomenon(Hughes et al., 2012).

8. Ocular tumours

8.1. Choroidal naevus and melanoma

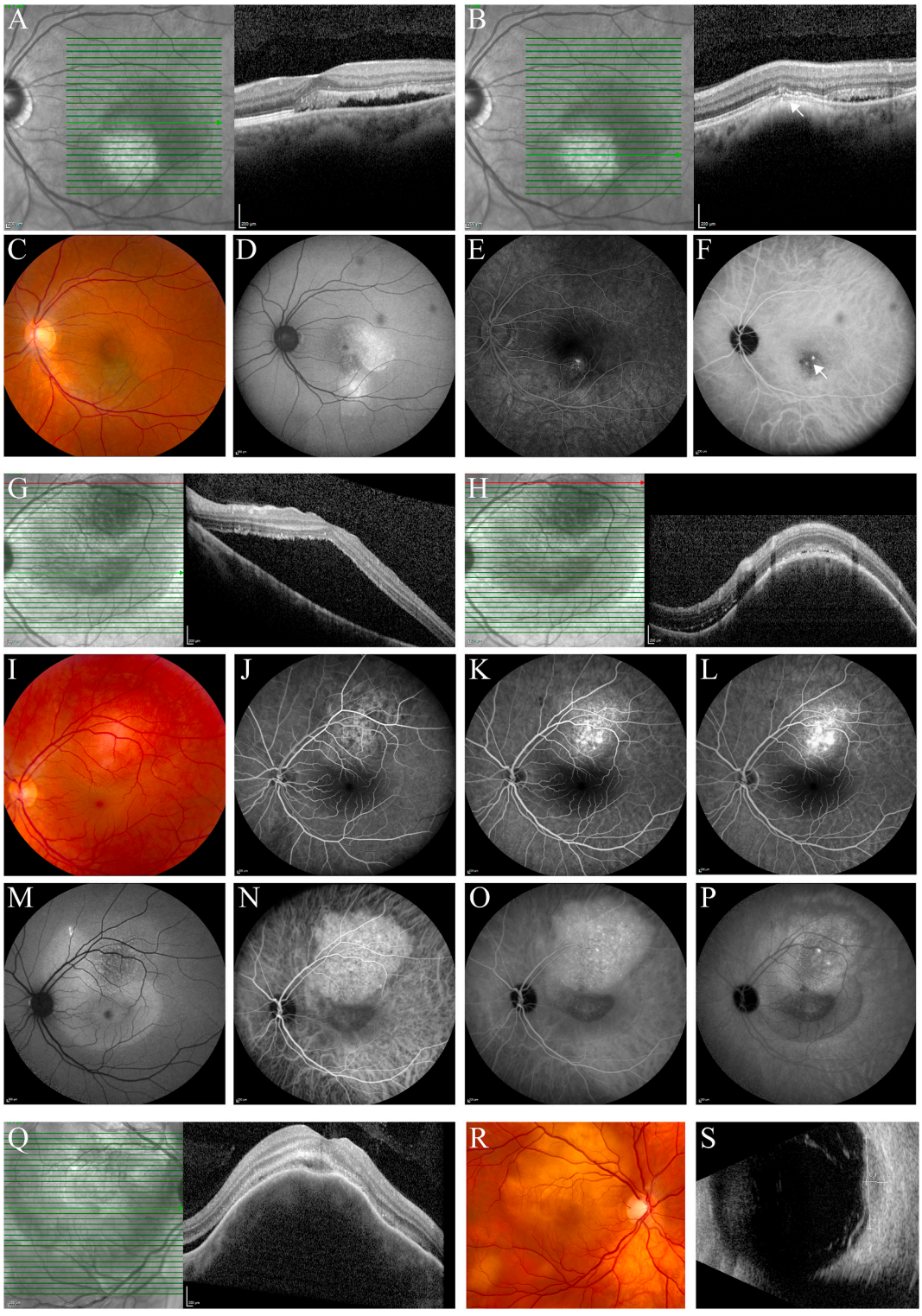
8.1.1. Clinical characteristics

Uveal melanoma is the most common primary intraocular tumour in adults, occurring in the iris (4% of cases), ciliary body (6% of cases), or choroid (90% of cases). A brown, dome-shaped choroidal mass is the most typical presentation of both a choroidal naevus (Fig. 6A–F) and a choroidal melanoma, although the degree of pigmentation can vary. Distinguishing between a choroidal naevus and a melanoma can be challenging, and the lesion can be either partially or completely amelanotic. Several clinical findings can increase the likelihood of a melanoma diagnosis, including SRF in the region of the lesion, visual complaints, orange pigment on the tumour surface, and tumour thickness >2 mm(Shields et al., 2019). Both choroidal naevi and choroidal melanomas have low internal reflectivity on B-scan ultrasonography. Although a choroidal melanoma and CSC can have overlapping clinical features such as the presence of RPE alterations and/or SRF due to a serous retinal detachment, findings on fundoscopy and multimodal imaging can be used to differentiate between these 2 disease entities. Distinguishing between a choroidal naevus or melanoma and CSC can be challenging in cases with a relatively flat tumour that presents without prominent hypopigmentation or hyperpigmentation. Although a bullous inferior retinal detachment can be present in melanoma, a bullous retinal detachment has also been reported in severe, profusely leaking cases of chronic CSC(Balaratnasingam et al., 2016a). On enhanced-depth imaging OCT, several findings can be present in both CSC and choroidal melanoma, including RPE atrophy, IRF, loss of the external limiting membrane, and loss of the ellipsoid zone (Shields et al., 2014); however, choroidal melanoma presents as a dome-shaped choroidal lesion with a smooth surface on enhanced-depth imaging OCT. With the accompanying SRF accumulation, 'shaggy' photoreceptors – representing either swollen photoreceptors or lipofuscin-containing macrophages – can be detected(Shields et al., 2014). With choroidal melanoma, multiple areas of pinpoint leakage at the tumour surface are typical on FA, which is in contrast to the focal 'hot spots' of leakage in the posterior pole in CSC(Higgins et al., 2016). A mixed pattern of fluorescence on ICGA can be found in choroidal melanoma, which differs from the typical 'ink blot' pattern of hyperfluorescence with a relatively indistinct border in CSC(Shields et al., 1995). Finally, the macular elevation in CSC is non-echogenic, in contrast to the low internal reflectivity on B-scan ultrasonography in both choroidal naevus and choroidal melanoma(Doro et al., 2005).

Early diagnosis is essential with choroidal melanoma, as treating a smaller tumour is generally associated with improved long-term outcome and survival(Singh et al., 2011).

8.1.2. Pathogenesis

Choroidal naevi often occur as benign tumours originating from uveal melanocytes. In patients with a choroidal naevus, a serous detachment of the RPE – or even the neurosensory retina – occurs only in cases with relatively high metabolic activity and secondary degenerative RPE changes(Pro et al., 1978). Patients with a choroidal melanoma often have leakage of SRF in the context of an inferior serous retinal detachment that can affect the macula; in these patients, the



(caption on next page)

Fig. 6. An overview of ocular tumours that are part of the differential diagnosis of central serous chorioretinopathy.
(**A-F**) Multimodal imaging of the left eye of a 48-year-old female patient with a **choroidal naevus.** On the foveal optical coherence tomography (OCT) scan (A), an accumulation of subretinal fluid (SRF) and hyperreflective subretinal material was seen. The OCT scan from the region inferiorly to the fovea (B) showed an elevated solid hyperreflective lesion in the choroid. In addition, a flat irregular detachment of the retinal pigment epithelium was present (white arrow), with some mid-reflective – possibly neovascular – material beneath it. Fundus photograph (C) showed a pigmented choroidal naevus, that was mildly elevated, with the presence of some orange pigment and without drusen. Fundus autofluorescence (FAF) imaging (D) showed mainly hyperautofluorescent abnormalities. Fluorescein angiography (FA; E) showed focal leakage, while mid-phase indocyanine green angiography (ICGA; F) showed focal hyperfluorescence in combination with a well-demarcated zone of potential neovascularisation (white arrow). Half-dose photodynamic therapy in combination with 3 intravitreal injections with the anti-vascular endothelial growth factor receptor medication bevacizumab led to complete resolution of SRF on OCT.
(G-P) Multimodal imaging of the left eye of a 36-year-old male patient with a **circumscribed cavernous choroidal haemangioma.**
The foveal OCT scan (G) in this patient showed a large central serous retinal detachment. The OCT scan that was obtained in the area superiorly in the macula (H) showed that this SRF originated from an elevated choroidal lesion with mixed reflectivity characteristics, compatible with the vascular nature of the tumour. On the fundus photograph (I), an elevated pinkish lesion could be appreciated superiorly in the macula. Characteristic mild irregular hyperfluorescence of RPE and underlying choroidal vessels was seen in the early-phase FA (J), which increased and became more confluent with increasing accumulation of dye in the later phases (K–L). FAF (M) showed mainly irregular hyperfluorescent abnormalities that were atypical and can be seen in many diseases associated with prolonged SRF accumulation. On ICGA, characteristic early (N) hyperfluorescence (filling of the tumour vessels) was observed, with a 'wash out phenomenon' of the dye during the late phase (O–P). (**Q-S**) Multimodal imaging of the right eye of a 46-year-old female patient with **choroidal metastases of breast carcinoma.**
The foveal OCT scan (Q) in this patient revealed an elevated lesion, that had its origin in the choroid, together with adjacent SRF. Fundoscopy (R) showed several amelanotic elevated lesions, which were surrounded by SRF. On ultrasonography (S), mid-reflective choroidal lesions were seen, which were compatible with choroidal metastases, together with a serous retinal detachment.

outer blood-retinal barrier is chronically damaged, with subsequent accumulation of IRF and SRF due to the tumour's increased metabolic activity(Shields et al., 2019).

8.2. Choroidal metastases

8.2.1. Clinical characteristics

Because of its abundant vascular supply, the choroid is the most common site for the occurrence of ocular metastases. Choroidal metastases are usually yellow in colour, can be multifocal and/or bilateral on fundoscopy, and often present with SRF, making this condition a differential diagnosis of CSC.

To aid in diagnosis, the primary tumour is usually already known in most patients at the onset of ocular complaints associated with choroidal metastases. Breast cancer and lung cancer are the most commonly diagnosed malignancies that induce choroidal metastases.

The findings on OCT differ markedly between choroidal metastases and CSC. For example, irregular hyperreflective spots in the photoreceptor layer and RPE are characteristic of choroidal metastases. Moreover, a slightly irregular ('lumpy, bumpy') tumour surface can be appreciated using enhanced-depth imaging OCT, together with anterior choriocapillaris compression and posterior shadowing(Al-Dahmash et al., 2014; Shields et al., 2014). FA usually shows hypofluorescence in the early phase and late leakage, which differs from the early hyperfluorescent changes typically seen in CSC. With choroidal metastases, blockage of choroidal fluorescence at the location of the tumour is generally visible on ICGA (Fig. 6Q–S).(Arepalli et al., 2015; Shields et al., 1997b; van Rijssen et al., 2019b).

Different treatment options depend on the number, location, and laterality of the metastatic tumour, as well the systemic status. Observation may be the method of choice for patients with poor systemic status and prognosis. For other patients, multifocal and bilateral tumours can be treated with systemic chemotherapy, immunotherapy, hormone therapy, and/or whole-eye irradiation. For solitary choroidal metastases, either plaque radiotherapy or transpupillary thermotherapy can be considered(Arepalli et al., 2015; Shields et al., 1997a, 1997b).

8.2.2. Pathogenesis

Uveal metastases of primary tumours occur most commonly in the choroid, as this tissue receives the highest flow of tumour emboli due to its abundant blood supply from the posterior ciliary arteries(Shields et al., 1997b). Retinal detachments in patients with choroidal metastases are usually exudative due to the tumour's high metabolic activity, and the detachment can be relatively large compared to the size of the metastases(Stephens and Shields, 1979).

8.3. Circumscribed cavernous choroidal haemangioma

8.3.1. Clinical characteristics

A circumscribed cavernous choroidal haemangioma is a benign vascular hamartoma and is virtually always solitary and unilateral. On fundoscopy, a haemangioma is visible as an orange-red round or oval choroidal prominence (Fig. 6I). Distinguishing between a choroidal haemangioma and CSC can be challenging, as the tumour is often located in the posterior pole, with increased choroidal thickness and signs of vascularity on OCT, RPE alterations, a serous retinal detachment, and IRF (Fig. 6G and H) (Rahman et al., 2013)

Importantly, a circumscribed cavernous choroidal haemangioma typically presents with a characteristic 'honeycomb'-like multilobular pattern, with hyporeflective oval zones corresponding to the lumen of the vascular spaces in the tumour, together with hyperreflective areas representing the vessel walls and connective tissue on OCT(Flores-Moreno et al., 2016). A focal 'hot spot' of leakage on FA is usually not present in a choroidal haemangioma; in contrast, FA typically shows mild diffuse hyperfluorescence in the early phase, with increasing diffuse leakage throughout the later phases (Fig. 6J and K). Moreover, and in contrast to CSC, ICGA shows early hyperfluorescent filling of the tumour vessels, with a 'wash out phenomenon' during the late phases (Fig. 6M–P)(Daruich et al., 2015; Shields et al., 2001). A choroidal haemangioma has high internal reflectivity on B-scan ultrasonography, in contrast to the acoustic hollowness seen in choroidal melanoma (Shields et al., 2001).

A circumscribed cavernous choroidal haemangioma can often be treated effectively with PDT according to the standard protocol with full settings (Boixadera et al., 2009; van Dijk et al., 2020b); however, effective results have been observed when giving the verteporfin as a bolus over a 1-min period (instead of the standard 10 min) and starting treatment 5–6 min after infusion (instead of the standard 15 min)(Verbraak et al., 2003, 2006). At the 5-year follow-up, an increase of $\geq$2 lines in best-corrected visual acuity in Early Treatment of Diabetic Retinopathy Study letters has been reported in 76% of patients, and complete resolution of macular SRF was reported in up to 100% of patients with a choroidal haemangioma treated using the standard PDT protocol(Blasi et al., 2010; Ho et al., 2018; van Dijk et al., 2020b). Moreover, no difference in outcome has been reported between the standard infusion and bolus infusion protocols(Pilotto et al., 2011). However, treated patients should be followed up at regular intervals, as a circumscribed cavernous choroidal haemangioma has a reported long-term recurrence rate of up to 35%(Michels et al., 2005; Stehouwer et al., 2020).

8.3.2. Pathogenesis

Circumscribed cavernous choroidal haemangiomas consist of large,

dilated vessels with a relatively thin vessel wall. These tumours blend almost imperceptibly into the normal choroidal tissue(Witschel and Font, 1976). The blood vessels in a choroidal haemangioma act as high-flow arteriovenous shunts with incompetent walls; thus, IRF and SRF may accumulate through a damaged RPE, with exudative leakage, cystoid degeneration, and/or subretinal fibrous RPE hyperplasia in some cases. The fluid presents mainly in the macula, due to either centripetal subretinal flow or perifoveal ischaemia with secondary increased capillary permeability(Havener, 1985; Shields et al., 2001).

8.4. Choroidal osteoma

8.4.1. Clinical characteristics

A choroidal osteoma often presents in young women, in whom well-defined mature bone tissue occurs in the papillary or macular region. Initially, these tumours have an orange appearance on fundoscopy and are only slightly elevated. Over time, a cream-coloured tumour with well-defined borders appears, often with grey pigment on the surface. A choroidal osteoma can cause visual symptoms due to the occurrence of CNV and/or SRF, which may be accompanied by chorioretinal atrophy. On OCT, hyperreflective horizontal lamellar lines between the tumour tissue and the choroid – presumably representing bone lamellae – can be seen (Shields et al., 2007, 2015). B-scan ultrasonography shows an absence of echoes posterior to the tumour. Findings on FA and ICGA may be relatively similar between a choroidal osteoma and CSC; specifically, diffuse mottled hyperfluorescence – with focal leakage in some cases – is generally observed on FA, whereas hyperfluorescent changes are seen on ICGA. However, uptake of the contrast dyes is relatively slow with choroidal osteoma (Fig. 7A–D) (Yahia et al., 2008).

Most patients with a choroidal osteoma do not require treatment, although standard-fluence PDT was recently reported as an effective treatment for choroidal osteoma without CNV(Mazloumi et al., 2020). Intravitreal anti-VEGF therapy is indicated when the choroidal osteoma is complicated by CNV(Khan et al., 2014; Rao and Gentile, 2010; Song et al., 2010).

8.4.2. Pathogenesis

Choroidal osteomas consist of cancellous bone located between the choriocapillaris and the outer choroidal circulation, with communication between the outer choroidal circulation and the choriocapillaris occurring via canals running through the bone tissue(Williams et al., 1978). Focal RPE leakage due to damage to the outer blood-retinal barrier has been found to induce SRF accumulation in patients with a choroidal osteoma with no evidence of CNV(Browning, 2003). Finally, a serous retinal detachment can also be caused by CNV in patients with a choroidal osteoma(Browning, 2003; Yahia et al., 2008).

9. Haematological malignancies

9.1. Waldenström macroglobulinaemia

9.1.1. Clinical characteristics

Waldenström macroglobulinaemia is a lymphoproliferative B cell disorder commonly involving secondary organ infiltration. The most typical feature of this disease is an overproduction of monoclonal immunoglobulin type M (IgM)(Baker et al., 2013; Thomas et al., 1983). The excessive circulating levels and deposition of large IgM pentamers cause increased blood viscosity (hyperviscosity) in approximately 17% of patients, and increased bleeding due to a low platelet count, neurological complaints, and cardiorespiratory symptoms are the major clinical features in these patients(Merlini et al., 2003). Moreover, up to 37% of patients with Waldenström macroglobulinaemia present with hyperviscosity-related retinopathy, which typically includes retinal haemorrhages, microaneurysms, vascular tortuosity, and optic disc oedema(Deuel et al., 1983). Bilateral serous retinal detachments have also been described in several cases(Baker et al., 2013; Lin et al., 2019). CSC and Waldenström macroglobulinaemia generally present with overlapping features, including bilateral presentation and a combination of both SRF and IRF(Baker et al., 2013; Mohabati et al., 2020b). In contrast to CSC, however, abnormalities on OCT are usually highly symmetrical in Waldenström macroglobulinaemia, and the cystoid lesions in the outer retina are strikingly columnar (as in retinoschisis). Intraretinal deposits are visible around the photoreceptors. Moreover, and also in contrast with CSC, both hyperfluorescent and hypofluorescent changes on FA and ICGA can be observed in Waldenström macroglobulinaemia, with no leakage (Fig. 8A–D) (Roy et al., 2015).

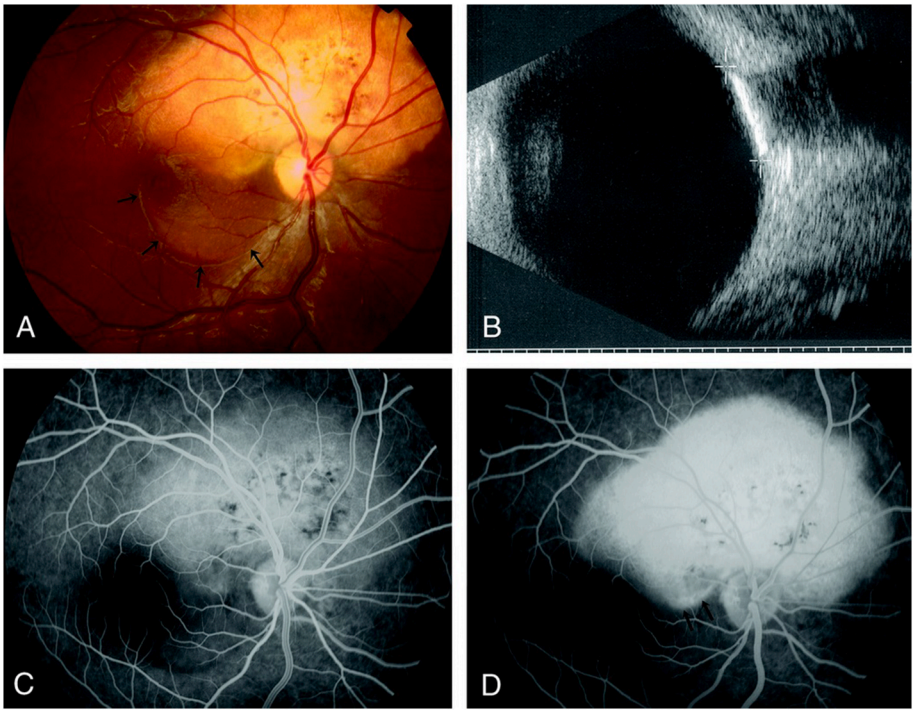
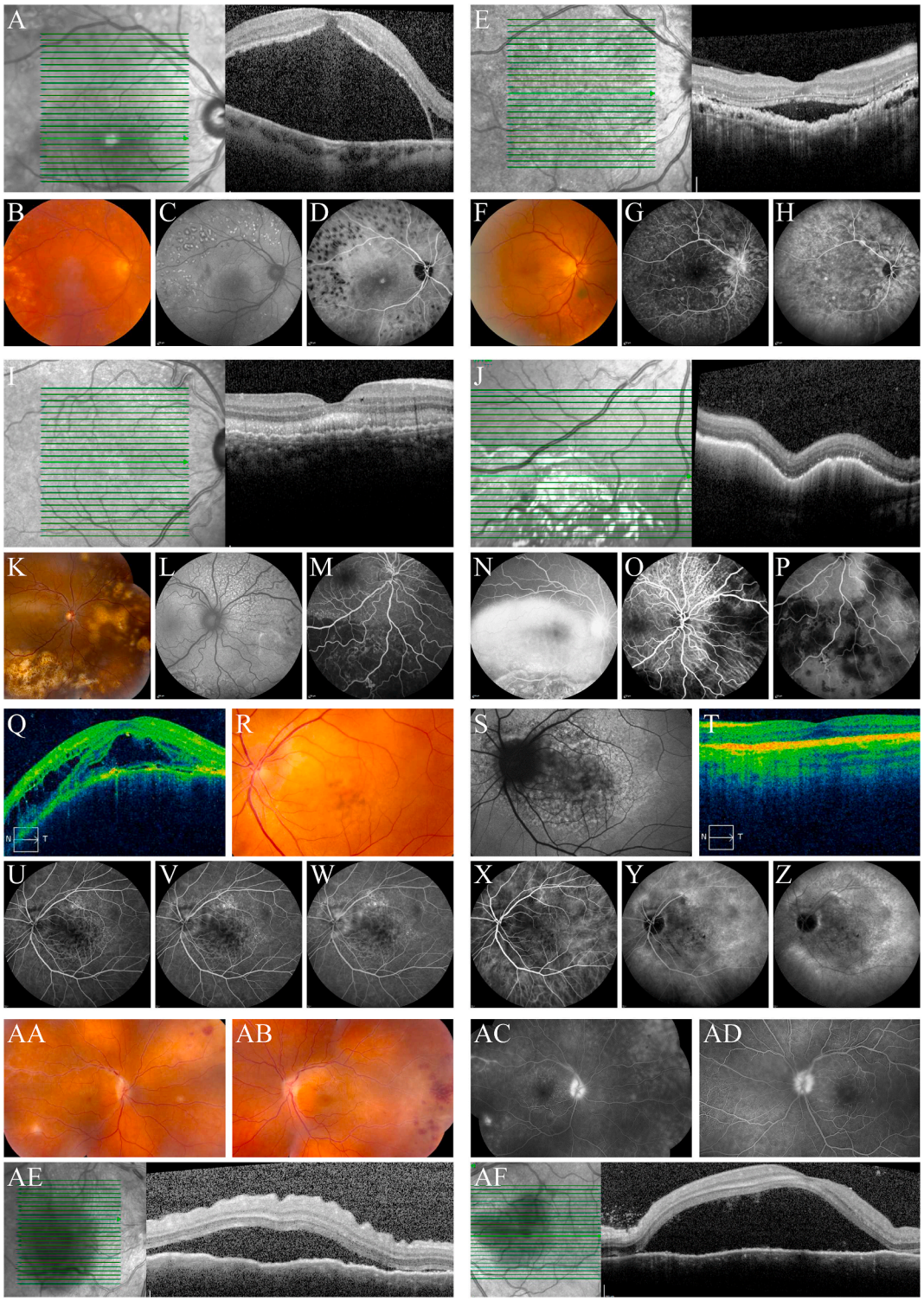


Fig. 7. [Courtesy of Salim Ben Yahia, MD].
(**A**) Colour fundus photograph of the right eye shows a **choroidal osteoma** located in the superior juxtapapillary area associated with serous retinal detachment extending to the macula (arrows). (**B**) B-scan ultrasonography. The tumour is highly reflective with associated acoustic orbital shadowing. Fluorescein angiography (**C**, early-phase and **D**, late-phase) shows a diffuse mottled hyperfluorescence of the tumour, associated with a moderately leaking area at its inferior border within the area of serous retinal detachment (arrows).



(caption on next page)

Fig. 8. An overview of hematological malignancies and a paraneoplastic syndrome that are part of the differential diagnosis of central serous chorioretinopathy.
(**A-D**) Multimodal imaging of the right eye of an 81-year-old male patient with **Waldenström macroglobulinaemia.**
This patient was also known with diabetic retinopathy, for which he previously received panretinal photocoagulation of both eyes. The optical coherence tomography (OCT) scan (A) of this patient revealed an extensive accumulation of serous subretinal fluid (SRF) in the macular area, with some intraretinal fluid nasally at the edge of the serous retinal detachment. In the left eye, a similar clinical picture was present. Fundoscopy (B) showed a central accumulation of serous SRF, together with mild atrophic changes of the retinal pigment epithelium (RPE) in the fovea. Fundus autofluorescence (FAF) imaging (C) showed mild hyperautofluorescent changes in the macula, corresponding to the area of SRF accumulation, as well as the midperipheral laser spots that are also visible in B. No leakage was seen on the fluorescein angiogram (FA) and indocyanine green angiogram (ICGA; D). The visual acuity in this eye was 20/200. The lesion did not respond to photodynamic therapy or intravitreal anti-vascular endothelial growth factor injections.
(**E-H**) Multimodal imaging of the right eye of a 52-year-old female patient with a metastasised colon carcinoma, for which she received chemotherapy, and **bilateral diffuse uveal melanocytic proliferation (BDUMP).**
This patient complained of a progressive decrease of visual acuity of both eyes, since 3 months. The OCT scan (E) showed a central serous SRF accumulation, together with a diffuse accumulation of variably reflective material below an irregular and thickened RPE layer. The left eye showed a similar clinical picture. On fundoscopy (F), several elevated, variably pigmented lesions were seen, especially around the optic disc and along the temporal retinal vascular arcades. A small pigmented naevus was also present below the optic disc. Mid-phase FA (G) revealed extensive multifocal granular hyperfluorescent areas, corresponding with the RPE changes and RPE detachments, as well as some optic disc leakage. There was no focal leakage through the RPE. Mid-phase ICGA (H) shows granular hyperfluorescent changes, that correspond mostly with the RPE changes that are also seen on FA, as well as some hypofluorescent reticular patterns. The visual acuity in this eye was 20/40.
(**I–P**) Multimodal imaging of the right eye of a 45-year-old female patient with **primary B cell choroidal lymphoma** with an otherwise unremarkable medical history.
This patient complained of a decrease in visual acuity of her right eye since 1 week, and her visual acuity had decreased to 20/100 at presentation. OCT scanning showed a bilateral symmetrical hyperreflective accumulation between the neuroretina and the RPE (I), while there was an irregular broad RPE detachment with material of moderate to low reflectivity beneath it. The OCT from the region inferiorly to the macula (J) showed large RPE detachments, with a hyperreflective accumulation beneath it. Fundoscopy (K) revealed a yellowish discolouration in the macula, whereas multifocal lobular yellow-white subretinal lesions with secondary hyperpigmented spots and beginning atrophy were seen in the midperiphery, mostly in the nasal and inferior fundus. These OCT changes and fundus changes raised a high index of suspicion of a (previously undiagnosed) primary B cell choroidal lymphoma. Some vitreous cells were present. FAF (L) did not provide much additional information, showing atypical salt and pepper-like retinal pigmentary changes. On early-phase FA (M) some diffuse punctate hyperfluorescent changes and fluorescein blockage by a subretinal accumulation in the midperiphery were seen, with profuse leakage in the late phase (N). Early- (O) and late-phase ICGA (P) showed blockage of choroidal fluorescence, that seem to correspond to the subretinal yellowish accumulation on fundoscopy and OCT.
Due to the suspicion of a lymphoma, a PET-CT scan was performed, revealing thickening of the gastric wall with high metabolic activity. Moreover, at least 4 foci were seen in the liver, and a supraclavicular lymph node was present, which was accessible for ultrasound-guided puncture. With this puncture the diagnosis of B cell lymphoma was established. Despite the fact that chemotherapy was started, patient deceased less than 9 months after the diagnosis was established.
(Q–Z) Multimodal imaging of the left eye of a 50-year-old male patient with **primary B cell choroidal lymphoma** with an otherwise unremarkable medical history.
This patient had presented with a sudden decrease in the visual acuity of the left eye. Findings on multimodal imaging had initially been considered to be typical of chronic central serous chorioretinopathy, for which half-dose photodynamic therapy had been performed twice. However, SRF increased and intraretinal fluid occurred on the OCT (Q) scan at the evaluation visit after the second half-dose photodynamic therapy, with increased thickening of the choroid. On fundoscopy (R) at that follow-up visit, the macula had developed a yellow-white aspect, together with RPE alterations. FAF (S) showed irregular hypoautofluorescent and hyperautofluorescent changes in the macula and surrounding the optic disc. This extensive and irregular pattern of autofluorescence, which can sometimes also assume a 'leopard spot' pattern, often appearing symmetrically, led to the suspicion of an underlying choroidal lymphoma. On early-phase FA (U) some diffuse punctate hyperfluorescent changes and some fluorescein blockage by the subretinal accumulation in the macula were seen (V–W). On early- (X), mid- (Y), and late-phase ICGA (Z) blockage of choroidal fluorescence was present, that seemed to correspond to the subretinal yellowish accumulation on fundoscopy and OCT. Due to the suspicion of a primary B cell choroidal lymphoma a vitreous biopsy was performed, which proved to be non-conclusive. However, a following choroidal biopsy confirmed that this patient had a primary B cell choroidal lymphoma. Ocular radiotherapy, which was performed in 15 fractions, led to complete resolution of SRF and intraretinal fluid and led to a decrease in choroidal thickness on OCT (T).
(AA-AF) Multimodal imaging of both eyes of a 33-year-old male patient with leukaemia (blastic plasmacytoid dendritic cell neoplasm) in his medical history who developed acute bilateral vision loss.
His visual acuity had decreased to 20/150 in his right eye and 20/100 in his left eye, at presentation. Fundoscopy of the right (Q) and the left eye (R) revealed papilloedema, a central accumulation of SRF, perivascular sheathing, and (mid)peripheral areas of retinal whitening and haemorrhages.
Moreover, vitreous cells were present. On FA (S–T) papillary leakage could be seen. The OCT of both eyes (U–V) showed a large central serous retinal detachment, some epiretinal membrane in the right eye, together with bilateral choroidal folds and thickening. These acute-onset ocular abnormalities were the presenting symptom of recurrence of the leukaemia. In this patient, herpes simplex virus, varicella zoster virus, and cytomegalovirus were not present on PCR analysis on an aqueous humor sample taken at 2 different visits.

Waldenström macroglobulinaemia should be treated promptly with chemotherapy in order to reduce IgM levels, as prolonged elevated levels of IgM can cause severe systemic complications, as well as fundoscopic abnormalities. However, systemic treatment has only a limited effect on the macular detachment, without significantly improving visual function; moreover, ophthalmic treatments also do not appear to be effective(Lin et al., 2019).

9.1.2. Pathogenesis

Unlike CSC, choroidal hyperpermeability, focal leakage through the RPE, and/or CNV do not appear to play a primary pathogenic role in Waldenström macroglobulinaemia-associated maculopathy. Moreover, the pathological mechanism underlying SRF accumulation in Waldenström macroglobulinaemia is a subject of debate. For example, IgM accumulation in the subretinal space has been suggested to cause an increased osmotic gradient, thus drawing IRF subretinally(Baker et al., 2013; Freidman et al., 1980). Moreover, a disruption in the outer retina on OCT has been reported in a subset of patients, with this disruption potentially creating a 'track' through which intraretinal IgM can travel from the retinal arterioles to the subretinal space, consistent with the aforementioned hypothesis(Baker et al., 2013).

9.2. Choroidal lymphoma

9.2.1. Clinical characteristics

Nearly all intraocular lymphomas are non-Hodgkin lymphomas, the majority of which are B cell in origin. Primary uveal lymphomas are low-grade (i.e. well-differentiated) lymphomas, generally with no systemic or central nervous system lymphoma at the time of ocular diagnosis. Choroidal lymphomas occur predominantly in men, typically present between the fifth and seventh decade, and are usually unilateral. Similar to CSC, patients with intraocular lymphoma often present with blurred vision due to macular SRF; however, the presence of vitreous cells and multifocal, yellow-whitish choroidal infiltrates on fundoscopy, together

with diffuse choroidal thickening on B-scan ultrasonography, are typical findings in choroidal lymphoma. Moreover, early hypofluorescence on FA is common in choroidal lymphoma, which further help discriminate between choroidal lymphoma and CSC. ICGA does not provide any benefit, as hypo- and hyperfluorescent abnormalities can be observed in both choroidal lymphoma (Fig. 8I-P) and CSC (Fig. 8Q–Z)(Arias et al., 2013; Barry et al., 2018; Matsuo et al., 1998). In contrast, primary vitreoretinal lymphomas are lymphomas of the central nervous system and are high-grade (i.e. poorly differentiated) lymphomas that may manifest initially in the eye. In addition to SRF on OCT, choroidal lymphoma cases can present with either homogenous hyperreflective sub-RPE infiltration or deep choroidal infiltration, which are characteristic of primary vitreoretinal lymphoma and choroidal lymphoma, respectively (Barry et al., 2018).

An interleukin-10 assay from a vitreous sample is a useful tool in primary intraocular lymphoma(Chan et al., 1995). However, a choroidal biopsy is the gold standard for diagnosing choroidal lymphoma, as it reveals evidence of malignant lymphocytes. However, this should be performed only in difficult diagnostic cases and should not be used for patients for whom the diagnosis can be established using other, non-invasive ocular procedures(Doycheva et al., 2015; Gunduz et al., 1999). Localised treatment consists of either intravitreal chemotherapy or ocular irradiation(Frenkel et al., 2008; Margolis et al., 1980; Sagoo et al., 2014; Yeh and Wilson, 2010). In addition, systemic screening should be performed in order to screen for the presence of a systemic or central nervous system lymphoma(Arias et al., 2013; Barry et al., 2018; Matsuo et al., 1998).

9.2.2. Pathogenesis

Intraocular lymphoma cells are commonly found between the RPE and BM, where these malignant cells can cause fluid exudates – particularly in areas over the sub-RPE infiltrates – and may infiltrate the retina. Moreover, areas of geographic atrophy in the RPE may disrupt the outer blood-retinal barrier. Finally, direct infiltration of malignant cells into the vitreous can occur when cells pass through the internal limiting membrane(Matsuo et al., 1998; Peterson et al., 1993; Ridley et al., 1992).

9.3. Leukaemia

9.3.1. Clinical characteristics

Ocular abnormalities can occur in up to 80% of patients with leukaemia and can manifest as cotton wool spots, haemorrhages, vascular tortuosity, and choroidal infiltrates. These manifestations can be associated with either acute or chronic forms of leukaemia, but are most common in patients with acute leukaemia during relapse with associated severe anaemia. A central serous retinal detachment is rare (Fig. 8AA-AF), and macular SRF accumulation as the primary ocular manifestation of leukaemia is even more rare; however, when present this accumulation is often bilateral and may resemble CSC(Kincaid and Green, 1983; Moulin et al., 2010). On FA, focal 'smokestack' leakage can be present both in choroidal leukaemic infiltration and in CSC(Moulin et al., 2010). Moreover, abnormalities similar to those found in CSC have been described in leukaemia, particularly among middle-aged patients (Moulin et al., 2010). Increased choroidal thickness has also been described in both diseases(Kishimoto et al., 2019). Importantly, ICGA may help distinguish between the 2 diseases; dot-like hyperfluorescence without choroidal leakage is often visible in leukaemia, but not in CSC.

The treatment of leukaemia currently includes intensive chemotherapy, combined with radiation therapy and bone marrow transplantation in some cases. The central neurosensory detachment often resolves shortly after the start of adequate leukaemia treatment, without the need for local ophthalmic treatment(Moulin et al., 2010).

9.3.2. Pathogenesis

The choroid often is the primary – and most commonly involved – ocular structure in cases in which leukaemia involves the eye. Choroidal involvement can often go unnoticed, unless vision loss occurs. A serous retinal detachment is usually localised in areas that overlie either leukaemic choroidal masses or choroidal infiltrates (Rosenthal, 1983), and this SRF accumulation can be due to RPE dysfunction as a results of ischaemia of the choriocapillaris(Moulin et al., 2010; Rosenthal, 1983).

10. Paraneoplastic syndromes

Paraneoplastic syndromes are relatively rare, non-metastatic systemic manifestations of certain forms of cancer. These syndromes are caused by either humoral factors secreted by tumour cells or by an immune response against the tumour.

10.1. Bilateral diffuse uveal melanocytic proliferation

10.1.1. Clinical characteristics

Bilateral diffuse uveal melanocytic proliferation (BDUMP) is an extremely rare disorder characterised by multiple elevated, pigmented choroidal lesions. Progressive cataract is also common in BDUMP and may be related to involvement of the iris and ciliary body(Joseph et al., 2014). BDUMP is caused by the proliferation of 'benign' melanocytes in the uveal tissue and is associated with several types of tumours, most of which are non-ocular. These tumours are typically detected several months or even years after the onset of ocular abnormalities, stressing the importance of rigorously screening for an underlying systemic tumour in cases with a high index of suspicion of BDUMP(Klemp et al., 2017; van Noort et al., 2019). The sudden occurrence of a bilateral exudative retinal detachment is another characteristic feature of BDUMP, thus mimicking CSC. In both BDUMP and CSC, RPE atrophy, RPE irregularity, and photoreceptor loss can occur, and multifocal areas of early hyperfluorescence on FA may also be present in both diseases (Fig. 8E–H) (Gass et al., 1990).

Despite this clinical overlap, however, the differentiation between CSC and BDUMP is relatively straightforward. For example, the average age at onset is higher for BDUMP compared to CSC, and BDUMP is more prevalent among women(Klemp et al., 2017). In addition, unlike with CSC, the serous retinal detachment in BDUMP is often symmetrical and bilateral. Moreover, with BDUMP subretinal round red lesions are often visible on fundoscopy, together with the characteristic bilateral 'giraffe pattern' of pigmentary changes that extend into the periphery(Naysan et al., 2016). In contrast with CSC, hypofluorescence on ICGA is detected in BDUMP, corresponding to the naevus-like pigmented tumours on fundoscopy(Kniggendorf et al., 2018). Finally, the rapid progression of cataract in BDUMP is not a feature of CSC, and BDUMP can also present with glaucoma, ciliary body enlargement, dilated episcleral vessels, iridocyclitis, and/or iris cysts(Gass et al., 1990; Joseph et al., 2014; Sahoo et al., 2019). The treatment for BDUMP should focus on effectively treating the systemic non-ocular malignancy, and plasmapheresis and plasma exchange can be successful in terms of improving visual acuity and achieving SRF resolution. Phacoemulsification with an intraocular lens implantation can be performed in cases with clinically significant cataract. Unfortunately, the mean survival duration of patients with BDUMP is just over a year, as most patients succumb to the primary underlying malignancy(Duong et al., 2006; Klemp et al., 2017; van Noort et al., 2019).

10.1.2. Pathogenesis

BDUMP has been reported in patients with a wide variety of primary tumours; most cases in women are linked to urogenital carcinomas, while most cases in men are associated with lung carcinomas(Klemp et al., 2017). The pathogenesis of BDUMP is currently unclear, although the proliferation of melanocytes has been suggested to arise from an inadequate immune response, as the disease occurs markedly less often in immune-incompetent patients compared to immune-competent patients(Klemp et al., 2017). The putative role of the immune system in the

pathogenesis of BDUMP has also been suggested by several other studies that found melanocyte proliferation–stimulating factors in the serum of BDUMP patients(Jansen et al., 2015; Miles et al., 2012).

The cause of the serous retinal detachment in BDUMP is also unclear, although uveal tract changes may play a primary role. Moreover, thickening of the choroidal tissue appears to precede the retinal detachment and the elevated uveal lesions by several months(Leys et al., 1991).

10.2. Paraneoplastic vitelliform maculopathy

10.2.1. Clinical characteristics

Paraneoplastic retinopathies comprise a heterogeneous group of rare disorders caused by a variety of anti-RPE and anti-retinal auto-antibodies. These paraneoplastic diseases often occur several years after the onset of the primary malignancy(Eksandh et al., 2008). A subset of these retinopathies can present as a vitelliform lesion (Fig. 9).(Nagiel et al., 2017; Rahimy and Sarraf, 2013) The subretinal lesions can wax and wane, thus overlapping with the clinical picture of CSC. However, unlike with CSC the lesions are typically yellow-white on fundoscopy(Daruich et al., 2015; de Jong et al., 2015; van Dijk et al., 2016a, 2017b). In addition, and also unlike CSC, paraneoplastic vitelliform maculopathy presents with SRF that is usually multifocal on OCT, with no underlying RPE detachments and no choroidal thickening. Another difference with CSC is that the vitelliform lesion blocks the choroidal fluorescence on FA, with no focal leakage(Daruich et al., 2015; de Jong et al., 2015; van Dijk et al., 2016a, 2017b).

Eksandh et al. previously described a patient with a history of choroidal melanoma in 1 eye that had been enucleated, followed 10 years later by the onset of vision loss in the remaining eye, with a central yellowish vitelliform lesion similar to the lesions seen in Best vitelliform macular dystrophy (Boon et al., 2009b; Eksandh et al., 2008), and an accumulation of subretinal hyperreflective debris and SRF on OCT. Unlike with CSC, an electro-oculogram – which reflects panretinal RPE function – showed a markedly reduced light peak response in this patient. This patient had circulating antibodies against the bestrophin-1 protein, which is encoded by the *BEST1* gene(Eksandh et al., 2008). The RPE-specific bestrophin-1 protein has several important functions, including maintaining normal fluid homeostasis in the subretinal space and keeping fluid out of the subretinal space(Boon et al., 2009b; Eksandh et al., 2008).

10.2.2. Pathogenesis

Paraneoplastic vitelliform maculopathy has been suggested to arise as an immunologic response to antigens expressed in cancer cells with antigenic overlap with endogenous proteins expressed in the eye. Several anti-RPE auto-antibodies (e.g. against bestrophin-1) and anti-retinal auto-antibodies have been found in patients with paraneoplastic vitelliform maculopathy. However, the exact pathogenesis of the vitelliform lesions is currently unclear. Subretinal debris may accumulate due to auto-immune antibody–mediated RPE dysfunction, thus compromising 'retinal housekeeping' mechanisms such as the regulation of fluid homeostasis and phagocytosis of photoreceptor outer segments (Nagiel et al., 2017; Rahimy and Sarraf, 2013). This accumulated debris presumably contains remnants of photoreceptor outer segments, which appear as yellowish vitelliform lesions on fundoscopy(Nagiel et al., 2017; Rahimy and Sarraf, 2013).

Similar to Best vitelliform macular dystrophy and MEKAR, the abnormal electro-oculogram in paraneoplastic vitelliform maculopathy reflects panretinal, diffuse dysfunction of the RPE, despite the relatively localised vitelliform lesions(Boon et al., 2009b; van Dijk et al., 2015). In contrast, CSC is characterised by 1 or more focal disruptions of the RPE, with a normal electro-oculogram(Deutman, 1969; van Dijk et al., 2015).

11. Genetic diseases

Several monogenic retinal diseases, which are caused by a mutation in a specific gene, can present with a clinical picture that includes serous fluid-like changes, thus mimicking CSC. However, these retinal dystrophies can be differentiated from CSC relatively easily, based on a range of differential diagnostic clinical aspects discussed below.

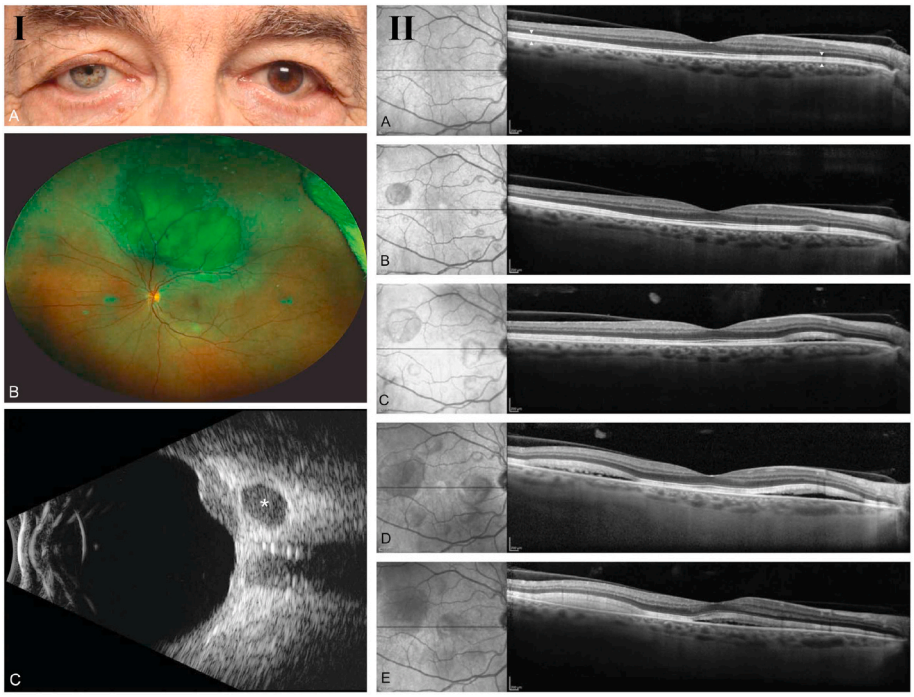


Fig. 9. Choroidal melanoma in the setting of ocular melanocytosis with the subsequent development of local recurrence 3 years after plaque brachytherapy, and evolution of **multifocal vitelliform lesions** on infrared scanning laser ophthalmoscopy and spectral-domain optical coherence tomography scanning [Courtesy of Aaron Nagiel, MD, PhD].
The patient had ocular melanocytosis of the left eye with iris heterochromia and mild scleral pigmentation (IA). Optos ultrawide field pseudocolour image (IB) demonstrating the choroidal melanoma at initial presentation. More than 3 years after plaque brachytherapy, extrasceral extension of the tumour was noted on ultrasound (IC) with a 5.5 mm diameter echolucent mass in the orbit (asterisk). Normal infrared image with optical coherence tomography scan (OCT; IIA) showing accumulation of vitelliform material at the level of the interdigitation zone (arrowheads). Three months later, the infrared image (IIB) shows scattered lesions in the macula. A small neurosensory detachment is present on this section through the fovea. At 7 months, the lesions are enlarging on infrared and OCT imaging (IIC). At 9 months, the lesions have enlarged substantially and vitelliform detachments are present nasal and temporal to the fovea (IID). At 1 year, the detachments have coalesced with involvement of the fovea. The temporal detachment has become filled with vitelliform material (IIE).

11.1. Best vitelliform macular dystrophy and autosomal recessive bestrophinopathy linked to mutations in the BEST1 gene

11.1.1. Clinical characteristics

Best disease (i.e. Best vitelliform macular dystrophy) is an autosomal dominant macular dystrophy caused by mutations in the *BEST1* gene (Boon et al., 2009b; Marquardt et al., 1998). Patients with Best disease present with macular vitelliform lesions similar to the central neuroretinal detachment in CSC(Zatreanu et al., 2020). These lesions are often bilateral and typically resemble an egg yolk in appearance at certain points in time, appearing sharply demarcated and yellowish, although the lesions can vary widely in aspect depending on the disease stage (Boon et al., 2009b, 2009c). Some lesions in Best disease contain largely transparent, relatively little yellowish material (Boon et al., 2009c), and the lesions can also be multifocal(Boon et al., 2007). Similar to CSC, the visual acuity can be relatively preserved in Best vitelliform macular dystrophy, and FA reveals hypofluorescence in vitelliform lesions, with some late staining. However, Best disease is not associated with focal leakage on FA and ICGA, and ICGA does not show the area(s) of indistinct hyperfluorescence that are typical of CSC (Fig. 3A–D).(Boon et al., 2009a; Guigui et al., 2009) With Best disease, areas of markedly increased fundus autofluorescence can be seen, particularly in the early stages of Best vitelliform macular dystrophy and in cases of autosomal recessive bestrophinopathy; these areas are often more prominent and more symmetrical compared to the clinical spectrum of CSC. Moreover, and in contrast with CSC, patients with bestrophinopathy typically have a markedly decreased – or even absent – light rise on the electro-oculogram(Deutman, 1969). In addition to noting these differences in clinical presentation between CSC and bestrophinopathy, obtaining a thorough family history (including an analysis of autosomal dominant inheritance in the case of Best disease) and genetic testing are essential for establishing a definitive diagnosis. Currently, no treatment is available for either Best vitelliform macular dystrophy or autosomal recessive bestrophinopathy, although gene therapy studies in animal models appear promising(Johnson et al., 2017). Nevertheless, complications such as angle-closure glaucoma and CNV can often be adequately treated(Boon et al., 2009b, 2013b).

11.1.2. Pathogenesis

The *BEST1* gene encodes bestrophin-1, a calcium-activated chloride channel expressed in the basolateral cell membrane of the RPE, where the protein plays an important role in maintaining ionic and fluid homeostasis and functions to regulate intracellular Ca^{2+} signalling(Boon et al., 2009b; Johnson et al., 2017; Kane Dickson et al., 2014). Although the precise consequences of mutations in the *BEST1* gene are currently unknown, some mutations may cause intracellular degradation of the protein; in contrast, some mutant forms of the bestrophin-1 protein are expressed in the RPE plasma membrane but exert a dominant-negative effect (Boon et al., 2009b; Johnson et al., 2017), possibly resulting in a loss of ion homeostasis and the subsequent accumulation of SRF. The vitelliform material present in the disease may correspond to unphagocytosed photoreceptor outer segments that accumulate secondary to RPE dysfunction(Boon et al., 2009b; Freund et al., 2011; Kane Dickson et al., 2014).

11.2. RP1L1-associated occult macular dystrophy

11.2.1. Clinical characteristics

Occult macular dystrophy is an autosomal dominant disease caused by mutations in the *RP1L1* gene, which encodes the retinitis pigmentosa-1-like-1 protein, a component of the photoreceptor cilium. Late-onset cases that resemble occult macular dystrophy but with no identified mutation in *RP1L1* have also been described. Occult macular dystrophy typically presents in childhood as with a progressive bilateral loss of central vision. Patients with occult macular dystrophy typically have very few abnormalities on fundoscopy, OCT, FAF, and FA. Retinal dysfunction is limited to the macula, as full-field electroretinogram shows a normal photoreceptor response. On OCT, the ellipsoid line is thickened and blurry in the early stage of the disease, and becomes disrupted and absent in the later stages. An 'optically empty' hyporeflective subretinal space – resembling a serous retinal detachment – may also be present (Fig. 10A and B).(Ruan et al., 2019) In this respect, the clinical picture overlaps superficially with CSC, although they can be easily distinguished based on an autosomal dominant family history of occult macular dystrophy, an early age at onset, extremely mild or absent abnormalities on fundoscopy, FAF, FA, and ICGA, as well as the relatively symmetrical and stable abnormalities on OCT, with no RPE detachment or irregularities(Takahashi et al., 2014). No therapeutic options are currently available for patients with *RP1L1*-associated ocular macular dystrophy.

11.2.2. Pathogenesis

The neuroretinal detachment in *RP1L1*-associated occult macular dystrophy has been referred to as foveal cavitation, a generic sign of cone dysfunction that manifests as a subfoveal, 'optically empty' hyporeflective space on OCT with an intact RPE(Leng et al., 2012; Takahashi et al., 2014). Why some patients with cone dysfunction or a cone dystrophy phenotype develop foveal cavitation, while other patients develop a more generalised thinning of the photoreceptors, is currently unknown(Leng et al., 2012; Takahashi et al., 2014).

11.3. Central areolar choroidal dystrophy linked to mutations in the PRPH2 gene

11.3.1. Clinical characteristics

In the early stages of central areolar choroidal dystrophy (CACD), the moderate atrophic changes in the RPE can mimic the changes seen in certain cases of chronic CSC. CACD is often inherited in an autosomal dominant pattern, although autosomal recessive inheritance has also been described. Autosomal dominant CACD is caused by mutations in the *PRPH2* gene (Boon et al., 2008a, 2009a), which encodes a photoreceptor-specific tetraspanin protein called peripherin-2/retinal degeneration slow.

Both our group and others (Boon et al., 2009a; Hoyng and Deutman, 1996) have described 4 disease stages of CACD. Stage 3 and stage 4 CACD are characterised by the presence of geographic atrophy; in contrast, geographic atrophy is extremely rare in CSC. Some patients with stage 2 CACD have a widened space between the outer neuroretina and the RPE (Fig. 10C–E), which is reminiscent of serous SRF and makes the distinction between CSC and atrophic AMD somewhat challenging, particularly given the low penetrance, variable expression, and relatively late onset of diseases linked to the *PRPH2* gene(Boon et al., 2008a, 2009a; Hoyng and Deutman, 1996; Smailhodzic et al., 2011). However, patients with CACD generally do not present with drusen or RPE detachments that are typical in AMD and CSC, respectively, nor do they present with the focal leakage spots on FA or hyperfluorescent areas on mid-phase ICGA that are typical in CSC(Boon et al., 2009a; Guigui et al., 2009). Patients with CACD often have a speckled pattern on FAF similar to advanced CSC cases; however, unlike CSC, these patients with CACD generally have highly symmetrical affected macular areas on FAF and no multifocal areas of speckled FAF abnormalities, nor do they present with the descending tracts seen in severe cases of chronic CSC(Daruich et al., 2015; Mohabati et al., 2020b; Smailhodzic et al., 2011).

No treatment is currently available for CACD, despite advances in developing gene therapy strategies(Conley and Naash, 2014; Perea-Romero et al., 2021).

11.3.2. Pathogenesis

The cause of the widened space between the outer photoreceptor border of the neuroretina and the underlying RPE is unclear. Animal studies have shown that photoreceptors containing a mutant form of *PRPH2* may have shorter photoreceptor outer segments, abnormal outer

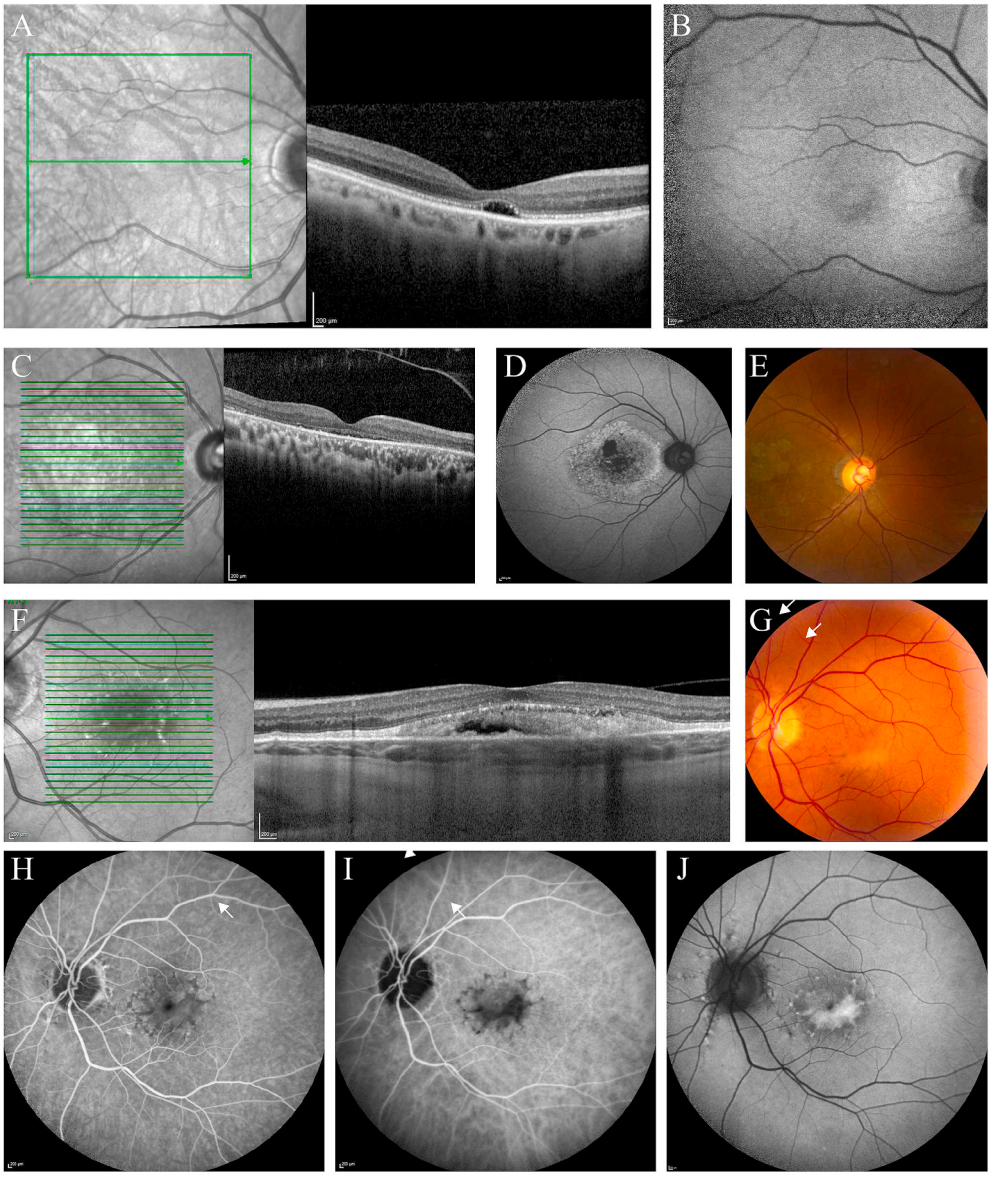


Fig. 10. Examples of genetic diseases that are part of the differential diagnosis of central serous chorioretinopathy.
(**A-B**) Multimodal imaging of the right eye of a 63-year-old female patient with **RP1L1-associated occult macular dystrophy.**
In this patient, a pathogenic c.133C>T (p.Arg45Trp) mutation was found in the *RP1L1* gene. Similar ophthalmological findings were found in her son, who carried the same mutation. On the foveal optical coherence tomography (OCT) scan (A), a hyporeflective space reminiscent of subretinal fluid (SRF) was present. The fundus autofluorescence (FAF) image (B) showed no clear abnormalities.
(**C-E**) Multimodal imaging of the right eye of a 49-year-old female patient with **autosomal dominant central areolar choroidal dystrophy due to a *PRPH2* gene mutation** (p.Arg172Trp).
Several other family members were also affected with macular dystrophy. On an OCT scan through the fovea (C), the ellipsoid zone appeared absent centrally, and a widened space between the outer neuroretina and the retinal pigment epithelium (RPE) was present, resembling serous SRF. On fundoscopy, beginning geographic atrophy was seen in the macula, with some yellow-white spots at the border of the atrophic area (E). The peripheral retina was normal. FAF (D) showed a variable, speckled FAF pattern: hypo-autofluorescent changes correspond to areas of atrophic RPE, while the markedly hyperautofluorescent changes correspond to increased levels of RPE lipofuscin.
(**F-J**) Multimodal imaging of the left eye of a 51-year-old female patient with **pseudoxanthoma elasticum (PXE) and serous fluid.**
In this patient, homozygous biallelic mutations (c.3421 C>T p.(Arg1141X) in the *ABCC6* gene were found. OCT (F) showed a vitelliform lesion, without signs of subretinal neovascularisation. The vitelliform lesion was also visible on colour fundus photography (G), surrounded by RPE changes. A similar picture was seen in the right eye. The mid-phase fluorescein angiography (H) and mid-phase indocyanine green angiography (I) showed that there was no (focal) leakage or choroidal hyperfluorescence – in contrast to central serous chorioretinopathy – but rather blockage of fluorescence by the vitelliform material and RPE hyperpigmentation. Subtle angioid streaks, typically seen in PXE, were also visible on these images (white arrows). FAF (J) mainly revealed hyperautofluorescence of the vitelliform material, as well as some surrounding granular autofluorescence changes, which were also present at the location of the angioid streaks. This patient had not been previously diagnosed with PXE, and did not have typical systemic features of this syndrome. Therefore, the retinal features, which can already be somewhat atypical and subtle as illustrated in this case, require a high index of suspicion for potential PXE. After all, patients with PXE should be screened for systemic involvement (e.g. gastrointestinal bleeding and cardiovascular disease) in an expertise centre to avoid complications.

segment membranes in the subretinal space, and changes in both the outer segment-RPE interface and disc phagocytosis(Boesze-Battaglia and Goldberg, 2002; Stuck et al., 2016). These changes could result in an increased hyporeflective space between the outer neuroretinal border and the apical RPE surface on OCT, thus simulating serous SRF.

11.4. *Pseudoxanthoma elasticum*

11.4.1. *Clinical characteristics*

Pseudoxanthoma elasticum is a predominantly autosomal recessive disorder caused by mutations in the *ABCC6* gene, which encodes ATP binding cassette subfamily C member 6. Patients with pseudoxanthoma elasticum present with abnormal elastic fibres in BM, the skin, and vascular walls. Findings on fundoscopy include a mottled RPE appearance (*peau d'orange*), angioid streaks, optic disc drusen, and round atrophic scars in the periphery. Among patients with angioid streaks, the most significant complication is the occurrence of CNV. Choroidal rupture can also occur in these patients, even after relatively minor trauma(Karampelas et al., 2013).

Patients with pseudoxanthoma elasticum can present with macular

SRF without CNV, and these cases can therefore mimic CSC. However, unlike CSC, pseudoxanthoma elasticum usually does not present with RPE detachments, and the choroid is often relatively thin. Pseudoxanthoma elasticum does not typically have focal leakage on FA, which is an important finding when attempting to distinguish between CSC and serous fluid due to RPE dysfunction in pseudoxanthoma elasticum (Fig. 10F–J).(Hansen et al., 2014) Finally, angioid streaks are easily visible on FAF and ICGA in pseudoxanthoma elasticum(Finger et al., 2009).

Pseudoxanthoma elasticum should be diagnosed as early as possible, as cardiovascular complications such as claudication, angina pectoris, stroke, and cardiomyopathy are commonly associated with this disorder (Finger et al., 2009).

11.4.2. Pathogenesis

The SRF accumulation seen in patients with pseudoxanthoma elasticum without CNV may be due to RPE dysfunction. This notion is supported by histopathological studies, which found decreased numbers of RPE cells in patients with pseudoxanthoma elasticum, and fewer pigmented granules present in the remaining RPE cells(Audo et al., 2007; Freund et al., 2011; Hansen et al., 2014).

12. Ocular developmental anomalies

Understanding the distinction between CSC and ocular developmental anomalies is extremely important, particularly given the marked differences with respect to the clinical course and therapeutic options.

12.1. Dome-shaped macula

12.1.1. Clinical characteristics

Dome-shaped macula presents as an inward macular deviation that usually occurs in myopic eyes; approximately half of all cases also present with a central accumulation of SRF(Caillaux et al., 2013; Errera et al., 2014; Gaucher et al., 2008). However, to date no clear difference in visual acuity has been found between dome-shaped macula with SRF and dome-shaped macula without SRF(Lorenzo et al., 2017). Findings on OCT, FA, and ICGA can be similar between dome-shaped macula and CSC, particularly in patients with a relatively small refractive error; thus, distinguishing between dome-shaped macula and CSC can be challenging (Fig. 11A–F).(Sahoo et al., 2019) However, dome-shaped macula can present with normal choroidal thickness and localised increased scleral thickness, in contrast with CSC, which is rare among patients with myopia. In addition, CSC does not present with an anterior bulge of the sclera underneath the macula visible on OCT(Imamura et al., 2011; Manayath et al., 2016). Notably, the dome-shaped macula can be detected more easily on the vertical OCT in approximately two-thirds of patients(Lorenzo et al., 2017). Dome-shaped macula generally responds poorly to currently available treatment options, including PDT and intravitreal injections of anti-VEGF medication (Lorenzo et al., 2017), although some cases can improve spontaneously (Daruich et al., 2015; Tamura et al., 2014).

12.1.2. Pathogenesis

Dome-shaped macula is caused by focal thickening of the sclera, which impairs choroidal blood flow by obstructing venous outflow, leading to RPE dysfunction and RPE detachment. Slow leakage from the dysfunctional RPE can cause an accumulation of SRF(Ellabban et al., 2013; Imamura et al., 2011; Ohsugi et al., 2014).

12.2. Tilted disc with inferior staphyloma

12.2.1. Clinical characteristics

Tilted disc syndrome has been estimated to be present in up to 2% of the general population, with affected individuals typically having an anterior position of the upper and temporal portions of their optic disc. In addition, the axis of the optic disc is oblique and has an inferonasal scleral crescent-shaped region of atrophy of the choroid and RPE. A minority of patients with tilted disc syndrome present with situs inversus of the retinal vessels(Cohen et al., 1998; Nakanishi et al., 2008). A rare complication of tilted disc with inferior staphyloma is serous retinal detachment(Cohen et al., 1998; Nakanishi et al., 2008). As in many differential diagnoses of CSC, the proper use of OCT is key in diagnosing tilted disc syndrome. Although a standard horizontal scan can show a focal serous retinal detachment in the macula and certain RPE irregularities, the inferior staphyloma can be difficult to appreciate; thus, a vertical OCT should be performed in order to clearly visualise the inferior staphyloma (Fig. 11G–L) (Maruko et al., 2011).

In patients with tilted disc with inferior staphyloma, SRF can generally be seen at the macular border of the inferior staphyloma (Fig. 11K), where the aforementioned changes in haemodynamic and/or mechanical factors can contribute to the development of SRF(Cohen et al., 1998). Both CSC and tilted disc with inferior staphyloma typically present with hyperfluorescent changes on late-phase ICGA. The hyperfluorescent areas on ICGA due to macular SRF in patients with tilted disc with inferior staphyloma are usually focalised along the border of the staphyloma (Fig. 11L); in contrast, CSC can present with more diffuse, multifocal abnormalities.

The SRF in patients with tilted disc with inferior staphyloma generally responds poorly to currently available treatment options, including PDT. However, similar to the clinical course in some CSC cases, the SRF can resolve spontaneously. As in CSC, patients with tilted disc with inferior staphyloma can develop complications such as CNV and/or PCV; in these cases, anti-VEGF is the primary treatment of choice (Cohen et al., 1998; Nakanishi et al., 2008).

12.2.2. Pathogenesis

The vertical OCT scan in patients with tilted disc with inferior staphyloma generally shows that the SRF accumulation often occurs at the watershed zone of the thicker choroid in the non-staphylomatous area and transitions to the thinner choroid in the inferior staphylomatous area. RPE irregularities and atrophic changes close to this transition zone may play a role in allowing SRF to enter the subretinal space through the impaired outer blood-retinal barrier of the RPE(Cohen et al., 1998; Maruko et al., 2011; Nakanishi et al., 2008).

12.3. Optic disc pit

12.3.1. Clinical characteristics

An optic disc pit is often unilateral and is believed to result from incomplete closure of the superior edge of the embryonic fissure, which causes congenital focal abnormalities in the head of the optic nerve. This leads to communication between the subretinal space, the vitreous cavity, and the subarachnoid space, which causes fluctuations in the gradient between the intraocular and intracranial spaces. Although these anomalies can be asymptomatic, patients usually develop visual complaints when a serous retinal detachment occurs. Many patients with optic disc pit have IRF and SRF (Fig. 11M) and therefore overlap clinically with CSC(Daruich et al., 2015; Jain and Johnson, 2014; Sahoo et al., 2019; Wang et al., 2008).

With an optic disc pit, fundoscopy reveals a relatively large disc with a round or oval greyish pit (Fig. 11N); moreover no focal leakage through the RPE and no hyperfluorescent choroidal changes are visible on FA and ICGA, respectively, thereby helping establish the correct diagnosis (Fig. 11O and P).(Jain and Johnson, 2014; Wang et al., 2008) Most patients with an optic disc pit and macular SRF and/or IRF have a relatively slow disease progression. Recent data suggest that a conservative approach may be preferred initially, unless marked worsening and/or complications such as a macular hole occur(Bloch et al., 2019). In these severe cases, no optimal treatment is currently available(Bloch et al., 2019). Many therapeutic approaches – most of which are surgical – have been advocated for severe patients and include pars plana

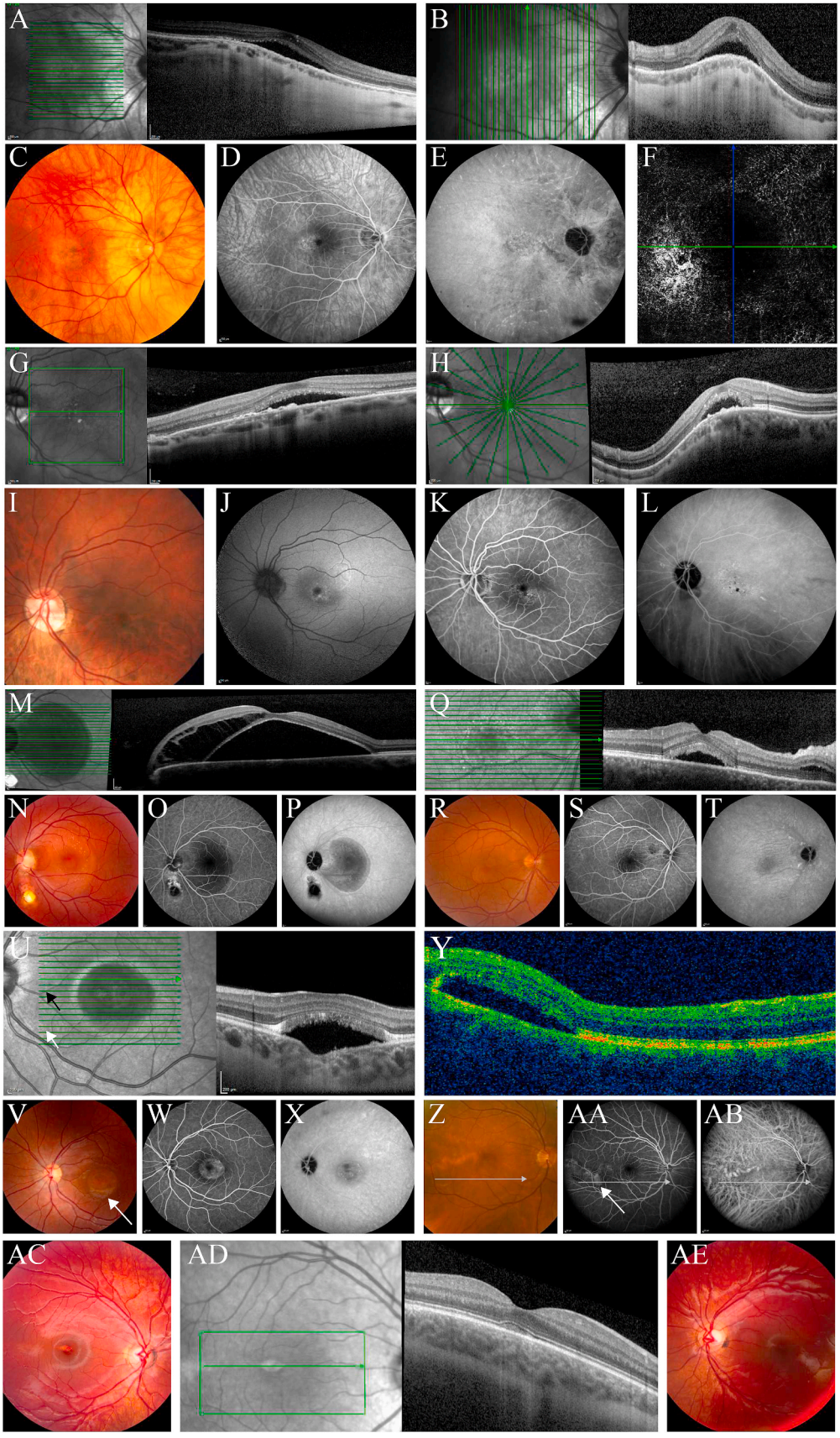


Fig. 11. An overview of ocular developmental anomalies that are part of the differential diagnosis of central serous chorioretinopathy (CSC).

(**A-F**) Multimodal imaging of the right eye in a 41-year-old highly myopic female patient with **dome-shaped macula** and serous fluid (SRF).

A horizontal foveal optical coherence tomography (OCT) scan (A) showed presence of SRF. From nasally to temporally, a gradual increase in choroidal thickness was present. The vertical OCT scan (B) revealed the inward macular deviation most clearly, with a thickened underlying sclera, together with a relatively thin choroid. Fundus photography (C) showed a sparsely pigmented fundus especially around the optic disc, compatible with the high myopia, and atrophic alterations of the retinal pigment epithelium (RPE) in the temporal macula. Mid-phase fluorescein angiography (FA; D) showed granular hyperfluorescence through the corresponding RPE window defect, without focal leakage. The mid-phase indocyanine green angiogram (ICGA; E) showed a broad area of moderately decreased fluorescence around the optic disc, due to the thin choroid in this area, in contrast to the hyperfluorescent choroidal abnormalities that are typically seen in CSC. On OCT angiography (F) it was difficult to appreciate the possible presence of a neovascularisation due to imaging artifacts. In this patient, there was no therapeutic effect of 3 intravitreal injections with anti-vascular endothelial growth factor receptor medication.

(**G-L**) Multimodal imaging of the left eye in a 48-year-old female patient with **tilted disc with inferior staphyloma.**

A horizontal OCT scan through the fovea (G) revealed SRF, small irregular RPE detachments, and a choroidal thickness that appeared within the normal range. In contrast, the vertical OCT scan (H) showed an inferior staphyloma, and a clearly thinner choroid in this inferior part as compared to the superior area. RPE irregularities and SRF appear to correspond roughly to the transition zone between the thicker choroid in the non-staphylomatous area and the thinner choroid in the inferior staphylomatous area. On fundoscopy (I), the tilted disc could be clearly seen, as well as a relatively depigmented inferior staphylomatous zone. Fundus autofluorescence (FAF) imaging (J) showed the changes delineating the contour of the area affected by SRF. On mid-phase FA (K) and mid-phase ICGA (L) granular hyperfluorescent changes were observed, without clear focal leakage or subretinal neovascularisation.

(**M-P**) Multimodal imaging of the left eye in a 38-year-old male patient with SRF due to an **optic disc pit.**

The foveal OCT scan (M) showed SRF, which seemed to be connected with the optic disc. In addition, intraretinal schisis-like fluid, mostly in the outer nuclear

layer, was seen nasally to the fovea. On fundoscopy (N), a relatively large disc with a round greyish pit was seen (black arrow), together with the macular fluid and some yellow-white punctiform subretinal deposits. This patient also had a microcoloboma (white arrow), which was also present in the other eye without an optic pit. On mid-phase FA (O) and ICGA (P), no clear leakage was observed in the macula. The visual acuity was 20/30. During 4 years of follow-up, the SRF and intraretinal fluid gradually disappeared spontaneously, while the visual acuity remained fairly stable.

(**Q-T**) Multimodal imaging of the right eye in a 52-year-old hyperopic male patient with **uveal effusion syndrome.**

SRF on OCT (Q) was seen in the fovea, together with some intraretinal fluid nasally to the fovea. On fundoscopy (R), SRF was seen, together with choroidal folds and peripheral choroidal detachments in 4 quadrants, typical of uveal effusion syndrome. Both mid-phase FA (S) and mid-phase ICGA (T) did not show evidence of hyperfluorescent areas of focal or diffuse leakage, in contrast to typical active central serous chorioretinopathy.

(**U-X**) Multimodal imaging of the left eye of a 22-year-old female patient with a **unilateral focal choroidal excavation with secondary serous SRF.**

This patient complained of a decrease in visual acuity since 4 months, and the visual acuity in this eye was 20/22. Serous SRF could be seen on OCT (U). Fundus photography (V) showed a central lesion with some yellowish subretinal changes, with a 'pseudohypopyon' of inferior gravitated yellowish debris (white arrow) that is reminiscent of Best vitelliform macular dystrophy (which was excluded by normal results on electro-oculography and genetic analysis of the *BEST1* gene, which did not reveal mutations). On FA (W) and ICGA, no (focal) leakage was present.

(**Y-AB**) Multimodal imaging of the right eye in a patient with SRF due to a **macular choroidal macrovessel** [Courtesy of Roselie Diederen, MD, PhD].

OCT (Y) showed SRF inferotemporally to the macula (scanning plane in Z, AA, and AB). Fundus photography (Z) revealed the large tortuous choroidal vessel that was located temporally in the macula, with corresponding RPE changes that are better visible as irregular hyperfluorescent changes without focal leakage on FA (AA). Some blockage of fluorescence by yellowish subretinal debris can also be seen, gravitating inferiorly in the serous retinal detachment (white arrow). Mid-phase ICGA (AB) showed characteristic early filling of the choroidal macrovessel.

(**AC-AE**) Fundus photography and OCT scan in a 6-year-old boy with **torpedo maculopathy** in his right eye.

On the fundus photograph of the right eye (AC), a hypopigmented torpedo lesion could be seen, which occurred temporally to the fovea with the characteristic tip pointing toward the fovea and slightly pigmented edges. On the OCT scan of the right eye (AD), a subretinal accumulation of hyperreflective material could be observed. No abnormalities were seen in the left eye (AE).

vitrectomy, laser photocoagulation, and macular buckling; however, the visual prognosis in these cases is guarded, and the SRF and IRF may be refractory to treatment(Moisseiev et al., 2015; Ooto et al., 2014).

12.3.2. Pathogenesis

The cause of the accumulation of SRF and IRF in optic disc pit is poorly understood but has been suggested to arise due to communication between the subretinal space, the vitreous cavity, and the subarachnoid space, which causes pressure fluctuations between the intraocular and intracranial spaces. Following a drop in intracranial pressure, a rise in intracranial pressure may force the vitreous fluid into the optic disc pit, which a subsequent accumulation of fluid in either the retina or the subretinal space(Daruich et al., 2015; Jain and Johnson, 2014; Wang et al., 2008). Finally, serous maculopathies often occur in cases with either a large or temporal optic disc pit(Brown et al., 1980).

12.4. Uveal effusion syndrome

12.4.1. Clinical characteristics

Uveal effusion syndrome can be caused by scleral thickening, abnormal scleral composition, and impaired venous outflow through the abnormal sclera. Moreover, nanophthalmos is a relatively common finding in patients with uveal effusion syndrome.

Both uveal effusion syndrome and CSC are most prevalent among middle-aged men, and both diseases have SRF of non-rhegmatogenous origin that can wax and wane during the disease course (Elagouz et al., 2010; Sahoo et al., 2019). However, the presence of a peripheral choroidal detachment – most easily seen on B-scan ultrasonography – points to a diagnosis of uveal effusion syndrome(Gass and Jallow, 1982; Uyama et al., 2000). Moreover, in contrast with CSC, uveal effusion syndrome often presents with early granular hyperfluorescence and secondary localised areas of RPE hypertrophy and hyperplasia (referred to as 'leopard spots') (Fig. 11Q–T).(Uyama et al., 2000) In severe cases, uveal effusion syndrome can be treated surgically with full-thickness sclerotomy in order to improve fluid drainage from the subchoroidal space(Elagouz et al., 2010). Unfortunately, however, even if treated uveal effusion syndrome often leads to severe, permanent bilateral loss of visual acuity(Elagouz et al., 2010).

12.4.2. Pathogenesis

In uveal effusion syndrome, obstruction of the vortex veins is caused by scleral thickening and relative obstruction of the scleral outlet. This can prevent the diffusion of proteins out of the eye via the uveoscleral route, giving rise to an osmotic gradient that favours the retention of intraocular fluid; this gradient arises from decreased removal of extravasated fluid and proteins and/or an increase in choroidal fluid leakage(Elagouz et al., 2010). In rare cases of uveal effusion syndrome with normal scleral thickness, altered choroidal permeability – possibly due to choroidal inflammation – has been observed on ICGA(Elagouz et al., 2010; Kumar et al., 2002).

12.5. Focal choroidal excavation with secondary serous subretinal fluid

12.5.1. Clinical characteristics

Focal choroidal excavation presents as either a congenital or an acquired concavity in the choroid. Focal choroidal excavation can be classified as either 'conforming' or 'non-conforming' based on OCT. In 'conforming' focal choroidal excavation, a normal retinal architecture overlies the choroid, visual acuity is unaffected, and there is no separation between the RPE and the photoreceptors. In contrast, 'non-conforming' focal choroidal excavation presents with a detachment of the neurosensory retina from the RPE; in addition, SRF accumulates in the area between below this detachment, and shed photoreceptor outer segments accumulate (Fig. 11U–X), often causing a slow decline in visual acuity(Chung et al., 2017; Margolis et al., 2011; Obata et al., 2013; Shinojima et al., 2014).

Together with the choroidal concavity on OCT, findings on FA and ICGA may be helpful in distinguishing between focal choroidal excavation and CSC. For example, focal choroidal excavation often presents with both hyperfluorescent and hypofluorescent changes due to RPE alterations, in contrast with the hyperfluorescent abnormalities present in CSC. In addition, in focal choroidal excavation early hypofluorescence close to the excavation can usually be seen on ICGA, in contrast with CSC. Finally, both CSC and focal choroidal excavation present with hyperfluorescent changes on late-phase ICGA, suggesting choroidal congestion and/or hyperpermeability, although these changes are generally more extensive and/or multifocal, particularly in chronic CSC (Chung et al., 2017; Daruich et al., 2015).

12.5.2. Pathogenesis

Focal choroidal excavation typically occurs in cases with no other forms of retinal or chorioretinal pathology, although it has been described in patients with a chorioretinal disease such as CSC, AMD, and vitelliform macular dystrophy (Margolis et al., 2011; Obata et al., 2013; Shinojima et al., 2014). For these diseases, the putative cause-and-effect relationship between these conditions and focal choroidal excavation remains unclear. Moreover, the precise aetiology of focal choroidal excavation is currently unknown. It has been suggested to reflect a congenital choroidal abnormality that does not change markedly over time. Some groups have suggested that focal choroidal excavation is either a developmental abnormality or other focal abnormality in the choroidal structure, while other groups suggest that focal choroidal excavation may develop secondary to ocular inflammatory diseases that primarily affect the choroid. Focal choroidal excavation has also been found in patients with pachychoroid spectrum disorder(Chung et al., 2017). Choroidal vascular disease and choroidal rupture can also cause thinning and/or scarring of the choroid, which can mimic focal choroidal excavation(Margolis et al., 2011; Nishikawa et al., 2014; Shinojima et al., 2014). The cause of the SRF accumulation in focal choroidal excavation is currently unknown. It may be purely mechanical in nature, arising secondary to the 'gap' that develops between the neuroretina and the RPE; however, it may also be due to a slow accumulation of SRF through the dysfunctional RPE at the site of choroidal thinning(Chung et al., 2017; Margolis et al., 2011; Obata et al., 2013).

12.6. Macular choroidal macrovessel

12.6.1. Clinical characteristics

A macular choroidal macrovessel is a large, tortuous, often hypopigmented choroidal vessel located temporally in the macular area (Fig. 11Y–AB). Fundus examination reveals a track-like choroidal vascular lesion with matching RPE changes. On ICGA, a macular choroidal macrovessel typically shows early filling (Fig. 11AB). SRF has been reported in a few cases with macular choroidal macrovessel; however, this SRF and the accompanying RPE changes may be mistaken for chronic CSC(Dalvin et al., 2021). Nevertheless, several findings on multimodal imaging can help distinguish macular choroidal macrovessel from CSC, including the presence of a choroidal vessel with an elevation in the macula on fundoscopy and OCT, no leakage on FA, and the ability to clearly delineating the extent of the vessel using ICGA. In addition, choroidal macrovessel appears to be more common in women (Dalvin et al., 2021; Lima et al., 2011). Observation is generally the procedure of choice in patients with a choroidal macrovessel, even in cases involving SRF(Dalvin et al., 2021; Lima et al., 2011).

12.6.2. Pathogenesis

The finding of early filling of a macular choroidal macrovessel on ICGA suggests an arterial origin. The cause of SRF accumulation in patients with choroidal macrovessel is currently unknown. However, the SRF may accumulate through a leak in the overlying RPE that arises from thinning and dysfunction of the underlying choriocapillaris due to compression by the dilated macrovessel. In this respect, the pathogenesis may be similar to the mechanism proposed in patients with choroidal 'pachyvessels' in Haller's layer in the context of pachychoroid disease(Gal-Or et al., 2018).

12.7. Torpedo maculopathy

12.7.1. Clinical characteristics

Torpedo maculopathy is either a hypo- or hyperpigmented lesion of the RPE that is typically unilateral and occurs temporally to the fovea with a tip pointing toward the fovea (Fig. 11AC).(Roseman and Gass, 1992) Affected patients are often diagnosed in childhood and are usually asymptomatic, with diagnosis occurring incidentally(Shirley et al., 2018). Torpedo maculopathy is generally considered to be a congenital, non-progressive disease, although in rare cases it can be complicated by CNV(Jurjevic et al., 2017; Shirley et al., 2018). Retinal thinning is often visible on OCT, whereas SRF and/or vitelliform material, as well as IRF, are relatively rare (Fig. 11AD).(Dolz-Marco et al., 2017; Sanabria et al., 2008; Shirley et al., 2018) Important findings that can help distinguish torpedo maculopathy from CSC include a lack of autofluorescence on FAF and no clear leakage on FA in the affected eye, unless CNV is present (Golchet et al., 2010; Shirley et al., 2018).

12.7.2. Pathogenesis

As noted above, torpedo maculopathy is believed to be a congenital abnormality closely related to the 'bulge' in the temporal macula that usually occurs around the fifth gestational month(Shirley et al., 2018). When present, the SRF in torpedo maculopathy may be caused by dysfunctional RPE in the affected area(Sanabria et al., 2008).

13. Medication-related conditions and toxicity-related diseases

Several types of medication can cause a clinical picture that overlaps with CSC. Thus, a thorough medical history, including medications, may provide important clues regarding the underlying cause of the disease.

13.1. Mitogen-activated protein kinase kinase inhibitor-associated retinopathy (MEKAR)

13.1.1. Clinical characteristics

MEK inhibitors such as binimetinib and trametinib are targeted therapies that are used as treatment of metastatic melanoma, lung carcinoma, and thyroid carcinoma. However, patients taking these compounds can develop macular or multifocal serous retinopathy resembling CSC(van Dijk et al., 2015). This side effect of MEK inhibitors (MEKAR) is generally bilaterally and relatively symmetrically. Although 4 morphologies of MEKAR have been described based on the fluid foci, the vast majority of patients present with a dome-shaped accumulation of SRF(Francis et al., 2017). The SRF in MEKAR causes visual symptoms such as blurred vision and flashes in only a minority of patients; when present, these symptoms are generally mild and transient, even in patients who continue taking MEK inhibitors(Urner-Bloch et al., 2014; van Dijk et al., 2015, 2018b). Therefore, the development of MEKAR is not considered a reason to discontinue taking MEK inhibitors, since the SRF will usually resolve spontaneously with a return of normal visual function.

Multimodal imaging can reveal several distinguishing features between MEKAR and CSC. For example, MEKAR typically does not present with RPE changes or pachychoroid on OCT, leakage on FA, or abnormalities on ICGA(Urner-Bloch et al., 2014; van Dijk et al., 2015, 2018b). In addition, MEKAR usually presents with multiple foci of SRF, which help distinguish MEKAR from CSC, which usually does not present with multifocal serous detachments (Fig. 12A–C). Moreover, neither gravitational dependency nor inferior tracking of SRF have been described in MEKAR.

13.1.2. Pathogenesis

MEKAR is believed to result from direct RPE toxicity induced by the MEK inhibitor, as the visual complaints and abnormalities on ophthalmological examination can occur within a few days after the start of treatment(Francis et al., 2017). This toxicity can be reflected in the electro-oculogram, which can be profoundly abnormal in patients with MEKAR, suggesting a panretinal disruption in the transepithelial electrical potential giving rise to RPE dysfunction(van Dijk et al., 2015). One possible mechanism may be a direct effect of the MEK inhibitor on the function of ion channels and pumps in the RPE, resulting in focal retinal detachments. Interestingly, post-mortem tissue obtained from patients suggests that the MEK inhibitor can inhibit the fibroblast growth factor receptor/mitogen-activated protein kinase pathway in several retinal components(van Dijk et al., 2016b). Finally, both anti-retinal and

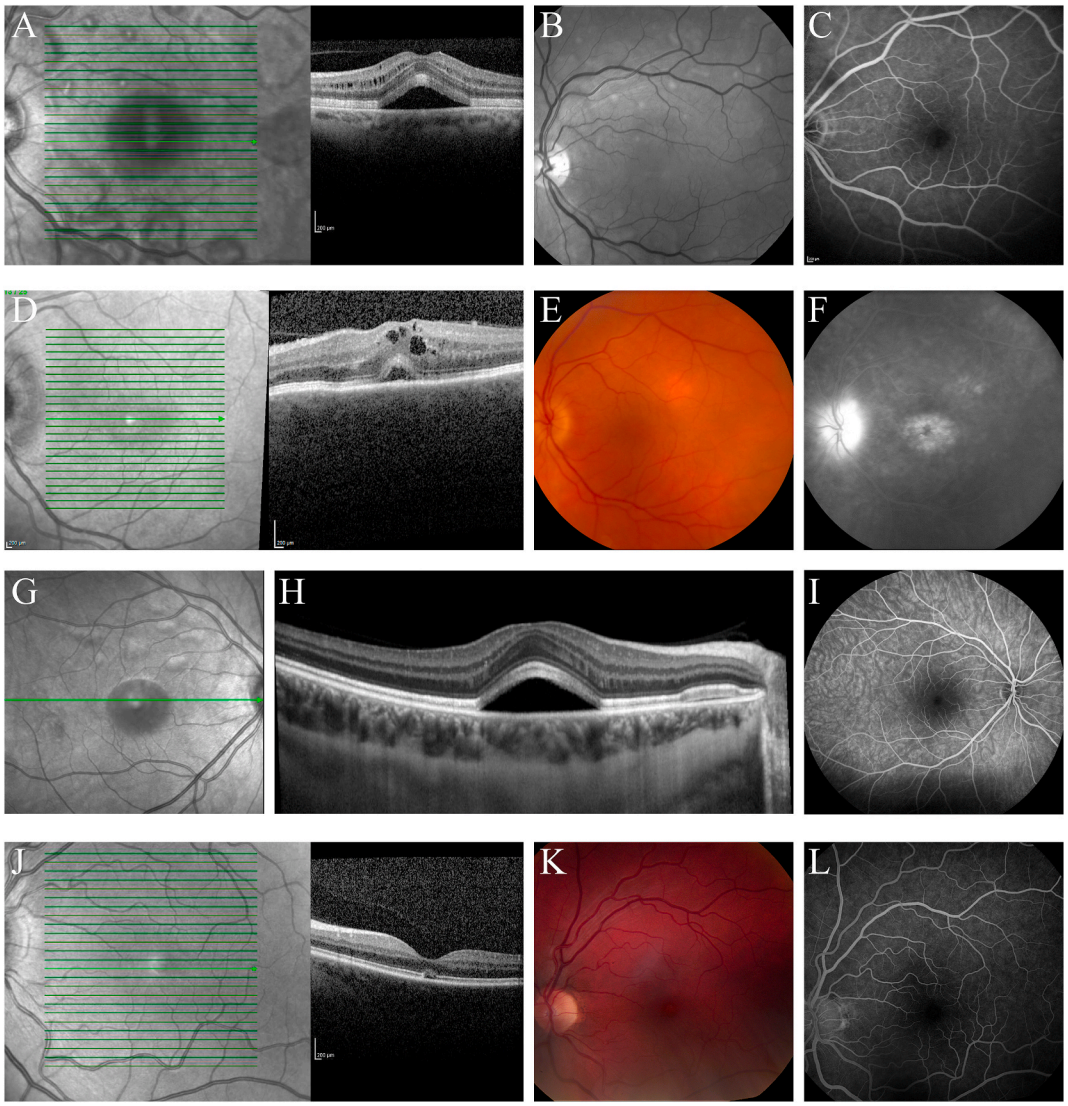


Fig. 12. An overview of medication-related conditions and toxicity-related diseases that are part of the differential diagnosis of central serous chorioretinopathy (CSC).
(**A-C**) Multimodal imaging of the left eye of a 64-year-old binimetinib-treated patient with metastatic cutaneous melanoma (**mitogen-activated protein kinase kinase inhibitor-associated retinopathy; MEKAR**).
Optical coherence tomography (OCT; A) showed mild intraretinal fluid and a dome-shaped serous neuroretinal detachment with an accumulation of subretinal fluid (SRF) in both eyes. Multifocal, variably-sized serous neuroretinal detachments were observed on red-free fundus photography (B) and infrared reflectance imaging (A). In contrast to typical CSC, MEKAR patients do not have retinal pigment epithelial detachments. Fluorescein angiography (FA; C) showed hardly any fluorescence changes, and no focal leakage, in contrast to typical active CSC.
(**D-F**) Multimodal imaging of the left eye in a 64-year-old male patient with **checkpoint inhibitors causing birdshot-like chorioretinopathy** (in this case pembrolizumab as a treatment for metastatic lung carcinoma).
The OCT scan (D) showed a small dome-shaped accumulation of SRF under the fovea, together with some intraretinal fluid. Fundoscopy (E) showed subtle macular oedema, and a superotemporal deep birdshot-like depigmented lesion. Mid-phase FA (F) showed the flower-petal leakage of the macula oedema, without CSC-like focal leakage, subtle hyperfluorescence of the deep superotemporal lesion, as well as papillary leakage.
(**G-I**) Multimodal imaging of the right eye in a 45-year-old woman with **serous retinopathy** similar to MEKAR, **caused by the use of hair dye containing aromatic amines** (para-phenylenediamine and 5-diamine sulphate) [Courtesy of Céline Faure, MD, and Martine Mauget-Faÿsse, MD].
Multifocal, variably-sized serous neuroretinal detachments were observed in the macula on infrared reflectance imaging (G). On the OCT scan (H), a dome-shaped accumulation of SRF was seen foveally, together with a more shallow SRF accumulation nasally. Mid-phase FA (I) showed no clear abnormalities. This clinical picture is very similar to the clinical spectrum of MEKAR, of which an example was shown in (A–C).
(**J-L**) Multimodal imaging of the left eye in a patient with **poppers maculopathy.**
The foveal OCT scan (J) revealed a characteristic disruption of the ellipsoid zone, which may resemble a small foveal SRF accumulation. A subtle yellow subfoveal lesion was seen on fundoscopy (K), whereas FA (L) was unremarkable.

anti-RPE auto-antibodies have been found in MEKAR patients, although their pathogenic role is currently unclear(van Dijk et al., 2015, 2016b).

13.2. Checkpoint inhibitors causing birdshot-like chorioretinopathy

13.2.1. Clinical characteristics

Ocular adverse events such as uveitis and conjunctivitis have been associated with the use of pembrolizumab, nivolumab, and ipilimumab,

which are immunotherapeutic agents – specifically, checkpoint inhibitors – that target either the programmed cell death protein 1 receptor (pembrolizumab and nivolumab) or cytotoxic T lymphocyte antigen-4 (ipilimumab) on T cells. In addition, these drugs – which are prescribed to treat metastatic melanoma, metastatic lung carcinoma, metastatic transitional cell carcinoma, metastatic renal cell carcinoma, and Hodgkin's lymphoma in order to boost the T cell response – have also been found to cause birdshot-like chorioretinopathy, an autoimmune complication that presents with multifocal uniform yellowish choroidal lesions typically concentrated nasally.

Birdshot-like chorioretinopathy associated with checkpoint inhibitors has clinical overlap with CSC, as these patients can present with SRF on OCT imaging (Fig. 12D). These patients can also present with macular oedema, retinal vasculitis, and CNV, as well as hypofluorescent lesions on FA and ICGA (Fig. 12E and F).(Minos et al., 2016; Miyakubo et al., 2019; Obata et al., 2019; Priem and Oosterhuis, 1988; Wong et al., 2012) Nevertheless, distinguishing between birdshot-like chorioretinopathy associated with checkpoint inhibitor treatment and CSC is relatively straightforward, as – in addition to the use of these immunotherapeutic agents – these clinical signs and the characteristic multifocal uniform yellow choroidal lesions are not seen on fundoscopy in patients with uncomplicated CSC. Moreover, patients with birdshot-like chorioretinopathy associated with checkpoint inhibitors can present with intraocular inflammation(Minos et al., 2016; Miyakubo et al., 2019; Obata et al., 2019; Priem and Oosterhuis, 1988; Wong et al., 2012).

With respect to treatment, regional injections of corticosteroids may be beneficial in birdshot-like chorioretinopathy associated with checkpoint inhibitors; however, systemic corticosteroids are not indicated, as it could interfere with the immune-based therapy in these gravely ill patients(Acaba-Berrocal et al., 2018).

13.2.2. Pathogenesis

As discussed above, the checkpoint inhibitors that cause birdshot-like chorioretinopathy increase the T cell response to tumours. These circulating T cells can also cause auto-immune complications, which has been suggested to induce a clinical picture that mimics birdshot chorioretinopathy(Acaba-Berrocal et al., 2018).

13.3. Hair dyes containing the aromatic amines para-phenylenediamine and 5-diamine sulphate causing serous retinopathy

13.3.1. Clinical characteristics

Commercial hair dyes containing high concentrations of aromatic amines have been found to increase the risk of developing bilateral serous retinopathy, a toxic effect that usually occurs within several days following exposure. This condition presents with multiple bilateral serous neuroretinal detachments that resemble both MEKAR and CSC on OCT(van Dijk et al., 2015). However, unlike CSC, patients exposed to aromatic amines have normal choroidal thickness, no RPE detachments, and no abnormalities on FA and ICGA (Fig. 12G–I); in this respect, the clinical picture is quite similar to MEKAR. SRF often resolves spontaneously, depending on the extent of the first exposure and possible repeat exposures(Faure et al., 2020).

13.3.2. Pathogenesis

Serous retinopathy associated with exposure to aromatic amines may be toxic in origin, as with MEKAR. Similar to MEK inhibitors, aromatic amines have been found to inhibit the fibroblast growth factor receptor/mitogen-activated protein kinase pathway in RPE cells, a pathway that plays a key role in the survival and maintenance of these cells(Faure et al., 2020; van der Noll et al., 2013).

13.4. Poppers maculopathy

13.4.1. Clinical characteristics

Poppers contain volatile aromatic nitrites, which are popular for their psychoactive effects. When inhaled, poppers can increase the sexual experience. Poppers are illegal, but they can still be purchased when sold in alternative products such as air fresheners(Romanelli et al., 2004).

Poppers maculopathy has been described as a side effect of using poppers and can occur after even 1 use. Poppers maculopathy presents as either unilateral or bilateral yellow subretinal deposits on fundoscopy (Fig. 12K). Moreover, OCT reveals a disruption of the ellipsoid zone often accompanied by retinal elevation, which could be interpreted as SRF (Fig. 12J).(Davies et al., 2012; Rewbury et al., 2017) In contrast with CSC, no thickened choroid and no RPE detachments are present on OCT with poppers maculopathy. Subtle hyperautofluorescent changes can be seen on FAF, corresponding to the lesions visible on fundoscopy. Finally, patients with poppers maculopathy typically do not present with leakage on FA or ICGA (Fig. 12L), providing an important diagnostic clue for differentiating between poppers maculopathy and CSC.

There is currently no known treatment for poppers maculopathy, other than discontinuing its use(Davies et al., 2012; Rewbury et al., 2017). The abnormalities seen on retinal imaging generally resolve over long-term follow-up, even after chronic use of the drug(Hui et al., 2020).

13.4.2. Pathogenesis

The cause of the retinal changes associated with poppers maculopathy is currently unknown, but may be toxic in origin. Nitrites have been found to upregulate the production of nitric oxide, which can be directly toxic to the retina, particularly the highly sensitive photoreceptors, consistent with the damage to the outer retina seen on OCT in patients with poppers maculopathy(Fawcett and Osborne, 2007; Rewbury et al., 2017).

14. Rhegmatogenous retinal detachment and tractional retinal detachment

14.1. Clinical characteristics

Both rhegmatogenous retinal detachment and tractional retinal detachment can cause an accumulation of fluid in the subretinal space that can progressively affect the macula. Rhegmatogenous retinal detachment usually presents with an acute onset of symptoms such as flashes and floaters, visual field loss, and – when the macula is detached – marked vision loss. However, in rare cases the retinal detachment can develop slowly, with few symptoms and a shallow, gradual retinal detachment that can be mistaken clinically for CSC (Fig. 13A–F and G-I). A slow rhegmatogenous retinal detachment is more common in individuals with high myopia, slowly occurring inferior retinal detachments associated with a small retinal break, and cases with retinal dialysis. A definitive diagnosis of rhegmatogenous retinal detachment can be based on the presence of pigment in the vitreous, 1 or more peripheral retinal breaks, and peripheral extension of the retinal detachment. If multimodal imaging is performed in rhegmatogenous retinal detachment, the findings differ from CSC, with peripheral extension of the SRF on OCT and an absence of leakage on FA and ICGA.

In tractional retinal detachment, which is commonly seen in patients with severe diabetic retinopathy, proliferative tissue from either the retina or the vitreous membrane pulls on the retina, causing retinal deformation and subsequent detachment(Ghazi and Green, 2002).

In general, surgery is indicated for treating both rhegmatogenous retinal detachment and tractional retinal detachment(Steel, 2014). After surgery, residual macular SRF can persist, particularly in chronic cases with a long duration of viscous SRF, mimicking CSC; this fluid can resolve at an extremely slow rate(Algethami et al., 2021; Veckeneer et al., 2012).



Fig. 13. An overview of miscellaneous diseases that are part of the differential diagnosis of central serous chorioretinopathy (CSC).
(**A-F**) Multimodal imaging of the right eye of a 56-year-old male highly myopic patient with **serous subretinal fluid (SRF) due to a long-lasting rhegmatogenous retinal detachment.**
Optical coherence tomography (OCT; A) shows SRF extending from temporally into the fovea. This SRF extended peripherally (B). Ophthalmological examination revealed a trace of pigment in the vitreous, inferotemporal atrophic pigmentary changes including some bone spicule hyperpigmentation, and a small peripheral retinal tear, indicative of a long-lasting rhegmatogenous retinal detachment as seen on the colour fundus photograph (C). These atrophic retinal pigment epithelium (RPE) changes we also clearly visible on the fundus autofluorescence (FAF) image (D), and corresponded to a granular hyperfluorescent window defect without focal hyperfluorescent leakage on fluorescein angiography (FA; E) and indocyanine green angiography (ICGA; F), which further excluded central serous chorioretinopathy as an aetiology.
(**G-I**) Multimodal imaging of the left eye of a 72-year-old highly myopic male patient with **SRF due to a rhegmatogenous retinal detachment secondary to progressive peripheral retinoschisis.** OCT (G) shows the retinal detachment with hyporeflective SRF. The fundus photograph (H) showed atrophic changes in the superotemporal region, and a retinal detachment, that already reached the fovea (white arrows point at the border between attached and detached retina). There was no leakage on FA (I).
(**J-L**) Multimodal imaging of the left eye of a 31-year-old **pregnant patient with acute central serous chorioretinopathy.** On the foveal OCT scan (G), SRF was present, which extended to more superiorly. FAF of the right eye (K) showed no abnormalities, whereas the left eye showed hyperautofluorescent changes superotemporally above the optic disc extending into the macula (L).
(**M-O**) Multimodal imaging of the right eye of a 66-year-old male patient with **serous maculopathy secondary to RPE dysfunction due to severe confluent drusen.**
The foveal OCT scan (M) in this patient showed an extensive amount of confluent (partly cuticular) drusen, together with SRF, which was also visible on fundoscopy (N). On FA (O), staining of the foveal lesion was seen, together with a typical 'stars-in-the-sky' appearance of the cuticular drusen surrounding this central lesion.

14.2. Pathogenesis

In rhegmatogenous retinal detachment, a combination of vitreoretinal traction and a retinal defect cause a movement of fluid from the vitreous cavity to the subretinal space through a break in the retina. The formation of a retinal break is most often associated with a posterior vitreous detachment, a naturally occurring phenomenon at increasing age(Steel, 2014). In cases of retinal dialysis – for example following blunt trauma – the posterior vitreous may still be attached.

In tractional retinal detachment, the retina is pulled away by a proliferative membrane from the retina itself or the vitreous, leading to retinal deformation and detachment(Ghazi and Green, 2002).

15. Retinal vascular diseases

A number of common retinal vascular diseases can masquerade superficially as CSC and are discussed below.

15.1. Diabetic macular oedema

15.1.1. Clinical characteristics

Approximately 15–30% of eyes with diabetic macular oedema present with a serous retinal detachment. Although an individual patient can present with both CSC and diabetic macular oedema, identifying other features typical in diabetic retinopathy (e.g. microaneurysms, cotton wool spots, and hard exudates) can provide a relatively easy differentiation between CSC and diabetic macula oedema with a serous retinal detachment(Catier et al., 2005; Otani et al., 1999; Ozdemir et al., 2005). In diabetic macular oedema, fluid may be present in all retinal layers. To exclude co-morbidity with CSC, both FA and ICGA can be helpful, as well as an assessment of the presence of RPE detachments and pachychoroid on OCT, which are suggestive of CSC(Daruich et al., 2015).

15.1.2. Pathogenesis

Diabetic macular oedema occurs due to changes in the blood-retinal barrier; the most relevant changes include loss of pericytes, damage to the endothelial cell-cell junction, and thickening of the basement membrane. In patients with diabetic retinopathy, leakage of plasma and lipids in the macula causes IRF and SRF(Das et al., 2015). Movement of fluid to the subretinal space is believed to be associated with systemic hypertension and high levels of glycosylated haemoglobin, subsequently leading to damage to the blood-retinal barrier(Gupta et al., 2014).

15.2. Retinal vein occlusion

15.2.1. Clinical characteristics

A serous retinal detachment in retinal vein occlusion can be caused by fluid leaking from either the retinal or choroidal circulation into the subretinal space. However, the clinical picture of retinal vein occlusion differs markedly from CSC; specifically, retinal haemorrhages, cotton wool spots, and an occlusion of a vein, as well as areas of non-perfusion on FA, are typical findings in patients with a retinal vein occlusion, all of which are not found in patients with CSC. Thus, distinguishing between retinal vein occlusion and CSC is straightforward(Celik et al., 2016; Gallego-Pinazo et al., 2013; Yamaguchi et al., 2006).

15.2.2. Pathogenesis

Leakage from congested retinal vessels located outside of the macula is the most common cause of foveal SRF in retinal vein occlusion (Yamaguchi et al., 2006). However, in some cases leakage from congested macular vessels can also cause SRF(Celik et al., 2016; Yamaguchi et al., 2006).

15.3. Acute hypertensive retinopathy

15.3.1. Clinical characteristics

Hypertensive retinopathy is the most common ocular complication associated with arterial hypertension and can present with microaneurysms, exudates, retinal haemorrhages, cotton wool spots, closure of blood vessels, and neovascularisation(Fraser-Bell et al., 2017; Grosso et al., 2005). Approximately one-third of patients with acute-onset severe hypertension present with IRF and SRF (Fig. 13J–L). Moreover, patients can present with increased choroidal thickness, similar to CSC. These abnormal findings generally resolve spontaneously (soon after the patient's blood pressure has normalised), which also overlaps with CSC (Ahn et al., 2014). Hypertensive retinopathy can be differentiated from CSC based on the combination of acute-onset, severe hypertension and the presence of widespread retinal abnormalities such as microaneurysms, retinal haemorrhages, and cotton wool spots(Daruich et al., 2015; Fraser-Bell et al., 2017; Grosso et al., 2005).

15.3.2. Pathogenesis

Retinal arterioles respond to increased blood flow with vasoconstriction. Moreover, a prolonged period of high blood pressure has been associated with damage to the blood-retinal barrier, as well as extravasation of plasma and erythrocytes, resulting in retinal haemorrhages, intraretinal lipids, and/or IRF(Wong and Mitchell, 2004). Hypertensive choroidopathy is characterised by necrosis of the choroidal arteries, which leads to impaired perfusion of the choriocapillaris and ischaemia of the RPE. SRF can also develop due to the reduced pumping capacity of the RPE as a result of these detrimental changes(Tso and Jampol, 1982).

15.4. Pregnancy-related serous maculopathy

15.4.1. Clinical characteristics

Pregnancy-induced hypertension occurs in approximately 5% of all pregnancies. It involves pre-eclampsia, in which arterial hypertension is associated with peripheral oedema and proteinuria, which can progress to eclampsia, when it also includes seizures. Approximately 10% of women with severe pregnancy-induced hypertension also develop haemolysis, elevated liver enzymes, and low platelets (HELLP) syndrome (Schönfeld, 2012; Sheth and Mieler, 2001), and up to 3.5% of women with this syndrome have SRF accumulation(Erbagci et al., 2008). As with CSC, patients with pregnancy-related serous maculopathy can present with multifocal areas of SRF on OCT, together with intraretinal cystoid changes and outer retinal changes(Van Rysselberge et al., 2020). Moreover, hyperfluorescent changes corresponding to dye staining in the subretinal space can be observed on FA(Van Rysselberge et al., 2020). In addition – and in contrast to CSC – patients with serous maculopathy in the context of HELLP syndrome and pre-eclampsia can present with early and late choroidal filling defects on ICGA, corresponding to choroidal ischaemia(Daruich et al., 2015; Komoto et al., 2019; Song et al., 2013; Van Rysselberge et al., 2020). In most cases, the SRF associated with HELLP syndrome resolves spontaneously within several weeks after delivery(Schönfeld, 2012; Sheth and Mieler, 2001).

15.4.2. Pathogenesis

The precise cause of serous maculopathy in pregnant patients with hypertension is currently unknown. However, young women may be more susceptible to developing hypertensive chorioretinopathy due to the high elasticity of their blood vessels; systemic hypertension may cause the relatively elastic choroidal arteries to constrict, reducing choroidal perfusion with subsequent hyperperfusion at the edge of these areas, thereby leading to secondary RPE dysfunction and SRF leakage through the damaged RPE outer blood-retinal barrier(Tso and Jampol, 1982).

16. Miscellaneous diseases

16.1. Serous maculopathy secondary to RPE dysfunction due to confluent drusen

16.1.1. Clinical characteristics

Central drusen in AMD can gradually expand, forming large confluent drusenoid RPE detachments, eventually reducing RPE function. Serous SRF can then accumulate in the subretinal space overlying these confluent 'megadrusen' (Fig. 13M–O).(de Jong, 2006; Mitchell et al., 2018) Mechanical separation of the neuroretina from the underlying RPE between several adjacent large dome-shaped drusenoid RPE detachments may also play a role. These confluent soft drusen in the macula have a poor prognosis, as 42% of cases develop advanced AMD within 5 years of diagnosis(Cukras et al., 2010). Soft drusen are associated with the occurrence of chorioretinal atrophy and CNV, both of which are common in late-stage AMD(Cukras et al., 2010). Nevertheless, it can be challenging to exclude the presence of CNV in cases of large drusenoid RPE detachments with accompanying SRF – even with OCT, OCTA, FA, and ICGA – due to blockage of the fluorescence signal by the drusenoid material and image artifacts. The simultaneous presence of IRF may indicate the presence of CNV.

Differentiating between AMD and large drusen and CSC is relatively straightforward, as patients with CSC are generally significantly younger and do not present with bilateral central macular drusen associated with their serous maculopathy. In addition, patients with CSC tend to have a thickened choroid on OCT, whereas patients with AMD and large drusen often have a relatively thin choroid(de Jong, 2006; Mitchell et al., 2018).

16.1.2. Pathogenesis

Drusen contain membranous and other materials such as uncharged lipids, proteins, and zinc and iron ions, and are located between the inner collagenous part of BM and the RPE basement membrane. The accumulation of drusen interferes with the RPE's normal function, causing subsequent failure of the RPE outer blood-retinal barrier and the RPE's pumping function(de Jong, 2006; Sparrow et al., 2010; Strauss, 2005).

In some cases, large confluent drusen can occur together with SRF. Because SRF can be present either in the depression between adjacent dome-shaped drusen or above the apex of a large drusenoid RPE detachment, or as low-lying SRF over confluent drusen, clusters of coalescent drusen have been hypothesised to apply mechanical strain to the outer retina, thereby pulling the retina away from its normal position and causing the aforementioned subretinal spaces(de Jong, 2006; Hilely et al., 2020; Mitchell et al., 2018).

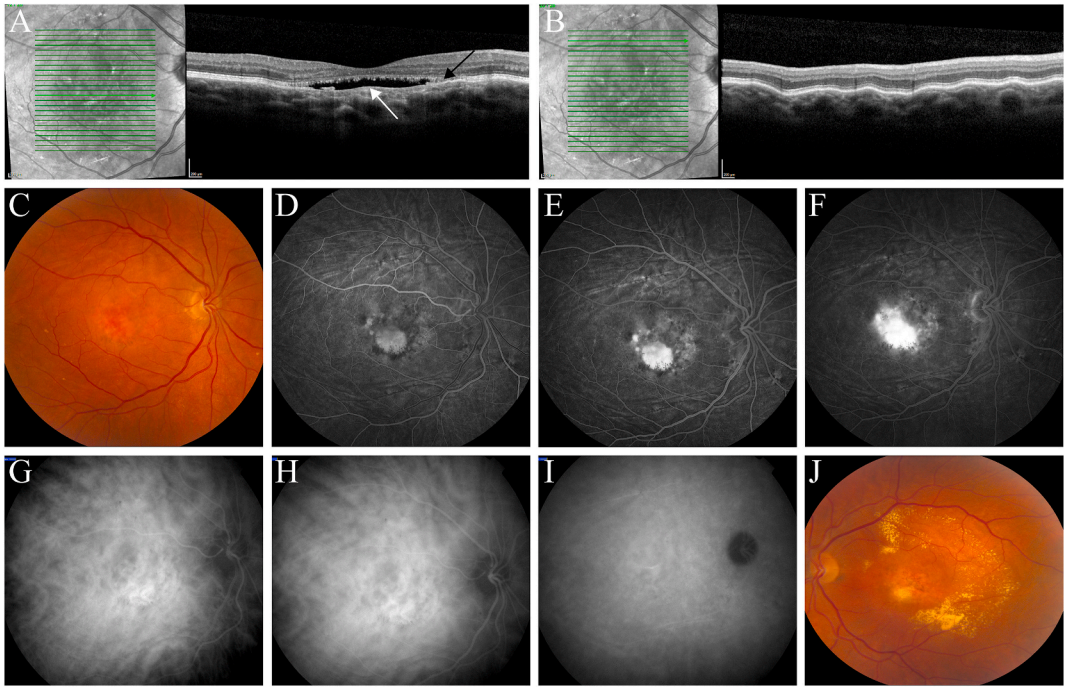


Fig. 14. Serous maculopathy with absence of retinal pigment epithelium (SMARPE).
(**A-J**) Multimodal imaging of the right eye of a 69-year-old female hyperopic patient (+4 dioptres) with **serous maculopathy with absent retinal pigment epithelium (SMARPE)**.
At presentation in our clinic, this patient did not have complaints of her right eye, and her visual acuity (20/30) had been stable for at least 2.5 years. Vision in the left eye was 20/150. In that eye, this patient had a therapy-resistant macular neovascularisation, for which she had received intravitreal injections with anti-vascular endothelial growth factor receptor medication, without effect and after which no further therapy was performed.
On the foveal optical coherence tomography (OCT) scan (A), subretinal fluid (SRF) was seen in the right eye, with a striking and relatively large area of absent retinal pigment epithelium (RPE; white arrow indicates the area of absent RPE, whereas black arrow indicates the area where the RPE line is still present), without any drusen or RPE detachments. The OCT scan that was obtained more superiorly (B) showed choroidal folds. On the fundus photograph of the right eye (C), a central well-delineated atrophic area of absent RPE was visible, with the choroidal vessels visible through this window defect, surrounded by mildly-atrophic RPE alterations, of which the inferonasal part was mildly hyperpigmented. The fundus photograph of the left eye (D) showed atrophic RPE changes in the macula, with an area of subretinal fibrosis, surrounded by a semicircular area of hard exudates. Fluorescein angiography (E–G) of the right eye revealed early hyperfluorescence due to RPE atrophy, with brightly hyperfluorescent pooling of fluorescein within the lesion in the late phase. Indocyanine green angiography showed large, densely packed choroidal vessels in the early- (H) and mid-phase (I), without clear CSC-like hyperfluorescent indistinct leakage in the mid- and late phase (I–J). Different anti-vascular endothelial growth factor medications were given, but no effect on the SRF on OCT was observed after injection of series of bevacizumab (3 injections), aflibercept (3 injections), and ranibizumab (5 injections) at monthly intervals. Moreover, this patient did not respond to indocyanine green angiography-guided half-dose photodynamic therapy.

16.2. Serous maculopathy with absence of RPE (SMARPE)

16.2.1. Clinical characteristics

In addition to the clinical recognised conditions described above, we can also characterise 2 additional forms of serous maculopathy that have not been previously described: serous maculopathy with absence of RPE (SMARPE; Fig. 14) and serous maculopathy due to aspecific choroidopathy (SMACH; Fig. 15).

In SMARPE, the presence of SRF on OCT is associated with a striking focal absence of the RPE, with no drusen, RPE detachments, or evidence of CNV (Fig. 14A). FA shows an early hyperfluorescent window defect due to RPE atrophy (Fig. 14D), with fluorescein pooling in the serous lesion in the mid- and late phases (Fig. 14E and F). Unlike CSC, SMARPE does not present with an RPE detachment on OCT, and no focal leakage on FA or ICGA, although a dense network of enlarged choroidal vessels and/or choroidal folds can be present (Fig. 14G–I). SMARPE can be distinguished from neovascular AMD by the lack of drusen or haemorrhage on fundoscopy, as well as no evidence of CNV on OCT, OCTA, FA, and ICGA. The serous SRF in SMARPE can reach a state of equilibrium, remaining extremely stable for years, with only a gradual decline in visual acuity.

Some degree of overlap between RPE apertures and SMARPE exists. However, in literature an RPE aperture has been found to occur in relatively large dome-shaped RPE detachments, whereas no RPE detachments were seen in SMARPE. In addition, the area of absent RPE in SMARPE appears much larger than in most cases of RPE aperture that have been described(Iovino et al., 2019; Querques et al., 2016).

16.2.2. Pathogenesis

In SMARPE, SRF can accumulate due to the absence of RPE in the macula and the subsequent failure of RPE's outer blood-retinal barrier and pumping function(Sparrow et al., 2010; Strauss, 2005). Serous SRF likely originates from the choriocapillaris through the relatively intact BM. As such, a clinical picture of SMARPE can be expected to result from several macular diseases in which the RPE is absent with no evidence of CNV. The presence of a thickened choroid and/or choroidal folds, in addition to the absent RPE, may also be an important diagnostic factor. The relatively stable visual acuity, which declines slowly over many years, is likely due to the exchange of molecules between the neuroretina, the residual RPE, and the choroid/choriocapillaris within the micro-environment of the foveal SRF accumulation. The presence of an alternative intraretinal visual cycle between the cone photoreceptors and the Müller cells may partly explain the relative preservation of visual acuity that may be present(Wang and Kefalov, 2011).

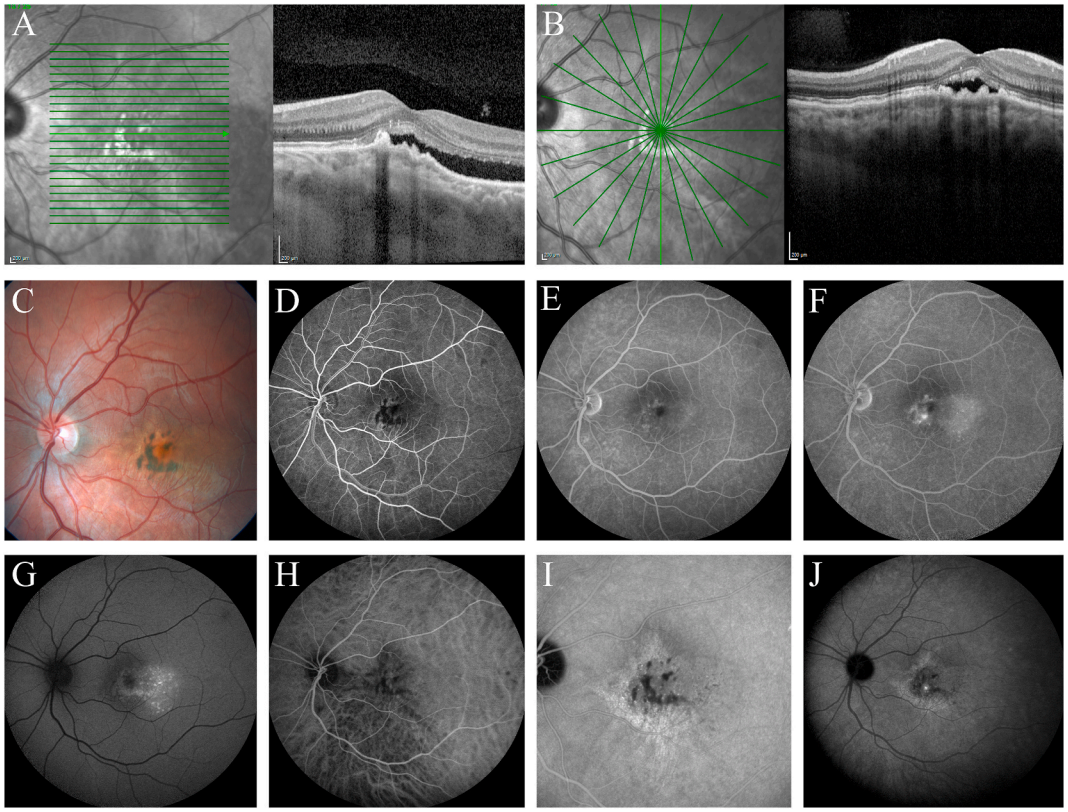


Fig. 15. Serous maculopathy due to aspecific choroidopathy (SMACH).
(**A-J**) Multimodal imaging of the left eye of a 19-year-old male patient with **serous maculopathy due to aspecific choroidopathy (SMACH)**.
At presentation in our clinic, this patient already had complaints of metamorphopsia of his left eye for months. At that time, his visual acuity was 20/20. In another hospital he had received half-fluence photodynamic therapy 4 months earlier, without an effect on the subretinal fluid (SRF). On the horizontal (A) and vertical foveal optical coherence tomography (OCT) scan (B), SRF was seen in the left eye. The retinal pigment epithelium (RPE) was irregular and appeared thickened, being elevated by an underlying thickened choroid. On the horizontal OCT scan, the inner part of the choroid appeared to have an irregular and relatively hyperreflective aspect. No clearly enlarged Haller's layer vessels ('pachyvessels') were present.
On the fundus photograph of the left eye (C), central irregular multifocal hyperpigmentation was seen, on a background of underlying yellow-white hypopigmentation. The hyperpigmented abnormalities were hyporeflective on the infrared reflectance image, and corresponded to areas of thickened irregular RPE on OCT (in A and B). Fluorescein angiography (D–F) showed early blockage of fluorescence by the hyperpigmented areas on a slightly hyperfluorescent background, with some hyperfluorescent staining in the mid- and late phase, and possibly some late focal leakage. Fundus autofluorescence imaging (G) revealed some indistinct hyperautofluorescent changes in the fovea, and a larger area of punctate hyperautofluorescent abnormalities temporally to the fovea. Early indocyanine green angiography (H) showed subtle hypofluorescence in the macula extending to the inferior periphery and some well-demarcated hyperfluorescent changes around the hypofluorescent area of hyperpigmentation in the macula. The right eye showed no abnormalities on multimodal imaging.

16.3. Serous maculopathy due to aspecific choroidopathy (SMACH)

16.3.1. Clinical characteristics

In SMACH, OCT shows SRF in the macula, irregular thickening of the underlying choroid, and hyperreflective material (Fig. 15A and B). The overlying RPE is parallel with the irregularity of the underlying choroid, with focal hyperplastic and hyperpigmented areas (Fig. 15A and B) and no evidence of subretinal or sub-RPE neovascularisation on FA, ICGA, and OCTA. Moreover, a degree of hyperfluorescent and hypofluorescent changes can be observed on FA, with no clear focal leakage between the early and late phases (Fig. 15D–F). Finally, unlike CSC, no focal hyperfluorescent changes are present on ICGA with SMACH (Fig. 15H–J).

16.3.2. Pathogenesis

The cause of SMACH and the associated SRF is currently unclear, although the choroidal abnormalities may be congenital, with gradually progressive dysfunction during life; alternatively, the abnormalities may develop later in life due to an unknown cause. The SRF leakage may be due to increased hydrostatic pressure from the abnormal, thickened underlying choroid. Finally, dysfunction of the RPE outer blood-retinal barrier and the RPE's pumping function may contribute to the persistence of SRF with no clear focal leakage(Sparrow et al., 2010; Strauss, 2005).

17. Future directions

The differential diagnosis of CSC and other diseases associated with SRF in the macula includes a broad spectrum of diseases, which can be categorised into 12 main pathogenic subgroups. New developments in multimodal imaging, such as OCTA, and improvements in quality of already available imaging modalities, such as OCT, FA, and ICGA, can help in the differentiation of these disease entities. However, despite all of these imaging techniques, the diagnosis of an underlying CNV, for example, can be challenging. Artificial intelligence and deep learning are expected to become an increasingly important aid in the correct diagnosis and distinction of choroidal and retinal diseases (Schmidt-Erfurth et al., 2018), and may also lead to better identification of subtle CNV, as well as the recognition of new diseases and pathogenic subgroups.

The exact pathogenesis is still unknown for many of the diseases that are part of the differential diagnosis of serous maculopathy, such as CSC, MEKAR, optic pit, tilted disc with inferior staphyloma, SMARPE, SMACH, and serous retinal detachments that occur in Waldenström macroglobulinaemia. A thorough insight into genetic and other risk factors of these diseases is crucial to unravel their pathogenesis. This is especially important for the diseases for which no effective treatment is currently available. After all, the mechanisms towards the common endpoint of serous SRF accumulation in the macula are diverse and many remain to be elucidated. These different pathways will probably require tailored treatment approaches.

18. Summary and conclusions

A strikingly wide spectrum of diseases and conditions can present with serous SRF in the macula, mimicking CSC. This spectrum ranges from inflammatory diseases and malignancies to genetic diseases and ocular developmental anomalies. Importantly, however, each of these conditions can be distinguished diagnostically from CSC using the appropriate clinical tools and ophthalmological examinations. Indeed, even a basic ophthalmological work-up using fundoscopy and OCT can already provide important clues regarding the correct diagnosis, and additional imaging tests such as FAF, FA, and ICGA can be considered for obtaining a more clear clinical picture. In this respect, using a combination of specific imaging and functional tests is essential for guiding the therapeutic decision-making process and can have important clinical consequences in terms of optimising patient outcome.

Author contributions

(To data curation, formal analysis, investigation, project administration, visualization, writing, reviewing, and editing): EHC van Dijk (65%) and CJF Boon (35%).

Funding sources

This research was supported by the following foundations: Stichting Macula Fonds; Retina Nederland Onderzoek Fonds; Stichting Blinden-Penning; Algemene Nederlandse Vereniging ter Voorkoming van Blindheid; Landelijke Stichting voor Blinden en Slechtzienden, which contributed through UitZicht (Delft, the Netherlands); Rotterdamse Stichting Blindenbelangen (Rotterdam, the Netherlands); Stichting Leids Oogheelkundig Ondersteuningsfonds (Leiden, the Netherlands); Stichting Blindenhulp (The Hague, the Netherlands); Stichting Ooglijders (Rotterdam, the Netherlands); the Gisela Thier Fellowship of Leiden University, Leiden, the Netherlands (to CJFB); and the Netherlands Organization for Scientific Research (VENI grant to CJFB).

These funding organizations provided unrestricted funding and had no role in the design or conduct of the study; the collection, management, analysis, or interpretation of the data; the preparation, review, or approval of the manuscript; or the decision to submit the manuscript for publication. The corresponding author has full access to all of the data in the study and was responsible for the decision to submit for publication.

Declaration of competing interest

None.

References

Acaba-Berrocal, L.A., Lucio-Alvarez, J.A., Mashayekhi, A., Ho, A.C., Dunn, J.P., Shields, C.L., 2018. Birdshot-like chorioretinopathy associated with pembrolizumab treatment. JAMA Ophthalmol 136, 1205–1207.

Agrawal, R., Lavric, A., Restori, M., Pavesio, C., Sagoo, M.S., 2016. Nodular posterior scleritis: clinico-sonographic characteristics and proposed diagnostic criteria. Retina 36, 392–401.

Aguilar, J.P., Green, W.R., 1984. Choroidal rupture. A histopathologic study of 47 cases. Retina 4, 269–275.

Ahlers, C., Geitzenauer, W., Stock, G., Golbaz, I., Schmidt-Erfurth, U., Prunte, C., 2009. Alterations of intraretinal layers in acute central serous chorioretinopathy. Acta Ophthalmol. 87, 511–516.

Ahmed, J., Braun, R.D., Dunn Jr., R., Linsenmeier, R.A., 1993. Oxygen distribution in the macaque retina. Invest. Ophthalmol. Vis. Sci. 34, 516–521.

Ahn, S.J., Woo, S.J., Park, K.H., 2014. Retinal and choroidal changes with severe hypertension and their association with visual outcome. Invest. Ophthalmol. Vis. Sci. 55, 7775–7785.

Ahnelt, P.K., 1998. The photoreceptor mosaic. Eye (Lond) 12 (Pt 3b), 531–540.

Al-Dahmash, S.A., Shields, C.L., Kaliki, S., Johnson, T., Shields, J.A., 2014. Enhanced depth imaging optical coherence tomography of choroidal metastasis in 14 eyes. Retina 34, 1588–1593.

Algethami, A., Talea, M., Alsakran, W.A., Mura, M., Alsulaiman, S.M., 2021 Feb. Persistent subretinal fluid following diabetic tractional retinal detachment repair: risk factors, natural history, and management outcomes. Int. Ophthalmol. 41 (2), 453–464.

Amer, R., Priel, E., Kramer, M., 2015. Spectral-domain optical coherence tomographic features of choroidal neovascular membranes in multifocal choroiditis and punctate inner choroidopathy. Graefes Arch. Clin. Exp. Ophthalmol. 253, 949–957.

Anderson, D.H., Mullins, R.F., Hageman, G.S., Johnson, L.V., 2002. A role for local inflammation in the formation of drusen in the aging eye. Am. J. Ophthalmol. 134, 411–431.

Anderson, D.H., Radeke, M.J., Gallo, N.B., Chapin, E.A., Johnson, P.T., Curletti, C.R., Hancox, L.S., Hu, J., Ebright, J.N., Malek, G., Hauser, M.A., Rickman, C.B., Bok, D., Hageman, G.S., Johnson, L.V., 2010. The pivotal role of the complement system in aging and age-related macular degeneration: hypothesis re-visited. Prog. Retin. Eye Res. 29, 95–112.

Arepalli, S., Kaliki, S., Shields, C.L., 2015. Choroidal metastases: origin, features, and therapy. Indian J. Ophthalmol. 63, 122–127.

Arias, J.D., Kumar, N., Fulco, E.A., Spaide, R., Yannuzzi, L., Shields, J.A., Shields, C.L., 2013. The seasick choroid: a finding on enhanced depth imaging spectral-domain optical coherence tomography of choroidal lymphoma. Retin. Cases Brief Rep. 7, 19–22.

Arnold, J.J., Sarks, J.P., Killingsworth, M.C., Kettle, E.K., Sarks, S.H., 2003. Adult vitelliform macular degeneration: a clinicopathological study. Eye (Lond) 17, 717–726.
Audo, I., Vanakker, O.M., Smith, A., Leroy, B.P., Robson, A.G., Jenkins, S.A., Coucke, P. J., Bird, A.C., De Paepe, A., Holder, G.E., Webster, A.R., 2007. Pseudoxanthoma elasticum with generalized retinal dysfunction, a common finding? Invest. Ophthalmol. Vis. Sci. 48, 4250–4256.
Baker, P.S., Garg, S.J., Fineman, M.S., Chiang, A., Alshareef, R.A., Belmont, J., Brown, G. C., 2013. Serous macular detachment in Waldenstrom macroglobulinemia: a report of four cases. Am. J. Ophthalmol. 155, 448–455.
Balaratnasingam, C., Freund, K.B., Tan, A.M., Mrejen, S., Hunyor, A.P., Keegan, D.J., Dansingani, K.K., Dayani, P.N., Barbazetto, I.A., Sarraf, D., Jampol, L.M., Yannuzzi, L.A., 2016a. Bullous variant of central serous chorioretinopathy: expansion of phenotypic features using multimethod imaging. Ophthalmology 123, 1541–1552.
Balaratnasingam, C., Hoang, Q.V., Inoue, M., Curcio, C.A., Dolz-Marco, R., Yannuzzi, N. A., Dhrami-Gavazi, E., Yannuzzi, L.A., Freund, K.B., 2016b. Clinical characteristics, choroidal neovascularization, and predictors of visual outcomes in acquired vitelliform lesions. Am. J. Ophthalmol. 172, 28–38.
Balaratnasingam, C., Lee, W.K., Koizumi, H., Dansingani, K., Inoue, M., Freund, K.B., 2016c. Polypoidal choroidal vasculopathy: a distinct disease or manifestation of many? Retina 36, 1–8.
Balaratnasingam, C., Messinger, J.D., Sloan, K.R., Yannuzzi, L.A., Freund, K.B., Curcio, C. A., 2017. Histologic and optical coherence tomographic correlates in drusenoid pigment epithelium detachment in age-related macular degeneration. Ophthalmology 124, 644–656.
Barbazetto, I., Dansingani, K.K., Dolz-Marco, R., Giovannini, A., Piccolino, F.C., Agarwal, A., Lima, L.H., Vianna, R.N., Yannuzzi, L.A., 2018. Idiopathic acute exudative polymorphous vitelliform maculopathy: clinical spectrum and multimodal imaging characteristics. Ophthalmology 125, 75–88.
Barry, R.J., Tasiopoulou, A., Murray, P.I., Patel, P.J., Sagoo, M.S., Denniston, A.K., Keane, P.A., 2018. Characteristic optical coherence tomography findings in patients with primary vitreoretinal lymphoma: a novel aid to early diagnosis. Br. J. Ophthalmol. 102, 1362–1366.
Bax, N.M., Valkenburg, D., Lambertus, S., Klevering, B.J., Boon, C.J.F., Holz, F.G., Cremers, F.P.M., Fleckenstein, M., Hoyng, C.B., Lindner, M., 2019. Foveal sparing in central retinal dystrophies. Invest. Ophthalmol. Vis. Sci. 60, 3456–3467.
Beck, A.P., Jampol, L.M., Glaser, D.A., Pollack, J.S., 2004. Is coxsackievirus the cause of unilateral acute idiopathic maculopathy? Arch. Ophthalmol. 122, 121–123.
Bergen, A.A., Arya, S., Koster, C., Pilgrim, M.G., Wiatrek-Moumoulidis, D., van der Spek, P.J., Hauck, S.M., Boon, C.J.F., Emri, E., Stewart, A.J., Lengyel, I., 2019. On the origin of proteins in human drusen: the meet, greet and stick hypothesis. Prog. Retin. Eye Res. 70, 55–84.
Bill, A., Sperber, G., Ujiie, K., 1983. Physiology of the choroidal vascular bed. Int. Ophthalmol. 6, 101–107.
Birnbaum, A.D., Blair, M.P., Tessler, H.H., Goldstein, D.A., 2010. Subretinal fluid in acute posterior multifocal placoid pigment epitheliopathy. Retina 30, 810–814.
Blaauwgeers, H.G., Holtkamp, G.M., Rutten, H., Witmer, A.N., Koolwijk, P., Partanen, T. A., Alitalo, K., Kroon, M.E., Kijlstra, A., van Hinsbergh, V.W., Schlingemann, R.O., 1999. Polarized vascular endothelial growth factor secretion by human retinal pigment epithelium and localization of vascular endothelial growth factor receptors on the inner choriocapillaris. Evidence for a trophic paracrine relation. Am. J. Pathol. 155, 421–428.
Blasi, M.A., Tiberti, A.C., Scupola, A., Balestrazzi, A., Colangelo, E., Valente, P., Balestrazzi, E., 2010. Photodynamic therapy with verteporfin for symptomatic circumscribed choroidal hemangioma: five-year outcomes. Ophthalmology 117, 1630–1637.
Bloch, E., Georgiadis, O., Lukic, M., da Cruz, L., 2019. Optic disc pit maculopathy: new Perspectives on the natural history. Am. J. Ophthalmol. 207, 159–169.
Boesze-Battaglia, K., Goldberg, A.F., 2002. Photoreceptor renewal: a role for peripherin/rds. Int. Rev. Cytol. 217, 183–225.
Boixadera, A., Garcia-Arumi, J., Martinez-Castillo, V., Encinas, J.L., Elizalde, J., Blanco-Mateos, G., Caminal, J., Capeans, C., Armada, F., Navea, A., Olea, J.L., 2009. Prospective clinical trial evaluating the efficacy of photodynamic therapy for symptomatic circumscribed choroidal hemangioma. Ophthalmology 116, 100–105 e101.
Booij, J.C., Baas, D.C., Beisekeeva, J., Gorgels, T.G., Bergen, A.A., 2010. The dynamic nature of Bruch's membrane. Prog. Retin. Eye Res. 29, 1–18.
Boon, C.J., den Hollander, A.I., Hoyng, C.B., Cremers, F.P., Klevering, B.J., Keunen, J.E., 2008a. The spectrum of retinal dystrophies caused by mutations in the peripherin/RDS gene. Prog. Retin. Eye Res. 27, 213–235.
Boon, C.J., Klevering, B.J., Cremers, F.P., Zonneveld-Vrieling, M.N., Theelen, T., Den Hollander, A.I., Hoyng, C.B., 2009a. Central areolar choroidal dystrophy. Ophthalmology 116, 771–782, 782.e771.
Boon, C.J., Klevering, B.J., den Hollander, A.I., Zonneveld, M.N., Theelen, T., Cremers, F. P., Hoyng, C.B., 2007. Clinical and genetic heterogeneity in multifocal vitelliform dystrophy. Arch. Ophthalmol. 125, 1100–1106.
Boon, C.J., Klevering, B.J., Hoyng, C.B., Zonneveld-Vrieling, M.N., Nabuurs, S.B., Blokland, E., Cremers, F.P., den Hollander, A.I., 2008b. Basal laminar drusen caused by compound heterozygous variants in the CFH gene. Am. J. Hum. Genet. 82, 516–523.
Boon, C.J., Klevering, B.J., Leroy, B.P., Hoyng, C.B., Keunen, J.E., den Hollander, A.I., 2009b. The spectrum of ocular phenotypes caused by mutations in the BEST1 gene. Prog. Retin. Eye Res. 28, 187–205.
Boon, C.J., Theelen, T., Hoefsloot, E.H., van Schooneveld, M.J., Keunen, J.E., Cremers, F. P., Klevering, B.J., Hoyng, C.B., 2009c. Clinical and molecular genetic analysis of best vitelliform macular dystrophy. Retina 29, 835–847.
Boon, C.J., van de Kar, N.C., Klevering, B.J., Keunen, J.E., Cremers, F.P., Klaver, C.C., Hoyng, C.B., Daha, M.R., den Hollander, A.I., 2009d. The spectrum of phenotypes caused by variants in the CFH gene. Mol. Immunol. 46, 1573–1594.
Boon, C.J., van de Ven, J.P., Hoyng, C.B., den Hollander, A.I., Klevering, B.J., 2013a. Cuticular drusen: stars in the sky. Prog. Retin. Eye Res. 37, 90–113.
Boon, C.J., van den Born, L.I., Visser, L., Keunen, J.E., Bergen, A.A., Booij, J.C., Riemslag, F.C., Florijn, R.J., van Schooneveld, M.J., 2013b. Autosomal recessive bestrophinopathy: differential diagnosis and treatment options. Ophthalmology 120, 809–820.
Boote, C., Sigal, I.A., Grytz, R., Hua, Y., Nguyen, T.D., Girard, M.J.A., 2020. Scleral structure and biomechanics. Prog. Retin. Eye Res. 74, 100773.
Borgersen, N.J., Møller-Lorentzen, T., Sørensen, T.L., Subhi, Y., 2020. Association between C-reactive protein and polypoidal choroidal vasculopathy: a systematic review and meta-analysis. Acta Ophthalmol. online ahead of print https://pubmed.ncbi.nlm.nih.gov/33124181/.
Boulton, M., Dayhaw-Barker, P., 2001. The role of the retinal pigment epithelium: topographical variation and ageing changes. Eye (Lond) 15, 384–389.
Boulton, M., Moriarty, P., Jarvis-Evans, J., Marcyniuk, B., 1994. Regional variation and age-related changes of lysosomal enzymes in the human retinal pigment epithelium. Br. J. Ophthalmol. 78, 125–129.
Bousquet, E., Beydoun, T., Zhao, M., Hassan, L., Offret, O., Behar-Cohen, F., 2013. Mineralocorticoid receptor antagonism in the treatment of chronic central serous chorioretinopathy: a pilot study. Retina 33, 2096–2102.
Bousquet, E., Dhundass, M., Lehmann, M., Rothschild, P.R., Bayon, V., Leger, D., Bergin, C., Dirani, A., Beydoun, T., Behar-Cohen, F., 2016. Shift work: a risk factor for central serous chorioretinopathy. Am. J. Ophthalmol. 165, 23–28.
Bouzas, E.A., Karadimas, P., Pournaras, C.J., 2002. Central serous chorioretinopathy and glucocorticoids. Surv. Ophthalmol. 47, 431–448.
Breukink, M.B., Dingemans, A.J., den Hollander, A.I., Keunen, J.E., MacLaren, R.E., Fauser, S., Querques, G., Hoyng, C.B., Downes, S.M., Boon, C.J., 2017. Chronic central serous chorioretinopathy: long-term follow-up and vision-related quality of life. Clin. Ophthalmol. (Auckland, N.Z.) 11, 39–46.
Breukink, M.B., Schellevis, R.L., Boon, C.J., Fauser, S., Hoyng, C.B., den Hollander, A.I., de Jong, E.K., 2015. Genomic copy number variations of the complement component C4B gene are associated with chronic central serous chorioretinopathy. Invest. Ophthalmol. Vis. Sci. 56, 5608–5613.
Brinks, J., van Dijk, E.H.C., Habeeb, M., Nikolaou, A., Tsonaka, R., Peters, H.A.B., Sips, H.C.M., van de Merbel, A.F., de Jong, E.K., Notenboom, R.G.E., Kielbasa, S.M., van der Maarel, S.M., Quax, P.H.A., Meijer, O.C., Boon, C.J.F., 2018. The effect of corticosteroids on human choroidal endothelial cells: a model to study central serous chorioretinopathy. Invest. Ophthalmol. Vis. Sci. 59, 5682–5692.
Brinks, J., van Haalen, F.M., van Rijssen, T.J., Biermasz, N.R., Meijer, O.C., Pereira, A.M., Boon, C.J.F., van Dijk, E.H.C., 2021. Central serous chorioretinopathy in active endogenous Cushing's syndrome. Sci. Rep. 11, 2748.
Brown, G.C., Shields, J.A., Goldberg, R.E., 1980. Congenital pits of the optic nerve head. II. Clinical studies in humans. Ophthalmology 87, 51–65.
Browning, D.J., 2003. Choroidal osteoma: observations from a community setting. Ophthalmology 110, 1327–1334.
Bujarborua, D., Borooah, S., Dhillon, B., 2013. Getting serious with retinopathy: approaching an integrated hypothesis for central serous chorioretinopathy. Med. Hypotheses 81, 268–273.
Bujarborua, D., Nagpal, P.N., Deka, M., 2010. Smokestack leak in central serous chorioretinopathy. Graefes Arch. Clin. Exp. Ophthalmol. 248, 339–351.
Caillaux, V., Gaucher, D., Gualino, V., Massin, P., Tadayoni, R., Gaudric, A., 2013. Morphologic characterization of dome-shaped macula in myopic eyes with serous macular detachment. Am. J. Ophthalmol. 156, 958–967 e951.
Carnevali, A., Capuano, V., Sacconi, R., Querques, L., Marchese, A., Rabiolo, A., Souied, E., Scorcia, V., Bandello, F., Querques, G., 2017. OCT angiography of treatment-naïve quiescent choroidal neovascularization in pachychoroid neovasculopathy. Ophthalmol Retina 1, 328–332.
Carvalho-Recchia, C.A., Yannuzzi, L.A., Negrao, S., Spaide, R.F., Freund, K.B., Rodriguez-Coleman, H., Lenharo, M., Iida, T., 2002. Corticosteroids and central serous chorioretinopathy. Ophthalmology 109, 1834–1837.
Castro-Correia, J., Coutinho, M.F., Rosas, V., Maia, J., 1992. Long-term follow-up of central serous retinopathy in 150 patients. Doc. Ophthalmol. 81, 379–386.
Catier, A., Tadayoni, R., Paques, M., Erginay, A., Haouchine, B., Gaudric, A., Massin, P., 2005. Characterization of macular edema from various etiologies by optical coherence tomography. Am. J. Ophthalmol. 140, 200–206.
Celik, E., Dogan, E., Turkoglu, E.B., Cakir, B., Alagoz, G., 2016. Serous retinal detachment in patients with macular edema secondary to branch retinal vein occlusion. Arq. Bras. Oftalmol. 79, 9–11.
Chan, C.C., Whitcup, S.M., Solomon, D., Nussenblatt, R.B., 1995. Interleukin-10 in the vitreous of patients with primary intraocular lymphoma. Am. J. Ophthalmol. 120, 671–673.
Chan, W.M., Lai, T.Y., Lai, R.Y., Liu, D.T., Lam, D.S., 2008. Half-dose verteporfin photodynamic therapy for acute central serous chorioretinopathy: one-year results of a randomized controlled trial. Ophthalmology 115, 1756–1765.
Chan, W.M., Lam, D.S., Lai, T.Y., Yuen, K.S., Liu, D.T., Chan, C.K., Chen, W.Q., 2003. Treatment of choroidal neovascularization in central serous chorioretinopathy by photodynamic therapy with verteporfin. Am. J. Ophthalmol. 136, 836–845.
Chang, Y.C., Cheng, C.K., 2020. Difference between pachychoroid and NONPACHYCHOROID polypoidal choroidal vasculopathy and their response to anti-vascular endothelial growth factor therapy. Retina 40, 1403–1411.

Chao, D.L., Marsiglia, M., Ahmad, B., Sridhar, J., Shah, G.K., de Souza, E.C., Yannuzzi, L. A., Albini, T.A., 2015. Peripapillary serous detachment in multiple evanescent white dot syndrome. Retina 35, 521–524.
Chatziralli, I., Kabanarou, S.A., Parikakis, E., Chatzirallis, A., Xirou, T., Mitropoulos, P., 2017. Risk factors for central serous chorioretinopathy: multivariate approach in a case-control study. Curr. Eye Res. 1–5.
Chatziralli, I., Saitakis, G., Dimitriou, E., Chatzirallis, A., Stoungioti, S., Theodossiadis, G., Theodossiadis, P., 2019. Angioid streaks: a comprehensive review from pathophysiology to treatment. Retina 39, 1–11.
Chen, G., Tzekov, R., Li, W., Jiang, F., Mao, S., Tong, Y., 2017. Subfoveal choroidal thickness in central serous chorioretinopathy: a meta-analysis. PLoS One 12, e0169152.
Cheung, C.M., Lai, T.Y., Chen, S.J., Chong, V., Lee, W.K., Htoon, H., Ng, W.Y., Ogura, Y., Wong, T.Y., 2014. Understanding indocyanine green angiography in polypoidal choroidal vasculopathy: the group experience with digital fundus photography and confocal scanning laser ophthalmoscopy. Retina (Philadelphia, Pa.) 34, 2397–2406.
Cheung, C.M.G., Lai, T.Y.Y., Ruamviboonsuk, P., Chen, S.J., Chen, Y., Freund, K.B., Gomi, F., Koh, A.H., Lee, W.K., Wong, T.Y., 2018. Polypoidal choroidal vasculopathy: definition, pathogenesis, diagnosis, and management. Ophthalmology 125, 708–724.
Cheung, C.M.G., Lee, W.K., Koizumi, H., Dansingani, K., Lai, T.Y.Y., Freund, K.B., 2019. Pachychoroid disease. Eye (Lond) 33, 14–33.
Chhablani, J., Cohen, F.B., 2020. Multimodal imaging-based central serous chorioretinopathy classification. Ophthalmol Retina 4, 1043–1046.
Chong, N.H., Keonin, J., Luthert, P.J., Frennesson, C.I., Weingeist, D.M., Wolf, R.L., Mullins, R.F., Hageman, G.S., 2005. Decreased thickness and integrity of the macular elastic layer of Bruch's membrane correspond to the distribution of lesions associated with age-related macular degeneration. Am. J. Pathol. 166, 241–251.
Chowers, I., Tiosano, L., Audo, I., Grunin, M., Boon, C.J., 2015. Adult-onset foveomacular vitelliform dystrophy: a fresh perspective. Prog. Retin. Eye Res. 47, 64–85.
Chung, H., Byeon, S.H., Freund, K.B., 2017. Focal choroidal excavation and its association with pachychoroid spectrum disorders: a review of the literature and multimodal imaging findings. Retina 37, 199–221.
Cohen, S.Y., Quentel, G., Guiberteau, B., Delahaye-Mazza, C., Gaudric, A., 1998. Macular serous retinal detachment caused by subretinal leakage in tilted disc syndrome. Ophthalmology 105, 1831–1834.
Conley, S.M., Naash, M.I., 2014. Gene therapy for PRPH2-associated ocular disease: challenges and prospects. Cold Spring Harbor Perspect. Med. 4 a017376.
Conrad, R., Geiser, F., Kleiman, A., Zur, B., Karpawitz-Godt, A., 2014. Temperament and character personality profile and illness-related stress in central serous chorioretinopathy. Sci. World J. 631687, 2014.
Coscas, G., Lupidi, M., Coscas, F., Benjelloun, F., Zerbib, J., Dirani, A., Semoun, O., Souied, E.H., 2015. Toward a specific classification of polypoidal choroidal vasculopathy: idiopathic disease or subtype of age-related macular degeneration. Invest. Ophthalmol. Vis. Sci. 56, 3187–3195.
Cowan, C.S., Renner, M., De Gennaro, M., Gross-Scherf, B., Goldblum, D., Hou, Y., Munz, M., Rodrigues, T.M., Krol, J., Szikra, T., Cuttat, R., Waldt, A., Papasaikas, P., Diggelmann, R., Patino-Alvarez, C.P., Galliker, P., Spirig, S.E., Pavlinic, D., Gerber-Hollbach, N., Schuierer, S., Srdanovic, A., Balogh, M., Panero, R., Kusnyerik, A., Szabo, A., Stadler, M.B., Orgül, S., Picelli, S., Hasler, P.W., Hierlemann, A., Scholl, H. P.N., Roma, G., Nigsch, F., Roska, B., 2020. Cell types of the human retina and its organoids at single-cell resolution. Cell 182, 1623–1640 e1634.
Cukras, C., Agron, E., Klein, M.L., Ferris 3rd, F.L., Chew, E.Y., Gensler, G., Wong, W.T., 2010. Natural history of drusenoid pigment epithelial detachment in age-related macular degeneration: age-Related Eye Disease Study Report No. 28. Ophthalmology 117, 489–499.
Curcio, C.A., 2001. Photoreceptor topography in ageing and age-related maculopathy. Eye (Lond) 15, 376–383.
Curcio, C.A., 2018. Soft drusen in age-related macular degeneration: biology and targeting via the oil spill strategies. Invest. Ophthalmol. Vis. Sci. 59, Amd160–amd181.
Curcio, C.A., Allen, K.A., Sloan, K.R., Lerea, C.L., Hurley, J.B., Klock, I.B., Milam, A.H., 1991. Distribution and morphology of human cone photoreceptors stained with anti-blue opsin. J. Comp. Neurol. 312, 610–624.
Curcio, C.A., Johnson, M., Huang, J.D., Rudolf, M., 2009. Aging, age-related macular degeneration, and the response-to-retention of apolipoprotein B-containing lipoproteins. Prog. Retin. Eye Res. 28, 393–422.
Curcio, C.A., Millican, C.L., Allen, K.A., Kalina, R.E., 1993. Aging of the human photoreceptor mosaic: evidence for selective vulnerability of rods in central retina. Invest. Ophthalmol. Vis. Sci. 34, 3278–3296.
Curcio, C.A., Sloan, K.R., Kalina, R.E., Hendrickson, A.E., 1990. Human photoreceptor topography. J. Comp. Neurol. 292, 497–523.
Dalvin, L.A., Pennington, J.D., Mashayekhi, A., Shields, C.L., 2021 May 1. Multimodal imaging OF macular choroidal macrovessel: a report OF TWO cases. Retin. Cases Brief Rep. 15 (3), 218–223.
Danjuma, M.I., Mukherjee, I., Makaronidis, J., Osula, S., 2014. Converging indications of aldosterone antagonists (spironolactone and eplerenone): a narrative review of safety profiles. Curr. Hypertens. Rep. 16, 414.
Dansingani, K.K., Balaratnasingam, C., Naysan, J., Freund, K.B., 2016. EN face imaging OF pachychoroid spectrum disorders with swept-source optical coherence tomography. Retina 36, 499–516.
Dansingani, K.K., Gal-Or, O., Sadda, S.R., Yannuzzi, L.A., Freund, K.B., 2018. Understanding aneurysmal type 1 neovascularization (polypoidal choroidal vasculopathy): a lesson in the taxonomy of 'expanded spectra' - a review. Clin. Exp. Ophthalmol. 46, 189–200.
Daruich, A., Matet, A., Dirani, A., Bousquet, E., Zhao, M., Farman, N., Jaisser, F., Behar-Cohen, F., 2015. Central serous chorioretinopathy: recent findings and new physiopathology hypothesis. Prog. Retin. Eye Res. 48, 82–118.
Daruich, A., Matet, A., Moulin, A., Kowalczuk, L., Nicolas, M., Sellam, A., Rothschild, P. R., Omri, S., Gélizé, E., Jonet, L., Delaunay, K., De Kozak, Y., Berdugo, M., Zhao, M., Crisanti, P., Behar-Cohen, F., 2018. Mechanisms of macular edema: beyond the surface. Prog. Retin. Eye Res. 63, 20–68.
Das, A., McGuire, P.G., Rangasamy, S., 2015. Diabetic macular edema: pathophysiology and novel therapeutic targets. Ophthalmology 122, 1375–1394.
Davies, A.J., Kelly, S.P., Naylor, S.G., Bhatt, P.R., Mathews, J.P., Sahni, J., Haslett, R., McKibbin, M., 2012. Adverse ophthalmic reaction in poppers users: case series of 'poppers maculopathy. Eye (Lond) 26, 1479–1486.
De Bats, F., Cornut, P.L., Wolff, B., Kodjikian, L., Mauget-Faÿsse, M., 2018. Dark and white lesions observed in central serous chorioretinopathy on optical coherence tomography angiography. Eur. J. Ophthalmol. 28, 446–453.
de Groot, E.L., Ten Dam-van Loon, N.H., de Boer, J.H., Ossewaarde-van Norel, J., 2020 Dec. The efficacy of corticosteroid-sparing immunomodulatory therapy in treating patients with central multifocal choroiditis. Acta Ophthalmol. 98 (8), 816–821.
de Jong, E.K., Breukink, M.B., Schellevis, R.L., Bakker, B., Mohr, J.K., Fauser, S., Keunen, J.E., Hoyng, C.B., den Hollander, A.I., Boon, C.J., 2015. Chronic central serous chorioretinopathy is associated with genetic variants implicated in age-related macular degeneration. Ophthalmology 122, 562–570.
de Jong, P.T., 2006. Age-related macular degeneration. N. Engl. J. Med. 355, 1474–1485.
de Laat, P., Smeitink, J.A., Janssen, M.C., Keunen, J.E., Boon, C.J., 2013. Mitochondrial retinal dystrophy associated with the m.3243A>G mutation. Ophthalmology 120, 2684–2696.
Demirel, S., Batioglu, F., Ozmert, E., Batioglu, F., 2014. Unilateral acute maculopathy related to hand, foot, and mouth disease: OCT and fluorescein angiography findings of a very rare disease. Eur. J. Ophthalmol. 24, 131–133.
Deuel, T.F., Davis, P., Avioli, L.V., 1983. Waldenstrom's macroglobulinemia. Arch. Intern. Med. 143, 986–988.
Deutman, A.F., 1969. Electro-oculography in families with vitelliform dystrophy of the fovea. Detection of the carrier state. Arch. Ophthalmol. 81, 305–316.
Dolz-Marco, R., Saffra, N.A., Freund, K.B., 2017. Torpedo maculopathy presenting with a vitelliform lesion. Retina 37, e19–e20.
Dorey, C.K., Wu, G., Ebenstein, D., Garsd, A., Weiter, J.J., 1989. Cell loss in the aging retina. Relationship to lipofuscin accumulation and macular degeneration. Invest. Ophthalmol. Vis. Sci. 30, 1691–1699.
Doro, D., Visentin, S., Maimone, P.E., Pilotto, E., 2005. High-resolution ultrasonography in central serous chorioretinopathy. Am. J. Ophthalmol. 139, 550–552.
Doycheva, D., Zierhut, M., Susskind, D., Bartz-Schmidt, K.U., Deuter, C., 2015. [Diagnostics and treatment of choroidal lymphoma]. Ophthalmologe 112, 217–222.
Du, L., Kijlstra, A., Yang, P., 2016. Vogt-Koyanagi-Harada disease: novel insights into pathophysiology, diagnosis and treatment. Prog. Retin. Eye Res. 52, 84–111.
Duong, H.V., McLean, I.W., Beahm, D.E., 2006. Bilateral diffuse melanocytic proliferation associated with ovarian carcinoma and metastatic malignant amelanotic melanoma. Am. J. Ophthalmol. 142, 693–695.
Dvoriashyna, M., Foss, A.J.E., Gaffney, E.A., Repetto, R., 2020. Fluid and solute transport across the retinal pigment epithelium: a theoretical model. J. R. Soc. Interface 17, 20190735.
Eandi, C.M., Ober, M., Iranmanesh, R., Peiretti, E., Yannuzzi, L.A., 2005. Acute central serous chorioretinopathy and fundus autofluorescence. Retina 25, 989–993.
Eksandh, L., Adamus, G., Mosgrove, L., Andreasson, S., 2008. Autoantibodies against bestrophin in a patient with vitelliform paraneoplastic retinopathy and a metastatic choroidal malignant melanoma. Arch. Ophthalmol. 126, 432–435.
Elagouz, M., Stanescu-Segall, D., Jackson, T.L., 2010. Uveal effusion syndrome. Surv. Ophthalmol. 55, 134–145.
Ellabban, A.A., Tsujikawa, A., Matsumoto, A., Yamashiro, K., Oishi, A., Ooto, S., Nakata, I., Akagi-Kurashige, Y., Miyake, M., Elnahas, H.S., Radwan, T.M., Zaky, K.A., Yoshimura, N., 2013. Three-dimensional tomographic features of dome-shaped macula by swept-source optical coherence tomography. Am. J. Ophthalmol. 155, 320–328 e322.
Entezari, M., Karimi, S., Ramezani, A., Nikkhah, H., Fekri, Y., Kheiri, B., 2018. Choroidal thickness in healthy subjects. J. Ophthalmic Vis. Res. 13, 39–43.
Erbagci, I., Karaca, M., Ugur, M.G., Okumus, S., Bekir, N.A., 2008. Ophthalmic manifestations of 107 cases with hemolysis, elevated liver enzymes and low platelet count syndrome. Saudi Med. J. 29, 1160–1163.
Errera, M.H., Michaelides, M., Keane, P.A., Restori, M., Paques, M., Moore, A.T., Yeoh, J., Chan, D., Egan, C.A., Patel, P.J., Tufail, A., 2014. The extended clinical phenotype of dome-shaped macula. Graefes Arch. Clin. Exp. Ophthalmol. 252, 499–508.
Ersoz, M.G., Arf, S., Hocaoglu, M., Sayman Muslubas, I., Karacorlu, M., 2019. Patient characteristics and risk factors for central serous chorioretinopathy: an analysis of 811 patients. Br. J. Ophthalmol. 103, 725–729.
Faure, C., Salame, N., Cahuzac, A., Mauget-Faysse, M., Scemama, C., 2020. Hair dye-induced retinopathy mimicking MEK-inhibitor retinopathy. Retin. Cases Brief Rep. online ahead of print https://pubmed.ncbi.nlm.nih.gov/31971924/.
Fawcett, R.J., Osborne, N.N., 2007. Flupirtine attenuates sodium nitroprusside-induced damage to retinal photoreceptors, in situ. Brain Res. Bull. 73, 278–288.
Federman, J.L., Shields, J.A., Tomer, T.L., 1975. Angioid streaks. II. Fluorescein angiographic features. Arch. Ophthalmol. 93, 951–962.
Feeney-Burns, L., Hilderbrand, E.S., Eldridge, S., 1984. Aging human RPE: morphometric analysis of macular, equatorial, and peripheral cells. Invest. Ophthalmol. Vis. Sci. 25, 195–200.
Ficker, L., Vafidis, G., While, A., Leaver, P., 1988. Long-term follow-up of a prospective trial of argon laser photocoagulation in the treatment of central serous retinopathy. Br. J. Ophthalmol. 72, 829–834.

Fields, M.A., Del Priore, L.V., Adelman, R.A., Rizzolo, L.J., 2020. Interactions of the choroid, Bruch's membrane, retinal pigment epithelium, and neurosensory retina collaborate to form the outer blood-retinal-barrier. Prog. Retin. Eye Res. 76, 100803.
Finger, R.P., Charbel Issa, P., Ladewig, M.S., Götting, C., Szliska, C., Scholl, H.P., Holz, F. G., 2009. Pseudoxanthoma elasticum: genetics, clinical manifestations and therapeutic approaches. Surv. Ophthalmol. 54, 272–285.
Flores-Moreno, I., Caminal, J.M., Arias-Barquet, L., Rubio-Caso, M.J., Catala-Mora, J., Vidal-Martí, M., Muñoz-Blanco, A., Filloy, A., Ruiz-Moreno, J.M., Duker, J.S., Arruga, J., 2016. En face mode of swept-source optical coherence tomography in circumscribed choroidal haemangioma. Br. J. Ophthalmol. 100, 360–364.
Fok, A.C., Chan, P.P., Lam, D.S., Lai, T.Y., 2011. Risk factors for recurrence of serous macular detachment in untreated patients with central serous chorioretinopathy. Ophthalmic Res. 46, 160–163.
Francis, J.H., Habib, L.A., Abramson, D.H., Yannuzzi, L.A., Heinemann, M., Gounder, M. M., Grisham, R.N., Postow, M.A., Shoushtari, A.N., Chi, P., Segal, N.H., Yaeger, R., Ho, A.L., Chapman, P.B., Catalanotti, F., 2017. Clinical and morphologic characteristics of MEK inhibitor-associated retinopathy: differences from central serous chorioretinopathy. Ophthalmology 124, 1788–1798.
Fraser-Bell, S., Symes, R., Vaze, A., 2017. Hypertensive eye disease: a review. Clin. Exp. Ophthalmol. 45, 45–53.
Freidman, A.H., Marchevsky, A., Odel, J.G., Gerber, M.A., Thung, S.N., 1980. Immunofluorescent studies of the eye in Waldenström's macroglobulinemia. Arch. Ophthalmol. 98, 743–746.
Frenkel, S., Hendler, K., Siegal, T., Shalom, E., Pe'er, J., 2008. Intravitreal methotrexate for treating vitreoretinal lymphoma: 10 years of experience. Br. J. Ophthalmol. 92, 383–388.
Freund, K.B., Laud, K., Lima, L.H., Spaide, R.F., Zweifel, S., Yannuzzi, L.A., 2011. Acquired Vitelliform Lesions: correlation of clinical findings and multiple imaging analyses. Retina (Philadelphia, Pa.) 31, 13–25.
Freund, K.B., Yannuzzi, L.A., Barile, G.R., Spaide, R.F., Milewski, S.A., Guyer, D.R., 1996. The expanding clinical spectrum of unilateral acute idiopathic maculopathy. Arch. Ophthalmol. 114, 555–559.
Fujiwara, T., Imamura, Y., Margolis, R., Slakter, J.S., Spaide, R.F., 2009. Enhanced depth imaging optical coherence tomography of the choroid in highly myopic eyes. Am. J. Ophthalmol. 148, 445–450.
Fung, A.T., Yannuzzi, L.A., Freund, K.B., 2012. Type 1 (sub-retinal pigment epithelial) neovascularization in central serous chorioretinopathy masquerading as neovascular age-related macular degeneration. Retina (Philadelphia, Pa.) 32, 1829–1837.
Gackle, H.C., Lang, G.E., Freissler, K.A., Lang, G.K., 1998. [Central serous chorioretinopathy. Clinical, fluorescein angiography and demographic aspects]. Ophthalmologe 95, 529–533.
Gal-Or, O., Dansingani, K.K., Sebrow, D., Dolz-Marco, R., Freund, K.B., 2018. Inner choroidal flow signal attenuation IN pachychoroid disease: optical coherence tomography angiography. Retina 38, 1984–1992.
Gallego-Pinazo, R., Dolz-Marco, R., Pardo-Lopez, D., Martinez-Castillo, S., Lleo-Perez, A., Arevalo, J.F., Diaz-Llopis, M., 2013. Ranibizumab for serous macular detachment in branch retinal vein occlusions. Graefe's archive for clinical and experimental ophthalmology = Albrecht von Graefes Archiv fur klinische und experimentelle Ophthalmologie 251, 9–14.
Gass, J.D., 1974. A clinicopathologic study of a peculiar foveomacular dystrophy. Trans. Am. Ophthalmol. Soc. 72, 139–156.
Gass, J.D., Chuang, E.L., Granek, H., 1988. Acute exudative polymorphous vitelliform maculopathy. Trans. Am. Ophthalmol. Soc. 86, 354–366.
Gass, J.D., Gieser, R.G., Wilkinson, C.P., Beahm, D.E., Pautler, S.E., 1990. Bilateral diffuse uveal melanocytic proliferation in patients with occult carcinoma. Arch. Ophthalmol. 108, 527–533.
Gass, J.D., Jallow, S., 1982. Idiopathic serous detachment of the choroid, ciliary body, and retina (uveal effusion syndrome). Ophthalmology 89, 1018–1032.
Gaucher, D., Erginay, A., Lecleire-Collet, A., Haouchine, B., Puech, M., Cohen, S.Y., Massin, P., Gaudric, A., 2008. Dome-shaped macula in eyes with myopic posterior staphyloma. Am. J. Ophthalmol. 145, 909–914.
Geerlings, M.J., de Jong, E.K., den Hollander, A.I., 2017. The complement system in age-related macular degeneration: a review of rare genetic variants and implications for personalized treatment. Mol. Immunol. 84, 65–76.
Gemenetzi, M., De Salvo, G., Lotery, A.J., 2010. Central serous chorioretinopathy: an update on pathogenesis and treatment. Eye (London, England) 24, 1743–1756.
Ghazi, N.G., Green, W.R., 2002. Pathology and pathogenesis of retinal detachment. Eye (Lond) 16, 411–421.
Gilbert, C.M., Owens, S.L., Smith, P.D., Fine, S.L., 1984. Long-term follow-up of central serous chorioretinopathy. Br. J. Ophthalmol. 68, 815–820.
Gliem, M., Finger, R.P., Fimmers, R., Brinkmann, C.K., Holz, F.G., Charbel Issa, P., 2013. Treatment of choroidal neovascularization due to angioid streaks: a comprehensive review. Retina 33, 1300–1314.
Goichot, B., Weibel, L., Chapotot, F., Gronfier, C., Piquard, F., Brandenberger, G., 1998. Effect of the shift of the sleep-wake cycle on three robust endocrine markers of the circadian clock. Am. J. Physiol. 275, E243–E248.
Golchet, P.R., Jampol, L.M., Mathura Jr., J.R., Daily, M.J., 2010. Torpedo maculopathy. Br. J. Ophthalmol. 94, 302–306.
Gomi, F., Sawa, M., Mitarai, K., Tsujikawa, M., Tano, Y., 2007. Angiographic lesion of polypoidal choroidal vasculopathy on indocyanine green and fluorescein angiography. Graefe's archive for clinical and experimental ophthalmology = Albrecht von Graefes Archiv fur klinische und experimentelle Ophthalmologie 245, 1421–1427.
Granstam, E., Nilsson, S.F., 1990. Non-adrenergic sympathetic vasoconstriction in the eye and some other facial tissues in the rabbit. Eur. J. Pharmacol. 175, 175–186.
Green, W.R., 1999. Histopathology of age-related macular degeneration. Mol. Vis. 5, 27.
Grisanti, S., Tatar, O., 2008. The role of vascular endothelial growth factor and other endogenous interplayers in age-related macular degeneration. Prog. Retin. Eye Res. 27, 372–390.
Grosso, A., Veglio, F., Porta, M., Grignolo, F.M., Wong, T.Y., 2005. Hypertensive retinopathy revisited: some answers, more questions. Br. J. Ophthalmol. 89, 1646–1654.
Guigui, B., Semoun, O., Querques, G., Coscas, G., Soubrane, G., Souied, E.H., 2009. Indocyanine green angiography features of central areolar choroidal dystrophy. Retin. Cases Brief Rep. 3, 434–437.
Gunduz, K., Shields, J.A., Shields, C.L., Eagle Jr., R.C., Diniz, W., Mercado, G., Chang, W., 1999. Transscleral choroidal biopsy in the diagnosis of choroidal lymphoma. Surv. Ophthalmol. 43, 551–555.
Gupta, A., Raman, R., Kulothungan, V., Sharma, T., 2014. Association of systemic and ocular risk factors with neurosensory retinal detachment in diabetic macular edema: a case-control study. BMC Ophthalmol. 14, 47.
Guymer, R., Luthert, P., Bird, A., 1999. Changes in Bruch's membrane and related structures with age. Prog. Retin. Eye Res. 18, 59–90.
Habot-Wilner, Z., Zur, D., Goldstein, M., Goldenberg, D., Shulman, S., Kesler, A., Giladi, M., Neudorfer, M., 2011. Macular findings on optical coherence tomography in cat-scratch disease neuroretinitis. Eye (Lond) 25, 1064–1068.
Hageman, G.S., Luthert, P.J., Victor Chong, N.H., Johnson, L.V., Anderson, D.H., Mullins, R.F., 2001. An integrated hypothesis that considers drusen as biomarkers of immune-mediated processes at the RPE-Bruch's membrane interface in aging and age-related macular degeneration. Prog. Retin. Eye Res. 20, 705–732.
Haimovici, R., Koh, S., Gagnon, D.R., Lehrfeld, T., Wellik, S., 2004. Risk factors for central serous chorioretinopathy: a case-control study. Ophthalmology 111, 244–249.
Haimovici, R., Rumelt, S., Melby, J., 2003. Endocrine abnormalities in patients with central serous chorioretinopathy. Ophthalmology 110, 698–703.
Hansen, M.S., Klefter, O.N., Larsen, M., 2014. Retinal degeneration and persistent serous detachment in the absence of active choroidal neovascularization in pseudoxanthoma elasticum. Acta Ophthalmol. 92, e156–157.
Havener, W.H., 1985. Centripetal subretinal flow. Ann. Ophthalmol. 17 (270), 272–273.
Hayreh, S.S., 1975. Segmental nature of the choroidal vasculature. Br. J. Ophthalmol. 59, 631–648.
Hayreh, S.S., 1990. In vivo choroidal circulation and its watershed zones. Eye (Lond) 4 (Pt 2), 273–289.
Hayreh, S.S., 2004. Posterior ciliary artery circulation in health and disease: the Weisenfeld lecture. Invest. Ophthalmol. Vis. Sci. 45, 749–757, 748.
Higgins, T.P., Khoo, C.T., Magrath, G., Shields, C.L., 2016. Flat choroidal melanoma masquerading as central serous chorioretinopathy. Oman J. Ophthalmol. 9, 174–176.
Hilely, A., Au, A., Freund, K.B., Loewenstein, A., Souied, E.H., Zur, D., Sacconi, R., Borrelli, E., Peiretti, E., Iovino, C., Sugiura, Y., Ellabban, A.A., Monés, J., Waheed, N. K., Ozdek, S., Yalinbas, D., Thiele, S., de Moura Mendonça, L.S., Lee, M.Y., Lee, W.K., Turcotte, P., Capuano, V., Filali Ansary, M., Chakravarthy, U., Lommatzsch, A., Gunnemann, F., Pauleikhoff, D., Ip, M.S., Querques, G., Holz, F.G., Spaide, R.F., Sadda, S., Sarraf, D., 2020. Non-neovascular age-related macular degeneration with subretinal fluid. Br. J. Ophthalmol. online ahead of print https://pubmed.ncbi.nlm.nih.gov/32920528/.
Ho, I.V., Yannuzzi, L., 2008. Chronic central serous chorioretinopathy and fundus autofluorescence. Retin. Cases Brief Rep. 2, 1–5.
Ho, Y.F., Chao, A., Chen, K.J., Chao, A.N., Wang, N.K., Liu, L., Chen, Y.P., Hwang, Y.S., Wu, W.C., Lai, C.C., Chen, T.L., 2018. Clinical outcomes and predictors of response to photodynamic therapy in symptomatic circumscribed choroidal hemangioma: a retrospective case series. PLoS One 13, e0197088.
Hollenberg, M.J., Lea, P.J., 1988. High resolution scanning electron microscopy of the retinal pigment epithelium and Bruch's layer. Invest. Ophthalmol. Vis. Sci. 29, 1380–1389.
Hosoda, Y., Yoshikawa, M., Miyake, M., Tabara, Y., Ahn, J., Woo, S.J., Honda, S., Sakurada, Y., Shiragami, C., Nakanishi, H., Oishi, A., Ooto, S., Miki, A., Iida, T., Iijima, H., Nakamura, M., Khor, C.C., Wong, T.Y., Song, K., Park, K.H., Yamada, R., Matsuda, F., Tsujikawa, A., Yamashiro, K., 2018. CFH and VIPR2 as susceptibility loci in choroidal thickness and pachychoroid disease central serous chorioretinopathy. Proc. Natl. Acad. Sci. U. S. A. 115, 6261–6266.
Hoyng, C.B., Deutman, A.F., 1996. The development of central areolar choroidal dystrophy. Graefes Arch. Clin. Exp. Ophthalmol. 234, 87–93.
Hu, W., Criswell, M.H., Fong, S.L., Temm, C.J., Rajashekhar, G., Cornell, T.L., Clauss, M. A., 2009. Differences in the temporal expression of regulatory growth factors during choroidal neovascular development. Exp. Eye Res. 88, 79–91.
Hughes, E.H., Hunyor, A.P., Gorbatov, M., Ho, I.V., 2012. Acute idiopathic maculopathy with coxsackievirus infection. Retin. Cases Brief Rep. 6, 19–21.
Hui, M., Galvin, J., Chilov, M., Gabrielle, P.H., Fung, A.T., 2020. Popper maculopathy: long-term follow-up and case series. Retin. Cases Brief Rep. 14, 195–199.
Hussain, A.A., Lee, Y., Marshall, J., 2020. Understanding the complexity of the matrix metalloproteinase system and its relevance to age-related diseases: age-related macular degeneration and Alzheimer's disease. Prog. Retin. Eye Res. 74, 100775.
Iannuzzi, M.C., Rybicki, B.A., Teirstein, A.S., 2007. Sarcoidosis. N. Engl. J. Med. 357, 2153–2165.
Ie, D., Yannuzzi, L.A., Spaide, R.F., Rabb, M.F., Blair, N.P., Daily, M.J., 1993. Subretinal exudative deposits in central serous chorioretinopathy. Br. J. Ophthalmol. 77, 349–353.
Iida, T., Kishi, S., Hagimura, N., Shimizu, K., 1999. Persistent and bilateral choroidal vascular abnormalities in central serous chorioretinopathy. Retina 19, 508–512.
Ikuno, Y., 2017. Overview OF the complications OF high myopia. Retina 37, 2347–2351.

Imamura, Y., Fujiwara, T., Margolis, R., Spaide, R.F., 2009. Enhanced depth imaging optical coherence tomography of the choroid in central serous chorioretinopathy. Retina (Philadelphia, Pa.) 29, 1469–1473.
Imamura, Y., Iida, T., Maruko, I., Zweifel, S.A., Spaide, R.F., 2011. Enhanced depth imaging optical coherence tomography of the sclera in dome-shaped macula. Am. J. Ophthalmol. 151, 297–302.
Iovino, C., Chhablani, J., Parameswarappa, D.C., Pellegrini, M., Giannaccare, G., Peiretti, E., 2019. Retinal pigment epithelium apertures as a late complication of longstanding serous pigment epithelium detachments in chronic central serous chorioretinopathy. Eye (Lond) 33, 1871–1876.
Ishibashi, K., Tian, J., Handa, J.T., 2004. Similarity of mRNA phenotypes of morphologically normal macular and peripheral retinal pigment epithelial cells in older human eyes. Invest. Ophthalmol. Vis. Sci. 45, 3291–3301.
Ishikawa, M., Sawada, Y., Yoshitomi, T., 2015. Structure and function of the interphotoreceptor matrix surrounding retinal photoreceptor cells. Exp. Eye Res. 133, 3–18.
Jain, N., Johnson, M.W., 2014. Pathogenesis and treatment of maculopathy associated with cavitary optic disc anomalies. Am. J. Ophthalmol. 158, 423–435.
Jansen, J.C., Van Calster, J., Pulido, J.S., Miles, S.L., Vile, R.G., Van Bergen, T., Cassiman, C., Spielberg, L.H., Leys, A.M., 2015. Early diagnosis and successful treatment of paraneoplastic melanocytic proliferation. Br. J. Ophthalmol. 99, 943–948.
Jiang, L.Q., Jorquera, M., Streilein, J.W., 1993. Subretinal space and vitreous cavity as immunologically privileged sites for retinal allografts. Invest. Ophthalmol. Vis. Sci. 34, 3347–3354.
Johnson, A.A., Guziewicz, K.E., Lee, C.J., Kalathur, R.C., Pulido, J.S., Marmorstein, L.Y., Marmorstein, A.D., 2017. Bestrophin 1 and retinal disease. Prog. Retin. Eye Res. 58, 45–69.
Joseph, A., Rahimy, E., Sarraf, D., 2014. Bilateral diffuse uveal melanocytic proliferation with multiple iris cysts. JAMA Ophthalmol 132, 756–760.
Jurjevic, D., Böni, C., Barthelmes, D., Fasler, K., Becker, M., Michels, S., Stemmle, J., Herbort, C., Zweifel, S.A., 2017. Torpedo maculopathy associated with choroidal neovascularization. Klin Monbl Augenheilkd 234, 508–514.
Kaarniranta, K., Uusitalo, H., Blasiak, J., Felszeghy, S., Kannan, R., Kauppinen, A., Salminen, A., Sinha, D., Ferrington, D., 2020. Mechanisms of mitochondrial dysfunction and their impact on age-related macular degeneration. Prog. Retin. Eye Res. 79, 100858.
Kane Dickson, V., Pedi, L., Long, S.B., 2014. Structure and insights into the function of a Ca(2+)-activated Cl(-) channel. Nature 516, 213–218.
Karampelas, M., Soumplis, V., Karagiannis, D., Parikakis, E., Webster, A.R., 2013. An atypical case of choroidal neovascularization associated with pseudoxanthoma elasticum treated with intravitreal bevacizumab: a case report. BMC Res. Notes 6, 530.
Kaye, R., Chandra, S., Sheth, J., Boon, C.J.F., Sivaprasad, S., Lotery, A., 2020. Central serous chorioretinopathy: an update on risk factors, pathophysiology and imaging modalities. Prog. Retin. Eye Res. 100865.
Khan, M.A., DeCroos, F.C., Storey, P.P., Shields, J.A., Garg, S.J., Shields, C.L., 2014. Outcomes of anti-vascular endothelial growth factor therapy in the management of choroidal neovascularization associated with choroidal osteoma. Retina 34, 1750–1756.
Kijlstra, A., Tian, Y., Kelly, E.R., Berendschot, T.T., 2012. Lutein: more than just a filter for blue light. Prog. Retin. Eye Res. 31, 303–315.
Kim, R.Y., Chung, D.H., Kim, M., Park, Y.H., 2020. Use OF choroidal vascularity index for choroidal structural evaluation IN central serous chorioretinopathy with choroidal neovascularization. Retina 40, 1395–1402.
Kincaid, M.C., Green, W.R., 1983. Ocular and orbital involvement in leukemia. Surv. Ophthalmol. 27, 211–232.
Kirchhof, B., Ryan, S.J., 1993. Differential permeance of retina and retinal pigment epithelium to water: implications for retinal adhesion. Int. Ophthalmol. 17, 19–22.
Kishimoto, T., Fukuda, K., Nishiuchi, T., Hayashi, N., Fukushima, A., 2019. Unilateral serous retinal detachment with choroidal thickening as a first presenting sign of acute myeloid leukemia. Am J Ophthalmol Case Rep 14, 51–54.
Kitajima, Y., Maruyama-Inoue, M., Ito, A., Sato, S., Inoue, T., Yamane, S., Kadonosono, K., 2020. One-year outcome of combination therapy with intravitreal anti-vascular endothelial growth factor and photodynamic therapy in patients with pachychoroid neovasculopathy. Graefes Arch. Clin. Exp. Ophthalmol. 258, 1279–1285.
Kitaya, N., Nagaoka, T., Hikichi, T., Sugawara, R., Fukui, K., Ishiko, S., Yoshida, A., 2003. Features of abnormal choroidal circulation in central serous chorioretinopathy. Br. J. Ophthalmol. 87, 709–712.
Kitzmann, A.S., Pulido, J.S., Diehl, N.N., Hodge, D.O., Burke, J.P., 2008. The incidence of central serous chorioretinopathy in Olmsted County, Minnesota, 1980-2002. Ophthalmology 115, 169–173.
Klaassen, I., Van Noorden, C.J., Schlingemann, R.O., 2013. Molecular basis of the inner blood-retinal barrier and its breakdown in diabetic macular edema and other pathological conditions. Prog. Retin. Eye Res. 34, 19–48.
Klemp, K., Kiilgaard, J.F., Heegaard, S., Norgaard, T., Andersen, M.K., Prause, J.U., 2017. Bilateral diffuse uveal melanocytic proliferation: case report and literature review. Acta Ophthalmol. 95, 439–445.
Kniggendorf, V.F., Neto, E.T., Maia, E.M., Grando, J.P.S., Bardal, A.M.C., Beato, P.M.M., Torres, C.C., Maia, M., 2018. Bilateral diffuse uveal melanocytic proliferation associated with renal cancer: the importance OF indocyanine green angiography and early diagnosis. Retin. Cases Brief Rep. 12, 166–171.
Kociok, N., Joussen, A.M., 2007. Varied expression of functionally important genes of RPE and choroid in the macula and in the periphery of normal human eyes. Graefes Arch. Clin. Exp. Ophthalmol. 245, 101–113.
Koh, A., Lee, W.K., Chen, L.J., Chen, S.J., Hashad, Y., Kim, H., Lai, T.Y., Pilz, S., Ruamviboonsuk, P., Tokaji, E., Weisberger, A., Lim, T.H., 2012. EVEREST study: efficacy and safety of verteporfin photodynamic therapy in combination with ranibizumab or alone versus ranibizumab monotherapy in patients with symptomatic macular polypoidal choroidal vasculopathy. Retina 32, 1453–1464.
Koh, A.H., Chen, L.J., Chen, S.J., Chen, Y., Giridhar, A., Iida, T., Kim, H., Yuk Yau Lai, T., Lee, W.K., Li, X., Han Lim, T., Ruamviboonsuk, P., Sharma, T., Tang, S., Yuzawa, M., 2013. Polypoidal choroidal vasculopathy: evidence-based guidelines for clinical diagnosis and treatment. Retina 33, 686–716.
Kohno, T., Miki, T., Shiraki, K., Kano, K., Hirabayashi-Matsushita, M., 2000. Indocyanine green angiographic features of choroidal rupture and choroidal vascular injury after contusion ocular injury. Am. J. Ophthalmol. 129, 38–46.
Kokame, G.T., Liu, K., Kokame, K.A., Kaneko, K.N., Omizo, J.N., 2019. Clinical characteristics of polypoidal choroidal vasculopathy and anti-vascular endothelial growth factor treatment response in Caucasians. Ophthalmologica 1–9.
Komoto, S., Maruyama, K., Hashida, N., Koh, S., Nishida, K., 2019. Bilateral serous retinal detachment associated with subretinal fibrin-like material in a case of pregnancy-induced hypertension. Am J Ophthalmol Case Rep 16, 100572.
Kowalczuk, L., Matet, A., Dor, M., Bararpour, N., Daruich, A., Dirani, A., Behar-Cohen, F., Thomas, A., Turck, N., 2018. Proteome and metabolome of subretinal fluid in central serous chorioretinopathy and rhegmatogenous retinal detachment: a pilot case study. Transl Vis Sci Technol 7, 3.
Kuiper, J., Rothova, A., de Boer, J., Radstake, T., 2015. The immunopathogenesis of birdshot chorioretinopathy; a bird of many feathers. Prog. Retin. Eye Res. 44, 99–110.
Kumar, A., Kedar, S., Singh, R.P., 2002. The indocyanine green findings in idiopathic uveal effusion syndrome. Indian J. Ophthalmol. 50, 217–219.
Lahousen, T., Painold, A., Luxenberger, W., Schienle, A., Kapfhammer, H.P., Ille, R., 2016. Psychological factors associated with acute and chronic central serous chorioretinopathy. Nord. J. Psychiatr. 70, 24–30.
Lainscak, M., Pelliccia, F., Rosano, G., Vitale, C., Schiariti, M., Greco, C., Speziale, G., Gaudio, C., 2015. Safety profile of mineralocorticoid receptor antagonists: spironolactone and eplerenone. Int. J. Cardiol. 200, 25–29.
Lakkaraju, A., Umapathy, A., Tan, L.X., Daniele, L., Philp, N.J., Boesze-Battaglia, K., Williams, D.S., 2020. The cell biology of the retinal pigment epithelium. Prog. Retin. Eye Res. 100846.
Lamb, T.D., Pugh Jr., E.N., 2004. Dark adaptation and the retinoid cycle of vision. Prog. Retin. Eye Res. 23, 307–380.
Lechner, J., Chen, M., Hogg, R.E., Toth, L., Silvestri, G., Chakravarthy, U., Xu, H., 2016. Higher plasma levels of complement C3a, C4a and C5a increase the risk of subretinal fibrosis in neovascular age-related macular degeneration: complement activation in AMD. Immun. Ageing 13, 4.
Lee, W.J., Lee, J.H., Lee, B.R., 2016. Fundus autofluorescence imaging patterns in central serous chorioretinopathy according to chronicity. Eye (Lond) 30, 1336–1342.
Lee, W.K., Iida, T., Ogura, Y., Chen, S.J., Wong, T.Y., Mitchell, P., Cheung, G.C.M., Zhang, Z., Leal, S., Ishibashi, T., 2018. Efficacy and safety of intravitreal aflibercept for polypoidal choroidal vasculopathy in the planet study: a randomized clinical trial. JAMA Ophthalmol 136, 786–793.
Lehmann, M., Bousquet, E., Beydoun, T., Behar-Cohen, F., 2015. PACHYCHOROID: an inherited condition? Retina 35, 10–16.
Lek, J.J., Caruso, E., Baglin, E.K., Sharangan, P., Hodgson, L.A.B., Harper, C.A., Rosenfeld, P.J., Luu, C.D., Guymer, R.H., 2018. Interpretation of subretinal fluid using OCT in intermediate age-related macular degeneration. Ophthalmol Retina 2, 792–802.
Leng, T., Marmor, M.F., Kellner, U., Thompson, D.A., Renner, A.B., Moore, W., Sowden, J.C., 2012. Foveal cavitation as an optical coherence tomography finding in central cone dysfunction. Retina 32, 1411–1419.
Leys, A.M., Dierick, H.G., Sciot, R.M., 1991. Early lesions of bilateral diffuse melanocytic proliferation. Arch. Ophthalmol. 109, 1590–1594.
Liew, G., Quin, G., Gillies, M., Fraser-Bell, S., 2013. Central serous chorioretinopathy: a review of epidemiology and pathophysiology. Clin. Exp. Ophthalmol. 41, 201–214.
Lim, T.H., Lai, T.Y.Y., Takahashi, K., Wong, T.Y., Chen, L.J., Ruamviboonsuk, P., Tan, C. S., Lee, W.K., Cheung, C.M.G., Ngah, N.F., Patalauskaite, R., Margaron, P., Koh, A., 2020. Comparison of ranibizumab with or without verteporfin photodynamic therapy for polypoidal choroidal vasculopathy: the EVEREST II randomized clinical trial. JAMA Ophthalmol 138, 935–942.
Lima, L.H., Laud, K., Chang, L.K., Yannuzzi, L.A., 2011. Choroidal macrovessel. Br. J. Ophthalmol. 95, 1333–1334.
Lima, L.H., Laud, K., Freund, K.B., Yannuzzi, L.A., Spaide, R.F., 2012. Acquired vitelliform lesion associated with large drusen. Retina 32, 647–651.
Lin, A.B., Sheyman, A.T., Jampol, L.M., 2019. Unusual serous retinal detachment IN a patient with waldenstrom macroglobulinemia: a case report. Retin. Cases Brief Rep. 13, 1–4.
Linsenmeier, R.A., Braun, R.D., 1992. Oxygen distribution and consumption in the cat retina during normoxia and hypoxemia. J. Gen. Physiol. 99, 177–197.
Liu, B., Deng, T., Zhang, J., 2016. Risk factors for central serous chorioretinopathy: a systematic review and meta-analysis. Retina 36, 9–19.
Lorentzen, T.D., Subhi, Y., Sorensen, T.L., 2018. Prevalence OF polypoidal choroidal vasculopathy IN white patients with exudative age-related macular degeneration: systematic review and meta-analysis. Retina 38, 2363–2371.
Lorenzo, D., Arias, L., Choudhry, N., Millan, E., Flores, I., Rubio, M.J., Cobos, E., Garcia-Bru, P., Filloy, A., Caminal, J.M., 2017. DOME-SHAPED macula IN myopic eyes: twelve-month follow-up. Retina 37, 680–686.
Lotery, A., Sivaprasad, S., O'Connell, A., Harris, R.A., Culliford, L., Ellis, L., Cree, A., Madhusudhan, S., Behar-Cohen, F., Chakravarthy, U., Peto, T., Rogers, C.A., Reeves, B.C., 2020. Eplerenone for chronic central serous chorioretinopathy in

patients with active, previously untreated disease for more than 4 months (VICI): a randomised, double-blind, placebo-controlled trial. Lancet 395, 294–303.
Luttrull, J.K., 2016. LOW-INTENSITY/HIGH-DENSITY subthreshold diode micropulse laser for central serous chorioretinopathy. Retina 36, 1658–1663.
Maggio, E., Polito, A., Freno, M.C., Pertile, G., 2015. Multimodal imaging findings in a case of severe Central Serous Chorioretinopathy in an uncomplicated pregnancy. BMC Ophthalmol. 15, 183.
Malik, R., Shah, A., Greaney, M.J., Dick, A.D., 2005. Bilateral serous macular detachment as a presenting feature of acute lymphoblastic leukemia. Eur. J. Ophthalmol. 15, 284–286.
Manayath, G.J., Arora, S., Parikh, H., Shah, P.K., Tiwari, S., Narendran, V., 2016. Is myopia a protective factor against central serous chorioretinopathy? Int. J. Ophthalmol. 9, 266–270.
Manayath, G.J., Shah, V.S., Saravanan, V.R., Narendran, V., 2018. Polypoidal choroidal vasculopathy associated with central serous chorioretinopathy: pachychoroid spectrum of diseases. Retina 38, 1195–1204.
Margolis, L., Fraser, R., Lichter, A., Char, D.H., 1980. The role of radiation therapy in the management of ocular reticulum cell sarcoma. Cancer 45, 688–692.
Margolis, R., Mukkamala, S.K., Jampol, L.M., Spaide, R.F., Ober, M.D., Sorenson, J.A., Gentile, R.C., Miller, J.A., Sherman, J., Freund, K.B., 2011. The expanded spectrum of focal choroidal excavation. Arch. Ophthalmol. 129, 1320–1325.
Margolis, R., Spaide, R.F., 2009. A pilot study of enhanced depth imaging optical coherence tomography of the choroid in normal eyes. Am. J. Ophthalmol. 147, 811–815.
Marmor, M.F., 1990. Control of subretinal fluid: experimental and clinical studies. Eye (Lond) 4 (Pt 2), 340–344.
Marquardt, A., Stöhr, H., Passmore, L.A., Krämer, F., Rivera, A., Weber, B.H., 1998. Mutations in a novel gene, VMD2, encoding a protein of unknown properties cause juvenile-onset vitelliform macular dystrophy (Best's disease). Hum. Mol. Genet. 7, 1517–1525.
Márquez, A., Cordero-Coma, M., Martín-Villa, J.M., Gorroño-Echebarría, M.B., Blanco, R., Díaz Valle, D., Del Rio, M.J., Blanco, A., Olea, J.L., Cordero, Y., Capella, M.J., Díaz-Llopis, M., Ortego-Centeno, N., Ruiz-Arruza, I., Llorenç, V., Adán, A., Fonollosa, A., Ten Berge, J., Atan, D., Dick, A.D., De Boer, J.H., Kuiper, J., Rothova, A., Martín, J., 2017. New insights into the genetic component of non-infectious uveitis through an Immunochip strategy. J. Med. Genet. 54, 38–46.
Maruko, I., Iida, T., Saito, M., Nagayama, D., Saito, K., 2007. Clinical characteristics of exudative age-related macular degeneration in Japanese patients. Am. J. Ophthalmol. 144, 15–22.
Maruko, I., Iida, T., Sugano, Y., Oyamada, H., Sekiryu, T., 2011. Morphologic choroidal and scleral changes at the macula in tilted disc syndrome with staphyloma using optical coherence tomography. Invest. Ophthalmol. Vis. Sci. 52, 8763–8768.
Matet, A., Daruich, A., Zola, M., Behar-Cohen, F., 2018. Risk factors for recurrences OF central serous chorioretinopathy. Retina 38, 1403–1414.
Matsumoto, H., Mukai, R., Kikuchi, Y., Morimoto, M., Akiyama, H., 2020. One-year outcomes of half-fluence photodynamic therapy combined with intravitreal injection of aflibercept for pachychoroid neovasculopathy without polypoidal lesions. Jpn. J. Ophthalmol. 64, 203–209.
Matsuo, T., Yamaoka, A., Shiraga, F., Matsuo, N., 1998. Two types of initial ocular manifestations in intraocular-central nervous system lymphoma. Retina 18, 301–307.
Mazloumi, M., Dalvin, L.A., Ancona-Lezama, D., Mashayekhi, A., Shields, C.L., 2020. Photodynamic therapy for extrafoveolar choroidal osteoma. Retina 40, 966–971.
McCluskey, P.J., Watson, P.G., Lightman, S., Haybittle, J., Restori, M., Branley, M., 1999. Posterior scleritis: clinical features, systemic associations, and outcome in a large series of patients. Ophthalmology 106, 2380–2386.
McMenamin, P.G., Saban, D.R., Dando, S.J., 2019. Immune cells in the retina and choroid: two different tissue environments that require different defenses and surveillance. Prog. Retin. Eye Res. 70, 85–98.
Mehta, H., Tufail, A., Daien, V., Lee, A.Y., Nguyen, V., Ozturk, M., Barthelmes, D., Gillies, M.C., 2018. Real-world outcomes in patients with neovascular age-related macular degeneration treated with intravitreal vascular endothelial growth factor inhibitors. Prog. Retin. Eye Res. 65, 127–146.
Mehta, P.H., Meyerle, C., Sivaprasad, S., Boon, C., Chhablani, J., 2017. Preferred practice pattern in central serous chorioretinopathy. Br. J. Ophthalmol. 101, 587–590.
Merlini, G., Baldini, L., Broglia, C., Comelli, M., Goldaniga, M., Palladini, G., Deliliers, G. L., Gobbi, P.G., 2003. Prognostic factors in symptomatic Waldenstrom's macroglobulinemia. Semin. Oncol. 30, 211–215.
Michels, S., Michels, R., Simader, C., Schmidt-Erfurth, U., 2005. Verteporfin therapy for choroidal hemangioma: a long-term follow-up. Retina 25, 697–703.
Miki, A., Kondo, N., Yanagisawa, S., Bessho, H., Honda, S., Negi, A., 2014. Common variants in the complement factor H gene confer genetic susceptibility to central serous chorioretinopathy. Ophthalmology 121, 1067–1072.
Miki, A., Sakurada, Y., Tanaka, K., Semba, K., Mitamura, Y., Yuzawa, M., Tajima, A., Nakatochi, M., Yamamoto, K., Matsuo, K., Imoto, I., Honda, S., 2018. Genome-wide association study to identify a new susceptibility locus for central serous chorioretinopathy in the Japanese population. Invest. Ophthalmol. Vis. Sci. 59, 5542–5547.
Miles, S.L., Niles, R.M., Pittock, S., Vile, R., Davies, J., Winters, J.L., Abu-Yaghi, N.E., Grothey, A., Siddiqui, M., Kaur, J., Hartmann, L., Kalli, K.R., Pease, L., Kravitz, D., Markovic, S., Pulido, J.S., 2012. A factor found in the IgG fraction of serum of patients with paraneoplastic bilateral diffuse uveal melanocytic proliferation causes proliferation of cultured human melanocytes. Retina 32, 1959–1966.
Minos, E., Barry, R.J., Southworth, S., Folkard, A., Murray, P.I., Duker, J.S., Keane, P.A., Denniston, A.K., 2016. Birdshot chorioretinopathy: current knowledge and new concepts in pathophysiology, diagnosis, monitoring and treatment. Orphanet J. Rare Dis. 11, 61.
Mitchell, P., Liew, G., Gopinath, B., Wong, T.Y., 2018. Age-related macular degeneration. Lancet 392, 1147–1159.
Miyakubo, T., Mukai, R., Nakamura, K., Matsumoto, H., Akiyama, H., 2019. A case of ipilimumab-induced unusual serous retinal detachment in bilateral eyes. Int. Med. Case Rep. J. 12, 355–361.
Mohabati, D., Boon, C.J.F., Yzer, S., 2020a. Risk of recurrence and transition to chronic disease in acute central serous chorioretinopathy. Clin. Ophthalmol. 14, 1165–1175.
Mohabati, D., Hoyng, C.B., Yzer, S., Boon, C.J.F., 2020b. Clinical characteristics and outcome OF posterior cystoid macular degeneration IN chronic central serous chorioretinopathy. Retina 40, 1742–1750.
Mohabati, D., Schellevis, R.L., van Dijk, E.H.C., Fauser, S., den Hollander, A.I., Hoyng, C. B., De Jong, E.K., Yzer, S., Boon, C.J.F., 2020c. Genetic risk factors IN severe, nonsevere and acute phenotypes OF central serous chorioretinopathy. Retina 40, 1734–1741.
Mohabati, D., van Dijk, E.H., van Rijssen, T.J., de Jong, E.K., Breukink, M.B., Martinez-Ciriano, J.P., Dijkman, G., Hoyng, C.B., Fauser, S., Yzer, S., Boon, C.J., 2018a. Clinical spectrum of severe chronic central serous chorioretinopathy and outcome of photodynamic therapy. Clin. Ophthalmol. 12, 2167–2176.
Mohabati, D., van Rijssen, T.J., van Dijk, E.H., Luyten, G.P., Missotten, T.O., Hoyng, C.B., Yzer, S., Boon, C.J., 2018b. Clinical characteristics and long-term visual outcome of severe phenotypes of chronic central serous chorioretinopathy. Clin. Ophthalmol. 12, 1061–1070.
Moisseiev, E., Moisseiev, J., Loewenstein, A., 2015. Optic disc pit maculopathy: when and how to treat? A review of the pathogenesis and treatment options. Int J Retina Vitreous 1, 13.
Moorthy, R.S., Inomata, H., Rao, N.A., 1995. Vogt-Koyanagi-Harada syndrome. Surv. Ophthalmol. 39, 265–292.
Morgan, I.G., French, A.N., Ashby, R.S., Guo, X., Ding, X., He, M., Rose, K.A., 2018. The epidemics of myopia: aetiology and prevention. Prog. Retin. Eye Res. 62, 134–149.
Moschos, M.M., Gazouli, M., Gatzioufas, Z., Brouzas, D., Nomikarios, N., Sivaprasad, S., Mitropoulos, P., Chatziralli, I.P., 2016. Prevalence OF the complement factor H and GSTM1 genes polymorphisms IN patients with central serous chorioretinopathy. Retina 36, 402–407.
Moulin, A.P., Bucher, M., Pournaras, J.A., Nguyen, C., Ambresin, A., 2010. Fluorescein and indocyanine green angiography findings in B cell lymphoblastic leukemia mimicking acute central serous chorioretinopathy. Klin Monbl Augenheilkd 227, 342–344.
Mrejen, S., Balaratnasingam, C., Kaden, T.R., Bottini, A., Dansingani, K., Bhavsar, K.V., Yannuzzi, N.A., Patel, S., Chen, K.C., Yu, S., Stoffels, G., Spaide, R.F., Freund, K.B., Yannuzzi, L.A., 2019. Long-term visual outcomes and causes of vision loss in chronic central serous chorioretinopathy. Ophthalmology 126, 576–588.
Mrejen, S., Spaide, R.F., 2013. Optical coherence tomography: imaging of the choroid and beyond. Surv. Ophthalmol. 58, 387–429.
Mullins, R.F., Schoo, D.P., Sohn, E.H., Flamme-Wiese, M.J., Workamelahu, G., Johnston, R.M., Wang, K., Tucker, B.A., Stone, E.M., 2014. The membrane attack complex in aging human choriocapillaris: relationship to macular degeneration and choroidal thinning. Am. J. Pathol. 184, 3142–3153.
Nagiel, A., Rootman, D.B., McCannel, T.A., 2017. Paraneoplastic vitelliform maculopathy IN the setting OF choroidal melanoma: evolution over one year. Retin. Cases Brief Rep. 11 (Suppl. 1), S7–s10.
Nakanishi, H., Tsujikawa, A., Gotoh, N., Hayashi, H., Iwama, D., Tamura, H., Otani, A., Yoshimura, N., 2008. Macular complications on the border of an inferior staphyloma associated with tilted disc syndrome. Retina (Philadelphia, Pa.) 28, 1493–1501.
Nathaniel Roybal, C., Sledz, E., Elshatory, Y., Zhang, L., Almeida, D.R.P., Chin, E.K., Critser, B., Abramoff, M.D., Russell, S.R., 2018. Dysfunctional autonomic regulation OF the choroid IN central serous chorioretinopathy. Retina 38, 1205–1210.
Naysan, J., Pang, C.E., Klein, R.W., Freund, K.B., 2016. Multimodal imaging of bilateral diffuse uveal melanocytic proliferation associated with an iris mass lesion. Int J Retina Vitreous 2, 13.
Newman, D.K., 2016. Photodynamic therapy: current role in the treatment of chorioretinal conditions. Eye (Lond) 30, 202–210.
Nicholson, B., Noble, J., Forooghian, F., Meyerle, C., 2013. Central serous chorioretinopathy: update on pathophysiology and treatment. Surv. Ophthalmol. 58, 103–126.
Nickla, D.L., Wallman, J., 2010. The multifunctional choroid. Prog. Retin. Eye Res. 29, 144–168.
Nishikawa, Y., Fujinami, K., Watanabe, K., Noda, T., Tsunoda, K., Akiyama, K., 2014. Clinical course of focal choroidal excavation in Vogt-Koyanagi-Harada disease. Clin. Ophthalmol. 8, 2461–2465.
Nozaki, M., Raisler, B.J., Sakurai, E., Sarma, J.V., Barnum, S.R., Lambris, J.D., Chen, Y., Zhang, K., Ambati, B.K., Baffi, J.Z., Ambati, J., 2006. Drusen complement components C3a and C5a promote choroidal neovascularization. Proc. Natl. Acad. Sci. U. S. A. 103, 2328–2333.
Nunes, H., Bouvry, D., Soler, P., Valeyre, D., 2007. Sarcoidosis. Orphanet J. Rare Dis. 2, 46.
O'Keefe, G.A., Rao, N.A., 2017. Vogt-Koyanagi-Harada disease. Surv. Ophthalmol. 62, 1–25.
Obana, A., Kusumi, M., Miki, T., 1996. Indocyanine green angiographic aspects of multiple evanescent white dot syndrome. Retina 16, 97–104.
Obata, R., Takahashi, H., Ueta, T., Yuda, K., Kure, K., Yanagi, Y., 2013. Tomographic and angiographic characteristics of eyes with macular focal choroidal excavation. Retina 33, 1201–1210.

Obata, S., Saishin, Y., Teramura, K., Ohji, M., 2019. Vogt-koyanagi-harada disease-like uveitis during nivolumab (Anti-PD-1 antibody) treatment for metastatic cutaneous malignant melanoma. Case Rep Ophthalmol 10, 67–74.
Ohsugi, H., Ikuno, Y., Oshima, K., Yamauchi, T., Tabuchi, H., 2014. Morphologic characteristics of macular complications of a dome-shaped macula determined by swept-source optical coherence tomography. Am. J. Ophthalmol. 158, 162–170 e161.
Ooto, S., Mittra, R.A., Ridley, M.E., Spaide, R.F., 2014. Vitrectomy with inner retinal fenestration for optic disc pit maculopathy. Ophthalmology 121, 1727–1733.
Ooto, S., Tsujikawa, A., Mori, S., Tamura, H., Yamashiro, K., Otani, A., Yoshimura, N., 2011. Retinal microstructural abnormalities in central serous chorioretinopathy and polypoidal choroidal vasculopathy. Retina 31, 527–534.
Organisciak, D.T., Vaughan, D.K., 2010. Retinal light damage: mechanisms and protection. Prog. Retin. Eye Res. 29, 113–134.
Otani, T., Kishi, S., Maruyama, Y., 1999. Patterns of diabetic macular edema with optical coherence tomography. Am. J. Ophthalmol. 127, 688–693.
Ozdemir, H., Karacorlu, M., Karacorlu, S., 2005. Serous macular detachment in diabetic cystoid macular oedema. Acta Ophthalmol. Scand. 83, 63–66.
Panda-Jonas, S., Jonas, J.B., Jakobczyk-Zmija, M., 1996. Retinal pigment epithelial cell count, distribution, and correlations in normal human eyes. Am. J. Ophthalmol. 121, 181–189.
Pang, C.E., Freund, K.B., 2015. Pachychoroid neovasculopathy. Retina 35, 1–9.
Pang, C.E., Shah, V.P., Sarraf, D., Freund, K.B., 2014. Ultra-widefield imaging with autofluorescence and indocyanine green angiography in central serous chorioretinopathy. Am. J. Ophthalmol. 158, 362–371 e362.
Parnell, J.R., Jampol, L.M., Yannuzzi, L.A., Gass, J.D., Tittl, M.K., 2001. Differentiation between presumed ocular histoplasmosis syndrome and multifocal choroiditis with panuveitis based on morphology of photographed fundus lesions and fluorescein angiography. Arch. Ophthalmol. 119, 208–212.
Parodi, M.B., Iacono, P., Mansour, A., Benedetto, U., Knutsson, K.A., Bandello, F., Ziemssen, F., Ness, T., Dodwell, D., 2013. Intravitreal bevacizumab for juxtafoveal choroidal neovascularization secondary to multifocal choroiditis. Retina 33, 953–956.
Parver, L.M., Auker, C., Carpenter, D.O., 1980. Choroidal blood flow as a heat dissipating mechanism in the macula. Am. J. Ophthalmol. 89, 641–646.
Parver, L.M., Auker, C.R., Carpenter, D.O., 1982. The stabilizing effect of the choroidal circulation on the temperature environment of the macula. Retina 2, 117–120.
Perea-Romero, I., Gordo, G., Iancu, I.F., Del Pozo-Valero, M., Almoguera, B., Blanco-Kelly, F., Carreño, E., Jimenez-Rolando, B., Lopez-Rodriguez, R., Lorda-Sanchez, I., Martin-Merida, I., Pérez de Ayala, L., Riveiro-Alvarez, R., Rodriguez-Pinilla, E., Tahsin-Swafiri, S., Trujillo-Tiebas, M.J., Garcia-Sandoval, B., Minguez, P., Avila-Fernandez, A., Corton, M., Ayuso, C., 2021. Genetic landscape of 6089 inherited retinal dystrophies affected cases in Spain and their therapeutic and extended epidemiological implications. Sci. Rep. 11, 1526.
Peterson, K., Gordon, K.B., Heinemann, M.H., DeAngelis, L.M., 1993. The clinical spectrum of ocular lymphoma. Cancer 72, 843–849.
Piccolino, F.C., Borgia, L., 1994. Central serous chorioretinopathy and indocyanine green angiography. Retina 14, 231–242.
Piccolino, F.C., De La Longrais, R.R., Manea, M., Cicinelli, S., 2008. Posterior cystoid retinal degeneration in central serous chorioretinopathy. Retina 28, 1008–1012.
Pierro, L., Tremolada, G., Introini, U., Calori, G., Brancato, R., 2002. Optical coherence tomography findings in adult-onset foveomacular vitelliform dystrophy. Am. J. Ophthalmol. 134, 675–680.
Pilotto, E., Urban, F., Parrozzani, R., Midena, E., 2011. Standard versus bolus photodynamic therapy in circumscribed choroidal hemangioma: functional outcomes. Eur. J. Ophthalmol. 21, 452–458.
Pino, R.M., 1985. Restriction to endogenous plasma proteins by a fenestrated capillary endothelium: an ultrastructural immunocytochemical study of the choriocapillary endothelium. Am. J. Anat. 172, 279–289.
Polak, B.C., Baarsma, G.S., Snyers, B., 1995. Diffuse retinal pigment epitheliopathy complicating systemic corticosteroid treatment. Br. J. Ophthalmol. 79, 922–925.
Priem, H.A., Oosterhuis, J.A., 1988. Birdshot chorioretinopathy: clinical characteristics and evolution. Br. J. Ophthalmol. 72, 646–659.
Pro, M., Shields, J.A., Tomer, T.L., 1978. Serous detachment of the macular associated with presumed choroidal nevi. Arch. Ophthalmol. 96, 1374–1377.
Prunte, C., Flammer, J., 1996. Choroidal capillary and venous congestion in central serous chorioretinopathy. Am. J. Ophthalmol. 121, 26–34.
Querques, G., Capuano, V., Costanzo, E., Corvi, F., Querques, L., Introini, U., Souied, E. H., Bandello, F., 2016. Retinal pigment epithelium aperture: a previously unreported finding in the evolution of avascular pigment epithelium detachment. Retina 36 (Suppl. 1), S65–s72.
Querques, G., delle Noci, N., 2007. Vitelliform macular dystrophy. Ophthalmology 114, 1234 author reply 1234-1235.
Querques, G., Forte, R., Querques, L., Massamba, N., Souied, E.H., 2011. Natural course of adult-onset foveomacular vitelliform dystrophy: a spectral-domain optical coherence tomography analysis. Am. J. Ophthalmol. 152, 304–313.
Quintyn, J.C., Brasseur, G., 2004. Subretinal fluid in primary rhegmatogenous retinal detachment: physiopathology and composition. Surv. Ophthalmol. 49, 96–108.
Rahimy, E., Sarraf, D., 2013. Paraneoplastic and non-paraneoplastic retinopathy and optic neuropathy: evaluation and management. Surv. Ophthalmol. 58, 430–458.
Rahman, W., Horgan, N., Hungerford, J., 2013. Circumscribed choroidal haemangioma mimicking chronic central serous chorioretinopathy. J. Fr. Ophtalmol. 36, e37–40.
Ramrattan, R.S., van der Schaft, T.L., Mooy, C.M., de Bruijn, W.C., Mulder, P.G., de Jong, P.T., 1994. Morphometric analysis of Bruch's membrane, the choriocapillaris, and the choroid in aging. Invest. Ophthalmol. Vis. Sci. 35, 2857–2864.
Rao, S., Gentile, R.C., 2010. Successful treatment of choroidal neovascularization complicating a choroidal osteoma with intravitreal bevacizumab. Retin. Cases Brief Rep. 4, 303–305.
Rashaed, S.A., 2013. Unusual presentation of residual subretinal fluid composition after surgery for acute rhegmatogenous retinal detachment. Clin. Ophthalmol. 7, 1069–1072.
Rathinam, S.R., Namperumalsamy, P., Nozik, R.A., Cunningham Jr., E.T., 1999. Vogt-Koyanagi-Harada syndrome after cutaneous injury. Ophthalmology 106, 635–638.
Read, R.W., Rao, N.A., 2000. Utility of existing Vogt-Koyanagi-Harada syndrome diagnostic criteria at initial evaluation of the individual patient: a retrospective analysis. Ocul. Immunol. Inflamm. 8, 227–234.
Read, R.W., Rao, N.A., Cunningham, E.T., 2000. Vogt-Koyanagi-Harada disease. Curr. Opin. Ophthalmol. 11, 437–442.
Reichhart, N., Strauss, O., 2014. Ion channels and transporters of the retinal pigment epithelium. Exp. Eye Res. 126, 27–37.
Reiner, A., Fitzgerald, M.E.C., Del Mar, N., Li, C., 2018. Neural control of choroidal blood flow. Prog. Retin. Eye Res. 64, 96–130.
Renner, A.B., Tillack, H., Kraus, H., Kohl, S., Wissinger, B., Mohr, N., Weber, B.H., Kellner, U., Foerster, M.H., 2004. Morphology and functional characteristics in adult vitelliform macular dystrophy. Retina (Philadelphia, Pa.) 24, 929–939.
Rewbury, R., Hughes, E., Purbrick, R., Prior, S., Baron, M., 2017. Poppers: legal highs with questionable contents? A case series of poppers maculopathy. Br. J. Ophthalmol. 101, 1530–1534.
Rezai, K.A., Eliott, D., 2004. Optical coherence tomographic findings in pregnancy-associated central serous chorioretinopathy. Graefes Arch. Clin. Exp. Ophthalmol. 242, 1014–1016.
Ridley, M.E., McDonald, H.R., Sternberg Jr., P., Blumenkranz, M.S., Zarbin, M.A., Schachat, A.P., 1992. Retinal manifestations of ocular lymphoma (reticulum cell sarcoma). Ophthalmology 99, 1153–1160 discussion 1160-1151.
Rizzolo, L.J., Peng, S., Luo, Y., Xiao, W., 2011. Integration of tight junctions and claudins with the barrier functions of the retinal pigment epithelium. Prog. Retin. Eye Res. 30, 296–323.
Robertson, D.M., 1986. Argon laser photocoagulation treatment in central serous chorioretinopathy. Ophthalmology 93, 972–974.
Robertson, D.M., Ilstrup, D., 1983. Direct, indirect, and sham laser photocoagulation in the management of central serous chorioretinopathy. Am. J. Ophthalmol. 95, 457–466.
Rocholz, R., Corvi, F., Weichsel, J., Schmidt, S., Staurenghi, G., 2019. OCT angiography (OCTA) in retinal diagnostics. In: Bille, J.F. (Ed.), High Resolution Imaging in Microscopy and Ophthalmology: New Frontiers in Biomedical Optics. Springer, pp. 135–160. Copyright 2019, The Author(s). Cham (CH).
Romanelli, F., Smith, K.M., Thornton, A.C., Pomeroy, C., 2004. Poppers: epidemiology and clinical management of inhaled nitrite abuse. Pharmacotherapy 24, 69–78.
Roorda, A., Williams, D.R., 1999. The arrangement of the three cone classes in the living human eye. Nature 397, 520–522.
Roseman, R.L., Gass, J.D., 1992. Solitary hypopigmented nevus of the retinal pigment epithelium in the macula. Arch. Ophthalmol. 110, 1358–1359.
Rosenthal, A.R., 1983. Ocular manifestations of leukemia. A review. Ophthalmology 90, 899–905.
Roy, K., Ghosh, S., Kumar, B., Ball, S., 2015. Characteristic OCT pattern in Waldenstrom macroglobulinemia. Optom. Vis. Sci. 92, e106–109.
Roy, R., Saurabh, K., Shah, D., Goel, S., 2019. Treatment outcomes of pachychoroid neovasculopathy with photodynamic therapy and anti-vascular endothelial growth factor. Indian J. Ophthalmol. 67, 1678–1683.
Rozing, M.P., Durhuus, J.A., Krogh Nielsen, M., Subhi, Y., Kirkwood, T.B., Westendorp, R.G., Sørensen, T.L., 2020. Age-related macular degeneration: a two-level model hypothesis. Prog. Retin. Eye Res. 76, 100825.
Ruan, M.Z., Hussnain, S.A., Thomas, A., Mansukhani, M., Tsang, S., Yannuzzi, L., 2019. Utility of en-face imaging in diagnosis of occult macular dystrophy with RP1L1 mutation: a case series. Am J Ophthalmol Case Rep 15, 100465.
Ruiz-Medrano, J., Montero, J.A., Flores-Moreno, I., Arias, L., García-Layana, A., Ruiz-Moreno, J.M., 2019. Myopic maculopathy: current status and proposal for a new classification and grading system (ATN). Prog. Retin. Eye Res. 69, 80–115.
Sagoo, M.S., Mehta, H., Swampillai, A.J., Cohen, V.M., Amin, S.Z., Plowman, P.N., Lightman, S., 2014. Primary intraocular lymphoma. Surv. Ophthalmol. 59, 503–516.
Sahin, A., Bez, Y., Kaya, M.C., Türkcü, F.M., Sahin, M., Yüksel, H., 2014. Psychological distress and poor quality of life in patients with central serous chorioretinopathy. Semin. Ophthalmol. 29, 73–76.
Sahoo, N.K., Singh, S.R., Rajendran, A., Shukla, D., Chhablani, J., 2019. Masqueraders of central serous chorioretinopathy. Surv. Ophthalmol. 64, 30–44.
Said-Ahmed, K., Moustafa, G., Fawzy, M., 2012. Incidence and natural course of symptomatic central serous chorioretinopathy in pregnant women in a maternity hospital in Kuwait. Middle East Afr. J. Ophthalmol. 19, 273–276.
Saint-Geniez, M., Kurihara, T., Sekiyama, E., Maldonado, A.E., D'Amore, P.A., 2009. An essential role for RPE-derived soluble VEGF in the maintenance of the choriocapillaris. Proc. Natl. Acad. Sci. U. S. A. 106, 18751–18756.
Saksens, N.T., Fleckenstein, M., Schmitz-Valckenberg, S., Holz, F.G., den Hollander, A.I., Keunen, J.E., Boon, C.J., Hoyng, C.B., 2014. Macular dystrophies mimicking age-related macular degeneration. Prog. Retin. Eye Res. 39, 23–57.
Sanabria, M.R., Coco, R.M., Sanchidrian, M., 2008. Oct findings in torpedo maculopathy. Retin. Cases Brief Rep. 2, 109–111.
Sawa, M., Ober, M.D., Freund, K.B., Spaide, R.F., 2006. Fundus autofluorescence in patients with pseudoxanthoma elasticum. Ophthalmology 113, 814–820 e812.
Schatz, H., Madeira, D., Johnson, R.N., McDonald, H.R., 1992. Central serous chorioretinopathy occurring in patients 60 years of age and older. Ophthalmology 99, 63–67.

Scheer, F.A., Hilton, M.F., Mantzoros, C.S., Shea, S.A., 2009. Adverse metabolic and cardiovascular consequences of circadian misalignment. Proc. Natl. Acad. Sci. U. S. A. 106, 4453–4458.
Schellevis, R.L., van Dijk, E.H.C., Breukink, M.B., Altay, L., Bakker, B., Koeleman, B.P.C., Kiemeney, L.A., Swinkels, D.W., Keunen, J.E.E., Fauser, S., Hoyng, C.B., den Hollander, A.I., Boon, C.J.F., de Jong, E.K., 2018. Role of the complement system in chronic central serous chorioretinopathy: a genome-wide association study. JAMA Ophthalmol 136, 1128–1136.
Schmidt-Erfurth, U., Sadeghipour, A., Gerendas, B.S., Waldstein, S.M., Bogunović, H., 2018. Artificial intelligence in retina. Prog. Retin. Eye Res. 67, 1–29.
Schmitz-Valckenberg, S., Pfau, M., Fleckenstein, M., Staurenghi, G., Sparrow, J.R., Bindewald-Wittich, A., Spaide, R.F., Wolf, S., Sadda, S.R., Holz, F.G., 2020. Fundus autofluorescence imaging. Prog. Retin. Eye Res. 100893.
Schönfeld, C.L., 2012. Bilateral exudative retinal detachment in HELLP syndrome. Case Rep Ophthalmol 3, 35–37.
Schubert, C., Pryds, A., Zeng, S., Xie, Y., Freund, K.B., Spaide, R.F., Merriam, J.C., Barbazetto, I., Slakter, J.S., Chang, S., Munch, I.C., Drack, A.V., Hernandez, J., Yzer, S., Merriam, J.E., Linneberg, A., Larsen, M., Yannuzzi, L.A., Mullins, R.F., Allikmets, R., 2014. Cadherin 5 is regulated by corticosteroids and associated with central serous chorioretinopathy. Hum. Mutat. 35, 859–867.
Senba, M., 1985. Autofluorescence of lipofuscin granules? Am. J. Clin. Pathol. 83, 134.
Setrouk, E., Hubault, B., Vankemmel, F., Zambrowski, O., Nazeyrollas, P., Delemer, B., Durlach, V., Ducasse, A., Arndt, C., 2016. Circadian disturbance and idiopathic central serous chorioretinopathy. Graefes Arch. Clin. Exp. Ophthalmol. 254, 2175–2181.
Sharon, D., Blackshaw, S., Cepko, C.L., Dryja, T.P., 2002. Profile of the genes expressed in the human peripheral retina, macula, and retinal pigment epithelium determined through serial analysis of gene expression (SAGE). Proc. Natl. Acad. Sci. U. S. A. 99, 315–320.
Sheth, B.P., Mieler, W.F., 2001. Ocular complications of pregnancy. Curr. Opin. Ophthalmol. 12, 455–463.
Sheth, J., Anantharaman, G., Kumar, N., Parachuri, N., Bandello, F., Kuppermann, B.D., Loewenstein, A., Sharma, A., 2020. Pachydrusen: the epidemiology of pachydrusen and its relevance to progression of pachychoroid disease spectrum. Eye (Lond) 34, 1501–1503.
Shields, C.L., Arepalli, S., Atalay, H.T., Ferenczy, S.R., Fulco, E., Shields, J.A., 2015. Choroidal osteoma shows bone lamella and vascular channels on enhanced depth imaging optical coherence tomography in 15 eyes. Retina 35, 750–757.
Shields, C.L., Dalvin, L.A., Ancona-Lezama, D., Yu, M.D., Di Nicola, M., Williams Jr., B.K., Lucio-Alvarez, J.A., Ang, S.M., Maloney, S., Welch, R.J., Shields, J.A., 2019. Choroidal nevus imaging features IN 3,806 cases and risk factors for TRANSFORMATION into melanoma IN 2,355 cases: the 2020 Taylor R. Smith and Victor T. Curtin lecture. Retina 39, 1840–1851.
Shields, C.L., Honavar, S.G., Shields, J.A., Cater, J., Demirci, H., 2001. Circumscribed choroidal hemangioma: clinical manifestations and factors predictive of visual outcome in 200 consecutive cases. Ophthalmology 108, 2237–2248.
Shields, C.L., Pellegrini, M., Ferenczy, S.R., Shields, J.A., 2014. Enhanced depth imaging optical coherence tomography of intraocular tumors: from placid to seasick to rock and rolling topography–the 2013 Francesco Orzalesi Lecture. Retina (Philadelphia, Pa.) 34, 1495–1512.
Shields, C.L., Perez, B., Materin, M.A., Mehta, S., Shields, J.A., 2007. Optical coherence tomography of choroidal osteoma in 22 cases: evidence for photoreceptor atrophy over the decalcified portion of the tumor. Ophthalmology 114, e53–58.
Shields, C.L., Shields, J.A., De Potter, P., 1995. Patterns of indocyanine green videoangiography of choroidal tumours. Br. J. Ophthalmol. 79, 237–245.
Shields, C.L., Shields, J.A., De Potter, P., Quaranta, M., Freire, J., Brady, L.W., Barrett, J., 1997a. Plaque radiotherapy for the management of uveal metastasis. Arch. Ophthalmol. 115, 203–209.
Shields, C.L., Shields, J.A., Gross, N.E., Schwartz, G.P., Lally, S.E., 1997b. Survey of 520 eyes with uveal metastases. Ophthalmology 104, 1265–1276.
Shin, W.B., Kim, M.K., Lee, C.S., Lee, S.C., Kim, H., 2015. Comparison of the clinical manifestations between acute vogt-koyanagi-harada disease and acute bilateral central serous chorioretinopathy. Kor. J. Ophthalmol. 29, 389–395.
Shinojima, A., Kawamura, A., Mori, R., Yuzawa, M., 2014. Morphologic features of focal choroidal excavation on spectral domain optical coherence tomography with simultaneous angiography. Retina 34, 1407–1414.
Shiragami, C., Takasago, Y., Osaka, R., Kobayashi, M., Ono, A., Yamashita, A., Hirooka, K., 2018. Clinical features of central serous chorioretinopathy with type 1 choroidal neovascularization. Am. J. Ophthalmol. 193, 80–86.
Shirley, K., O'Neill, M., Gamble, R., Ramsey, A., McLoone, E., 2018. Torpedo maculopathy: disease spectrum and associated choroidal neovascularisation in a paediatric population. Eye (Lond) 32, 1315–1320.
Sho, K., Takahashi, K., Yamada, H., Wada, M., Nagai, Y., Otsuji, T., Nishikawa, M., Mitsuma, Y., Yamazaki, Y., Matsumura, M., Uyama, M., 2003. Polypoidal choroidal vasculopathy: incidence, demographic features, and clinical characteristics. Arch. Ophthalmol. (Chicago, Ill: 1960) 121, 1392–1396.
Sikorski, B.L., Bukowska, D., Kaluzny, J.J., Szkulmowski, M., Kowalczyk, A., Wojtkowski, M., 2011. Drusen with accompanying fluid underneath the sensory retina. Ophthalmology 118, 82–92.
Silva, R.M., Ruiz-Moreno, J.M., Gomez-Ulla, F., Montero, J.A., Gregorio, T., Cachulo, M. L., Pires, I.A., Cunha-Vaz, J.G., Murta, J.N., 2013. Photodynamic therapy for chronic central serous chorioretinopathy: a 4-year follow-up study. Retina 33, 309–315.
Singh, A.D., Turell, M.E., Topham, A.K., 2011. Uveal melanoma: trends in incidence, treatment, and survival. Ophthalmology 118, 1881–1885.
Singh, S.R., Matet, A., van Dijk, E.H.C., Daruich, A., Fauser, S., Yzer, S., Peiretti, E., Sivaprasad, S., Lotery, A.J., Boon, C.J.F., Behar-Cohen, F., Freund, K.B., Chhablani, J., 2019. Discrepancy in current central serous chorioretinopathy classification. Br. J. Ophthalmol. 103, 737–742.
Sivaprasad, S., Elagouz, M., McHugh, D., Shona, O., Dorin, G., 2010. Micropulsed diode laser therapy: evolution and clinical applications. Surv. Ophthalmol. 55, 516–530.
Slakter, J.S., Giovannini, A., Yannuzzi, L.A., Scassellati-Sforzolini, B., Guyer, D.R., Sorenson, J.A., Spaide, R.F., Orlock, D., 1997. Indocyanine green angiography of multifocal choroiditis. Ophthalmology 104, 1813–1819.
Smailhodzic, D., Fleckenstein, M., Theelen, T., Boon, C.J., van Huet, R.A., van de Ven, J. P., Den Hollander, A.I., Schmitz-Valckenberg, S., Hoyng, C.B., Weber, B.H., Holz, F. G., Klevering, B.J., 2011. Central areolar choroidal dystrophy (CACD) and age-related macular degeneration (AMD): differentiating characteristics in multimodal imaging. Invest. Ophthalmol. Vis. Sci. 52, 8908–8918.
Solomon, S.G., Lennie, P., 2007. The machinery of colour vision. Nat. Rev. Neurosci. 8, 276–286.
Song, J.H., Bae, J.H., Rho, M.I., Lee, S.C., 2010. Intravitreal bevacizumab in the management of subretinal fluid associated with choroidal osteoma. Retina 30, 945–951.
Song, Y.S., Kinouchi, R., Ishiko, S., Fukui, K., Yoshida, A., 2013. Hypertensive choroidopathy with eclampsia viewed on spectral-domain optical coherence tomography. Graefe's archive for clinical and experimental ophthalmology = Albrecht von Graefes Archiv fur klinische und experimentelle Ophthalmologie 251, 2647–2650.
Spaide, R., 2008. Autofluorescence from the outer retina and subretinal space: hypothesis and review. Retina 28, 5–35.
Spaide, R.F., 2004. Deposition of yellow submacular material in central serous chorioretinopathy resembling adult-onset foveomacular vitelliform dystrophy. Retina 24, 301–304.
Spaide, R.F., 2018. Disease expression IN nonexudative age-related macular degeneration varies with choroidal thickness. Retina 38, 708–716.
Spaide, R.F., 2020. Choroidal blood flow: review and potential explanation for the choroidal venous anatomy including the vortex vein system. Retina 40, 1851–1864.
Spaide, R.F., 2021. The ambiguity of pachychoroid. Retina 41, 231–237.
Spaide, R.F., Campeas, L., Haas, A., Yannuzzi, L.A., Fisher, Y.L., Guyer, D.R., Slakter, J.S., Sorenson, J.A., Orlock, D.A., 1996. Central serous chorioretinopathy in younger and older adults. Ophthalmology 103, 2070–2079 discussion 2079-2080.
Spaide, R.F., Cheung, C.M.G., 2020. Choroidal venous remodeling documented by long-term follow-up. Retina 40, e60–e61.
Spaide, R.F., Curcio, C.A., 2010. Drusen characterization with multimodal imaging. Retina 30, 1441–1454.
Spaide, R.F., Fujimoto, J.G., Waheed, N.K., Sadda, S.R., Staurenghi, G., 2018a. Optical coherence tomography angiography. Prog. Retin. Eye Res. 64, 1–55.
Spaide, R.F., Jaffe, G.J., Sarraf, D., Freund, K.B., Sadda, S.R., Staurenghi, G., Waheed, N. K., Chakravarthy, U., Rosenfeld, P.J., Holz, F.G., Souied, E.H., Cohen, S.Y., Querques, G., Ohno-Matsui, K., Boyer, D., Gaudric, A., Blodi, B., Baumal, C.R., Li, X., Coscas, G.J., Brucker, A., Singerman, L., Luthert, P., Schmitz-Valckenberg, S., Schmidt-Erfurth, U., Grossniklaus, H.E., Wilson, D.J., Guymer, R., Yannuzzi, L.A., Chew, E.Y., Csaky, K., Monés, J.M., Pauleikhoff, D., Tadayoni, R., Fujimoto, J., 2020a. Consensus nomenclature for reporting neovascular age-related macular degeneration data: consensus on neovascular age-related macular degeneration nomenclature study group. Ophthalmology 127, 616–636.
Spaide, R.F., Ledesma-Gil, G., Gemmy Cheung, C.M., 2021 May 1. Intervortex venous anastomosis in pachychoroid-related disorders. Retina 41 (5), 997–1004.
Spaide, R.F., Ooto, S., Curcio, C.A., 2018b. Subretinal drusenoid deposits AKA pseudodrusen. Surv. Ophthalmol. 63, 782–815.
Spaide, R.F., Yannuzzi, L., Freund, K.B., Mullins, R., Stone, E., 2019. Eyes with subretinal drusenoid deposits and NO drusen: progression of macular findings. Retina 39, 12–26.
Spaide, R.F., Yannuzzi, L., Slakter, J.S., Sorenson, J., Orlach, D.A., 1995. Indocyanine green videoangiography of idiopathic polypoidal choroidal vasculopathy. Retina (Philadelphia, Pa.) 15, 100–110.
Sparrow, J.R., Boulton, M., 2005. RPE lipofuscin and its role in retinal pathobiology. Exp. Eye Res. 80, 595–606.
Sparrow, J.R., Gregory-Roberts, E., Yamamoto, K., Blonska, A., Ghosh, S.K., Ueda, K., Zhou, J., 2012. The bisretinoids of retinal pigment epithelium. Prog. Retin. Eye Res. 31, 121–135.
Sparrow, J.R., Hicks, D., Hamel, C.P., 2010. The retinal pigment epithelium in health and disease. Curr. Mol. Med. 10, 802–823.
Srour, M., Querques, G., Rostaqui, O., Souied, E.H., 2013. Early spectral-domain optical coherence tomography findings in unilateral acute idiopathic maculopathy. Retina 33, 2182–2184.
Steel, D., 2014. Retinal detachment. BMJ Clin Evid, 2014.
Stehouwer, M., Schlingemann, R.O., Verbraak, F.D., 2020 Nov. High recurrence rate in patients with choroidal hemangioma treated with limited single spot photodynamic therapy during long-term follow-up. Acta Ophthalmol. 98 (7), 679–686.
Stephens, R.F., Shields, J.A., 1979. Diagnosis and management of cancer metastatic to the uvea: a study of 70 cases. Ophthalmology 86, 1336–1349.
Strauss, O., 2005. The retinal pigment epithelium in visual function. Physiol. Rev. 85, 845–881.
Stuck, M.W., Conley, S.M., Naash, M.I., 2016. PRPH2/RDS and ROM-1: historical context, current views and future considerations. Prog. Retin. Eye Res. 52, 47–63.
Subhi, Y., Krogh Nielsen, M., Molbech, C.R., Oishi, A., Singh, A., Nissen, M.H., Sørensen, T.L., 2019a. Polypoidal choroidal vasculopathy associate with diminished regulatory T cells that are polarized into a T helper 2-like phenotype. Invest. Ophthalmol. Vis. Sci. 60, 2583–2590.
Subhi, Y., Nielsen, M.K., Molbech, C.R., Liisborg, C., Søndergaard, H.B., Sellebjerg, F., Sørensen, T.L., 2019b. The transcriptome of peripheral blood mononuclear cells in

patients with clinical subtypes of late age-related macular degeneration. Immun. Ageing 16, 20.
Subudhi, P., Kanungo, S., Subudhi, B.N., 2017. AN atypical case OF sympathetic ophthalmia after limbal corneal laceration. Retin. Cases Brief Rep. 11, 141–144.
Sundelin, S., Wihlmark, U., Nilsson, S.E., Brunk, U.T., 1998. Lipofuscin accumulation in cultured retinal pigment epithelial cells reduces their phagocytic capacity. Curr. Eye Res. 17, 851–857.
Takahashi, H., Hayashi, T., Tsuneoka, H., Nakano, T., Yamada, H., Katagiri, S., Fujino, Y., Noda, Y., Yoshimoto, M., Kawashima, H., 2014. Occult macular dystrophy with bilateral chronic subfoveal serous retinal detachment associated with a novel RP1L1 mutation (p.S1199P). Doc. Ophthalmol. 129, 49–56.
Tamura, N., Sakai, T., Tsuneoka, H., 2014. Spontaneous resolution of foveal detachment in dome-shaped macula observed by spectral domain optical coherence tomography. Clin. Ophthalmol. 8, 83–86.
Teussink, M.M., Breukink, M.B., van Grinsven, M.J., Hoyng, C.B., Klevering, B.J., Boon, C.J., de Jong, E.K., Theelen, T., 2015. OCT angiography compared to fluorescein and indocyanine green angiography in chronic central serous chorioretinopathy. Invest. Ophthalmol. Vis. Sci. 56, 5229–5237.
Thomas, E.L., Olk, R.J., Markman, M., Braine, H., Patz, A., 1983. Irreversible visual loss in Waldenstrom's macroglobulinaemia. Br. J. Ophthalmol. 67, 102–106.
Tittl, M., Maar, N., Polska, E., Weigert, G., Stur, M., Schmetterer, L., 2005. Choroidal hemodynamic changes during isometric exercise in patients with inactive central serous chorioretinopathy. Invest. Ophthalmol. Vis. Sci. 46, 4717–4721.
Tornquist, P., Alm, A., Bill, A., 1990. Permeability of ocular vessels and transport across the blood-retinal-barrier. Eye (Lond) 4 (Pt 2), 303–309.
Tso, M.O., Jampol, L.M., 1982. Pathophysiology of hypertensive retinopathy. Ophthalmology 89, 1132–1145.
Tsujikawa, A., Ojima, Y., Yamashiro, K., Ooto, S., Tamura, H., Nakagawa, S., Yoshimura, N., 2010. Punctate hyperfluorescent spots associated with central serous chorioretinopathy as seen on indocyanine green angiography. Retina 30, 801–809.
Urner-Bloch, U., Urner, M., Stieger, P., Galliker, N., Winterton, N., Zubel, A., Moutouh-de Parseval, L., Dummer, R., Goldinger, S.M., 2014. Transient MEK inhibitor-associated retinopathy in metastatic melanoma. Ann. Oncol. : Off. J. Eur. Soc. Med. Oncol/ESMO 25, 1437–1441.
Uyama, M., Takahashi, K., Kozaki, J., Tagami, N., Takada, Y., Ohkuma, H., Matsunaga, H., Kimoto, T., Nishimura, T., 2000. Uveal effusion syndrome: clinical features, surgical treatment, histologic examination of the sclera, and pathophysiology. Ophthalmology 107, 441–449.
Vaclavik, V., Ooi, K.G., Bird, A.C., Robson, A.G., Holder, G.E., Webster, A.R., 2007. Autofluorescence findings in acute exudative polymorphous vitelliform maculopathy. Arch. Ophthalmol. 125, 274–277.
Valeyre, D., Prasse, A., Nunes, H., Uzunhan, Y., Brillet, P.Y., Müller-Quernheim, J., 2014. Sarcoidosis. Lancet 383, 1155–1167.
van der Noll, R., Leijen, S., Neuteboom, G.H., Beijnen, J.H., Schellens, J.H., 2013. Effect of inhibition of the FGFR-MAPK signaling pathway on the development of ocular toxicities. Canc. Treat Rev. 39, 664–672.
van der Schaft, T.L., Mooy, C.M., de Bruijn, W.C., Oron, F.G., Mulder, P.G., de Jong, P.T., 1992. Histologic features of the early stages of age-related macular degeneration. A statistical analysis. Ophthalmology 99, 278–286.
van Dijk, E.H., Dijkman, G., Biermasz, N.R., van Haalen, F.M., Pereira, A.M., Boon, C.J., 2016a. Chronic central serous chorioretinopathy as a presenting symptom of Cushing syndrome. Eur. J. Ophthalmol. 26, 442–448.
van Dijk, E.H., Duits, D.E., Versluis, M., Luyten, G.P., Bergen, A.A., Kapiteijn, E.W., de Lange, M.J., Boon, C.J., van der Velden, P.A., 2016b. Loss of MAPK pathway activation in post-mitotic retinal cells as mechanism in MEK inhibition-related retinopathy in cancer patients. Medicine (Baltim.) 95, e3457.
van Dijk, E.H., van Herpen, C.M., Marinkovic, M., Haanen, J.B., Amundson, D., Luyten, G.P., Jager, M.J., Kapiteijn, E.H., Keunen, J.E., Adamus, G., Boon, C.J., 2015. Serous retinopathy associated with mitogen-activated protein kinase kinase inhibition (binimetinib) for metastatic cutaneous and uveal melanoma. Ophthalmology 122, 1907–1916.
van Dijk, E.H.C., Dijkman, G., Boon, C.J.F., 2017a. Photodynamic therapy in chronic central serous chorioretinopathy with subretinal fluid outside the fovea. Graefes Arch. Clin. Exp. Ophthalmol. 255, 2029–2035.
van Dijk, E.H.C., Fauser, S., Breukink, M.B., Blanco-Garavito, R., Groenewoud, J.M.M., Keunen, J.E.E., Peters, P.J.H., Dijkman, G., Souied, E.H., MacLaren, R.E., Querques, G., Downes, S.M., Hoyng, C.B., Boon, C.J.F., 2018a. Half-dose photodynamic therapy versus high-density subthreshold micropulse laser treatment in patients with chronic central serous chorioretinopathy: the PLACE trial. Ophthalmology 125, 1547–1555.
van Dijk, E.H.C., Kruit, W.H.J., Jager, M.J., Luyten, G.P.M., Vingerling, J.R., Boon, C.J.F., 2018b. Pimasertib-associated ophthalmological adverse events. Acta Ophthalmol. 96, 712–718.
van Dijk, E.H.C., Mohabati, D., Veselinovic, S., Chung, W.H., Dijkman, G., Boon, C.J.F., 2020a. The spectrum of polypoidal choroidal vasculopathy in Caucasians: clinical characteristics and proposal of a classification. Graefes Arch. Clin. Exp. Ophthalmol. online ahead of print https://pubmed.ncbi.nlm.nih.gov/32812132/.
van Dijk, E.H.C., Schellevis, R.L., Breukink, M.B., Mohabati, D., Dijkman, G., Keunen, J. E.E., Yzer, S., den Hollander, A.I., Hoyng, C.B., de Jong, E.K., Boon, C.J.F., 2019. Familial central serous chorioretinopathy. Retina 39, 398–407.
van Dijk, E.H.C., Schellevis, R.L., van Bergen, M., Breukink, M.B., Altay, L., Scholz, P., Fauser, S., Meijer, O.C., Hoyng, C.B., den Hollander, A.I., Boon, C.J.F., de Jong, E.K., 2017b. Association of a haplotype in the NR3C2 gene, encoding the mineralocorticoid receptor, with chronic central serous chorioretinopathy. JAMA Ophthalmol 135, 446–451.
van Dijk, E.H.C., Tsonaka, R., Klar-Mohamad, N., Wouters, D., de Vries, A.P.J., de Jong, E.K., van Kooten, C., Boon, C.J.F., 2017c. Systemic complement activation in central serous chorioretinopathy. PLoS One 12, e0180312.
van Dijk, E.H.C., van Rijssen, T.J., Subhi, Y., Boon, C.J.F., 2020b. Photodynamic therapy for chorioretinal diseases: a practical approach. Ophthalmol Ther 9, 329–342.
van Haalen, F.M., van Dijk, E.H.C., Andela, C.D., Dijkman, G., Biermasz, N.R., Pereira, A. M., Boon, C.J.F., 2019. Maladaptive personality traits, psychological morbidity and coping strategies in chronic central serous chorioretinopathy. Acta Ophthalmol. 97, e572–e579.
van Haalen, F.M., van Dijk, E.H.C., Dekkers, O.M., Bizino, M.B., Dijkman, G., Biermasz, N.R., Boon, C.J.F., Pereira, A.M., 2018. Cushing's syndrome and hypothalamic-pituitary-adrenal Axis hyperactivity in chronic central serous chorioretinopathy. Front. Endocrinol. (Lausanne) 9, 39.
van Noort, B.C., Keunen, J.E.E., Schlingemann, R.O., Marinkovic, M., 2019. Long survival and preservation of good visual acuity in a patient with bilateral diffuse uveal melanocytic proliferation. Ocul Oncol Pathol 5, 75–78.
van Rijssen, T.J., van Dijk, E.H.C., Dijkman, G., Boon, C.J.F., 2018. Clinical characteristics of chronic central serous chorioretinopathy patients with insufficient response to reduced-settings photodynamic therapy. Graefes Arch. Clin. Exp. Ophthalmol. 256, 1395–1402.
van Rijssen, T.J., van Dijk, E.H.C., Scholz, P., Breukink, M.B., Blanco-Garavito, R., Souied, E.H., Keunen, J.E.E., MacLaren, R.E., Querques, G., Fauser, S., Downes, S.M., Hoyng, C.B., Boon, C.J.F., 2019a. Focal and diffuse chronic central serous chorioretinopathy treated with half-dose photodynamic therapy or subthreshold micropulse laser: PLACE trial report No. 3. Am. J. Ophthalmol. 205, 1–10.
van Rijssen, T.J., van Dijk, E.H.C., Scholz, P., Breukink, M.B., Blanco-Garavito, R., Souied, E.H., Keunen, J.E.E., MacLaren, R.E., Querques, G., Fauser, S., Downes, S.M., Hoyng, C.B., Boon, C.J.F., 2020a. Reply to comment on: focal and diffuse chronic central serous chorioretinopathy treated with half-dose photodynamic therapy or subthreshold micropulse laser: PLACE trial report No. 3. Am. J. Ophthalmol. 212, 187–188.
van Rijssen, T.J., van Dijk, E.H.C., Scholz, P., Breukink, M.B., Dijkman, G., Peters, P.J.H., Tsonaka, R., MacLaren, R.E., Downes, S.M., Fauser, S., Boon, C.J.F., Hoyng, C.B., 2020b. Crossover to photodynamic therapy or micropulse laser after failure of primary treatment of chronic central serous chorioretinopathy: the REPLACE trial. Am. J. Ophthalmol. 216, 80–89.
van Rijssen, T.J., van Dijk, E.H.C., Yzer, S., Ohno-Matsui, K., Keunen, J.E.E., Schlingemann, R.O., Sivaprasad, S., Querques, G., Downes, S.M., Fauser, S., Hoyng, C.B., Piccolino, F.C., Chhablani, J.K., Lai, T.Y.Y., Lotery, A.J., Larsen, M., Holz, F.G., Freund, K.B., Yannuzzi, L.A., Boon, C.J.F., 2019b. Central serous chorioretinopathy: towards an evidence-based treatment guideline. Prog. Retin. Eye Res. 100770.
Van Rysselberge, C., Balikova, I., Judice, L., Makhoul, D., Postelmans, L., 2020. Multimodal imaging IN hellp-related chorioretinopathy. Retin. Cases Brief Rep. online ahead of print https://pubmed.ncbi.nlm.nih.gov/32028449/.
van Soest, S.S., de Wit, G.M., Essing, A.H., ten Brink, J.B., Kamphuis, W., de Jong, P.T., Bergen, A.A., 2007. Comparison of human retinal pigment epithelium gene expression in macula and periphery highlights potential topographic differences in Bruch's membrane. Mol. Vis. 13, 1608–1617.
Veckeneer, M., Derycke, L., Lindstedt, E.W., van Meurs, J., Cornelissen, M., Bracke, M., Van Aken, E., 2012. Persistent subretinal fluid after surgery for rhegmatogenous retinal detachment: hypothesis and review. Graefe's archive for clinical and experimental ophthalmology = Albrecht von Graefes Archiv fur klinische und experimentelle Ophthalmologie 250, 795–802.
Verbraak, F.D., Schlingemann, R.O., de Smet, M.D., Keunen, J.E., 2006. Single spot PDT in patients with circumscribed choroidal haemangioma and near normal visual acuity. Graefes Arch. Clin. Exp. Ophthalmol. 244, 1178–1182.
Verbraak, F.D., Schlingemann, R.O., Keunen, J.E., de Smet, M.D., 2003. Longstanding symptomatic choroidal hemangioma managed with limited PDT as initial or salvage therapy. Graefes Arch. Clin. Exp. Ophthalmol. 241, 891–898.
Verhagen, F.H., Bekker, C.P.J., Rossato, M., Hiddingh, S., de Vries, L., Devaprasad, A., Pandit, A., Ossewaarde-van Norel, J., Ten Dam, N., Moret-Pot, M.C.A., Imhof, S.M., de Boer, J.H., Radstake, T., Kuiper, J.J.W., 2018. A disease-associated MicroRNA cluster links inflammatory pathways and an altered composition of leukocyte subsets to noninfectious uveitis. Invest. Ophthalmol. Vis. Sci. 59, 878–888.
von Ruckmann, A., Fitzke, F.W., Bird, A.C., 1995. Distribution of fundus autofluorescence with a scanning laser ophthalmoscope. Br. J. Ophthalmol. 79, 407–412.
Wang, J.S., Kefalov, V.J., 2011. The cone-specific visual cycle. Prog. Retin. Eye Res. 30, 115–128.
Wang, M., Munch, I.C., Hasler, P.W., Prunte, C., Larsen, M., 2008. Central serous chorioretinopathy. Acta Ophthalmol. 86, 126–145.
Wang, S., Wang, Y., Gao, X., Qian, N., Zhuo, Y., 2015. Choroidal thickness and high myopia: a cross-sectional study and meta-analysis. BMC Ophthalmol. 15, 70.
Wangsa-Wirawan, N.D., Linsenmeier, R.A., 2003. Retinal oxygen: fundamental and clinical aspects. Arch. Ophthalmol. 121, 547–557.
Warrow, D.J., Hoang, Q.V., Freund, K.B., 2013. Pachychoroid pigment epitheliopathy. Retina 33, 1659–1672.
Watts, P.O., Mantry, S., Austin, M., 2000. Serous retinal detachment at the macula in sarcoidosis. Am. J. Ophthalmol. 129, 262–264.
Watzke, R.C., Packer, A.J., Folk, J.C., Benson, W.E., Burgess, D., Ober, R.R., 1984. Punctate inner choroidopathy. Am. J. Ophthalmol. 98, 572–584.
Weenink, A.C., Borsje, R.A., Oosterhuis, J.A., 2001. Familial chronic central serous chorioretinopathy. Ophthalmol. J. Int. d'ophtalmologie. Int. J. Ophthalmol. Zeitschrift fur Augenheilkunde 215, 183–187.

Weiter, J.J., Delori, F.C., Wing, G.L., Fitch, K.A., 1986. Retinal pigment epithelial lipofuscin and melanin and choroidal melanin in human eyes. Invest. Ophthalmol. Vis. Sci. 27, 145–152.
Wenkel, H., Streilein, J.W., 1998. Analysis of immune deviation elicited by antigens injected into the subretinal space. Invest. Ophthalmol. Vis. Sci. 39, 1823–1834.
Wenkel, H., Streilein, J.W., 2000. Evidence that retinal pigment epithelium functions as an immune-privileged tissue. Invest. Ophthalmol. Vis. Sci. 41, 3467–3473.
Williams, A.T., Font, R.L., Van Dyk, H.J., Riekhof, F.T., 1978. Osseous choristoma of the choroid simulating a choroidal melanoma. Association with a positive 32P test. Arch. Ophthalmol. 96, 1874–1877.
Witmer, A.N., Vrensen, G.F., Van Noorden, C.J., Schlingemann, R.O., 2003. Vascular endothelial growth factors and angiogenesis in eye disease. Prog. Retin. Eye Res. 22, 1–29.
Witschel, H., Font, R.L., 1976. Hemangioma of the choroid. A clinicopathologic study of 71 cases and a review of the literature. Surv. Ophthalmol. 20, 415–431.
Wong, C.W., Yanagi, Y., Lee, W.K., Ogura, Y., Yeo, I., Wong, T.Y., Cheung, C.M., 2016. Age-related macular degeneration and polypoidal choroidal vasculopathy in Asians. Prog. Retin. Eye Res. 53, 107–139.
Wong, R., Chopdar, A., Brown, M., 2004. Five to 15 year follow-up of resolved idiopathic central serous chorioretinopathy. Eye (London, England) 18, 262–268.
Wong, R.K., Lee, J.K., Huang, J.J., 2012. Bilateral drug (ipilimumab)-induced vitritis, choroiditis, and serous retinal detachments suggestive of vogt-koyanagi-harada syndrome. Retin. Cases Brief Rep. 6, 423–426.
Wong, R.L., Singh, S.R., Rasheed, M.A., Goud, A., Chhablani, G., Samantaray, S., AnkiReddy, S., Vupparaboina, K.K., Chhablani, J., 2021 Mar. En-face choroidal vascularity in central serous chorioretinopathy. Eur. J. Ophthalmol. 31 (2), 536–542.
Wong, T.Y., Mitchell, P., 2004. Hypertensive retinopathy. N. Engl. J. Med. 351, 2310–2317.
Wyszynski, R.E., Grossniklaus, H.E., Frank, K.E., 1988. Indirect choroidal rupture secondary to blunt ocular trauma. A review of eight eyes. Retina 8, 237–243.
Xia, T., Rizzolo, L.J., 2017. Effects of diabetic retinopathy on the barrier functions of the retinal pigment epithelium. Vis. Res. 139, 72–81.
Yahia, S.B., Zaouali, S., Attia, S., Messaoud, R., Ladjimi, A., Khairallah, M., 2008. Serous retinal detachment secondary to choroidal osteoma successfully treated with transpupillary thermotherapy. Retin. Cases Brief Rep. 2, 126–127.
Yamaguchi, Y., Otani, T., Kishi, S., 2006. Serous macular detachment in branch retinal vein occlusion. Retina 26, 1029–1033.
Yang, L., Jonas, J.B., Wei, W., 2013. Optical coherence tomography-assisted enhanced depth imaging of central serous chorioretinopathy. Invest. Ophthalmol. Vis. Sci. 54, 4659–4665.
Yannuzzi, L.A., 2010. Central serous chorioretinopathy: a personal perspective. Am. J. Ophthalmol. 149, 361–363.
Yannuzzi, L.A., Ciardella, A., Spaide, R.F., Rabb, M., Freund, K.B., Orlock, D.A., 1997. The expanding clinical spectrum of idiopathic polypoidal choroidal vasculopathy. Arch. Ophthalmol. 115, 478–485.
Yannuzzi, L.A., Jampol, L.M., Rabb, M.F., Sorenson, J.A., Beyrer, C., Wilcox Jr., L.M., 1991. Unilateral acute idiopathic maculopathy. Arch. Ophthalmol. 109, 1411–1416.
Yannuzzi, L.A., Sorenson, J., Spaide, R.F., Lipson, B., 1990. Idiopathic polypoidal choroidal vasculopathy (IPCV). Retina 10, 1–8.
Yeh, S., Wilson, D.J., 2010. Combination intravitreal rituximab and methotrexate for massive subretinal lymphoma. Eye (Lond) 24, 1625–1627.
Yoneya, S., Tso, M.O., 1987. Angioarchitecture of the human choroid. Arch. Ophthalmol. 105, 681–687.
Yoo, C., Kim, S.K., Huh, K., Oh, J., 2009. Atypical acute syphilitic posterior placoid chorioretinitis. Kor. J. Ophthalmol. 23, 108–111.
Yu, D.Y., Cringle, S.J., Su, E., Yu, P.K., Humayun, M.S., Dorin, G., 2005. Laser-induced changes in intraretinal oxygen distribution in pigmented rabbits. Invest. Ophthalmol. Vis. Sci. 46, 988–999.
Yung, M., Klufas, M.A., Sarraf, D., 2016. Clinical applications of fundus autofluorescence in retinal disease. Int J Retina Vitreous 2, 12.
Yzer, S., Fung, A.T., Barbazetto, I., Yannuzzi, L.A., Freund, K.B., 2012. Central serous chorioretinopathy in myopic patients. Arch. Ophthalmol. 130, 1339–1340.
Zamiri, P., Masli, S., Kitaichi, N., Taylor, A.W., Streilein, J.W., 2005. Thrombospondin plays a vital role in the immune privilege of the eye. Invest. Ophthalmol. Vis. Sci. 46, 908–919.
Zatreanu, L., Freund, K.B., Leong, B.C.S., Yu, H.G., Teke, M.Y., Yzer, S., Sadda, S.R., Sarraf, D., 2020. Serous macular detachment IN best disease: a masquerade syndrome. Retina (Philadelphia, Pa.) 40, 1456–1470.
Zhao, M., Celerier, I., Bousquet, E., Jeanny, J.C., Jonet, L., Savoldelli, M., Offret, O., Curan, A., Farman, N., Jaisser, F., Behar-Cohen, F., 2012. Mineralocorticoid receptor is involved in rat and human ocular chorioretinopathy. J. Clin. Invest. 122, 2672–2679.
Zola, M., Chatziralli, I., Menon, D., Schwartz, R., Hykin, P., Sivaprasad, S., 2018. Evolution of fundus autofluorescence patterns over time in patients with chronic central serous chorioretinopathy. Acta Ophthalmol. 96, e835–e839.